INFORMATION TO USERS

This manuscript has been reproduced from the microfilm master. UMI films the text directly from the original or copy submitted. Thus, some thesis and dissertation copies are in typewriter face, while others may be from any type of computer printer.

The quality of this reproduction is dependent upon the quality of the copy submitted. Broken or indistinct print, colored or poor quality illustrations and photographs, print bleedthrough, substandard margins, and improper alignment can adversely affect reproduction.

In the unlikely event that the author did not send UMI a complete manuscript and there are missing pages, these will be noted. Also, if unauthorized copyright material had to be removed, a note will indicate the deletion.

Oversize materials (e.g., maps, drawings, charts) are reproduced by sectioning the original, beginning at the upper left-hand corner and continuing from left to right in equal sections with small overlaps.

Photographs included in the original manuscript have been reproduced xerographically in this copy. Higher quality 6" x 9" black and white photographic prints are available for any photographs or illustrations appearing in this copy for an additional charge. Contact UMI directly to order.

ProQuest Information and Learning
300 North Zeeb Road, Ann Arbor, MI 48106-1346 USA
800-521-0600

UMI®

SPECTROSCOPIC STUDIES OF AGGREGATED MOLECULES ENCAPSULATED IN MESOPOROUS MATERIALS

by

WEI XU

A dissertation submitted to the Graduate Faculty in Chemistry in partial fulfillment of the requirements for degree of Doctor of Philosophy, The City University of New York

2001

UMI Number: 3024847

Bell & Howell Information and Learning Company
300 North Zeeb Road
P.O. Box 1346
Ann Arbor, MI 48106-1346

This manuscript has been read and accepted for the Graduate Faculty in Chemistry in satisfaction of the dissertation requirement for the degree of Doctor of Philosophy.

9/5/2001
Date

[required signature] Daniel L. Akins
Chair of Examining Committee

9/13/2001
Date

[required signature] Gerald Koppel
Executive Officer

[typed name] John R. Fuller

[typed name] Ron M. Lerner

[typed name] Raymond J. Dusch
Supervisory Committee

THE CITY UNIVERSITY OF NEW YORK

ABSTRACT

SPECTROSCOPIC STUDIES OF AGGREGATED MOLECULES ENCAPSULATED IN MESOPOROUS MATERIALS

By

Wei Xu

Advisor: Professor Daniel L. Akins

We report the formation of monomeric and aggregated tetrakis(*p*-sulfonatophenyl) porphyrin (TSPP), 1,1'-3,3'-tetraethyl-5,5',6,6'-tetrachlorobenzimidazolocarbocyanine (TTBC) as well as 1,1'-diethyl-3,3'-di(4-sulfobutyl)-5,5',6,6'-tetrachlorobenzimidazolo-carbocyanine (TDBC) encapsulated within aluminosilicate or silicate mesostructures, specifically, MCM-41 and SBA-15, under different pH conditions. It was necessary to stabilize the synthesized MCM-41 through use of a silylation reagent, aminopropyltriethoxysilane, which cross-links oxygen on the surface (thus rigidifying the walls of the mesoporous material) and functionalizes the interface for proper guest-host interaction. But in the case of SBA-15, due to its thicker walls, even though silylation was utilized, the main purpose it served was to modify SBA-15 is to meet the requirement of electrostatic interaction. NMR, XRD, UV-vis absorption, Raman scattering, and fluorescence measurements are used as spectroscopic tools to characterize the various products. Nitrogen adsorption/desorption isotherms and SEM were also applied to study the mesostructure of MCM-41 and SBA-15. Additionally, the difference between J-aggregated TSPP formed within modified MCM-41 and that formed in the

presence of an ionic vesicle suspension are compared and analyzed. The composites consisting of either J-aggregated TTBC or TDBC and the aluminosilicate/silicate represent new fluorescent nanomaterials that possess the properties of the aggregate, yet avoid the essentially unfettered topography and physical length that accompanies the formation of an aggregate in solution or adsorbed onto an interface.

PREFACE

Research dealing with spectral and optical dynamics properties of molecular aggregated structures is of continuing interest for a large number of scientists and engineers. Interest in aggregates derives from the realization that aggregated molecules play crucial roles in nature, such as in light harvesting and the primary charge-separation steps in photosynthesis. Through the study of the spectral properties of two kinds of molecular aggregates, i.e., those formed from porphyrins and cyanine dyes, an important outcome that is sought in this dissertation is to provide a great amount of fundamental and important information for potential applications of selected aggregated molecules as the active agents in molecular photonic devices or photonic materials.

The research described in this dissertation contributes original results to the body of knowledge concerned with aggregated molecules and mesoporous silicates and aluminosilicates. The silicates and aluminosilicates have one-dimensional channel structure and uniform pore size with 2 nm to 10 nm. The composites consisting of aggregates and mesoporous materials possess the properties of aggregate, yet avoid the uncertainty of topographic influence because of the constricted growth with the channels of mesoporous structures.

In Chapter 1, we report the formation of monomeric and aggregated tetrakis(*p*-sulfonatophenyl) porphyrin (TSPP) encapsulated within an aluminosilicate mesostructure, specifically MCM-41, under different pH conditions. It was necessary to stabilize the synthesized MCM-41 through use of a silylation reagent, aminopropyltriethoxysilane, which cross-links oxygen on the surface (thus rigidifying the

walls of the mesoporous material) and functionalizes the interface for proper guest-host interaction. NMR, XRD, UV-vis absorption and fluorescence measurements are used as spectroscopic tools to characterize the various products.

To compare the difference in structural and spectral properties of the formed aggregates in different environments, in Chapter 2, electronic absorption and vibrational Raman spectra of monomeric and aggregated TSPP within modified nanoporous MCM-41 and in the presence of an ionic vesicle suspension are acquired and analyzed. In dilute TSPP solution, a key factor in leading to formation of aggregates in didodecyldimethylammonium bromide (referred to as 3DMA) is the increase in the site concentration of the monomers promoted by the electrostatic attraction between the anionic porphyrin substituents and the positively charged binding sites of the vesicle. Due to the differences in the microenvironments, the Soret band shifts of the formed aggregates both on vesicle surface and within MCM-41 are observed when compared to homogeneous aggregate solution, and the changes in two enhanced Raman bands are demonstrated as well. The same mechanism of J-aggregate formation, i.e., the structural alignments of protonated monomers in TSPP aggregate, suggests the similar Raman patterns to that in solution phase. For occluded monomeric TSPP within modified MCM-41, due to strong electrostatic interaction between the end-group of TSPP (i.e., SO_3^-) and surface wall (i.e., $^+NH_3$-R), dramatic Raman shifts, especially for phenyl group, are observed.

One finds that aggregated TSPP/MCM-41 composite system shows low exciton emission because the exciton emission from aggregated S_2 state molecules to ground state S_1 is dipolar forbidden. For photonic device application making use of strong exciton

emission, a replacement of TSPP with cynanine dye molecules is imperative. In chapter 3, we report the formation of monomeric and J-aggregated 1,1',3,3'-tetraethyl-5,5',6,6'-tetrachlorobenzimidazolocarbocyanine (referred to as TTBC) encapsulated within modified MCM-41, under different pH conditions. Based on the same reason above, the modified MCM-41 by silylation is used in the preparation of the aggregated TTBC/composites so as to maintain its structural integration and meet the host-guest interaction as well. XRD, UV-vis absorption and fluorescence measurements are used as spectroscopic tools to characterize the various products. The composite consisting of J-aggregated TTBC and the aluminosilicate represents a new fluorescent nanomaterial whose properties derive from exciton energies and dynamics that result from quantum confinement.

It is to be noted that due to a substantial amount of monomer remained within the mesoporous channels, the amount of aggregated TTBC formed within the channels of MCM-41 does not dominate the emission from sample. Additionally, the structure of MCM-41 for aggregated composite is not completely remained, hence, composite system with more robust and manipulable physical form is desirable. To achieve the above goal, in Chapter 4, 1,1'-diethyl-3,3'-di(4-sulfobutyl)-5,5',6,6'-tetrachlorobenzimidazolo-carbo-cyanine (referred to as TDBC) and mesoporous SBA-15 are used in stead of TTBC and MCM-41. SBA-15 has similar pore structure but thicker wall than that of MCM-41. We report the formation of monomeric and J-aggregated TDBC encapsulated within SBA-15. The monolayer formed by silylation with $^{-}NH_2$ at the terminals results in formation of NH_3^+ surface species at low pH values, which facilitates the incorporation of anionic dye within the cores of SBA-15 by electrostatic interaction. XRD, UV-vis absorption and

fluorescence measurements are also used as spectroscopic tools to characterize SBA-15 host samples as well as composites consisting of the host and encapsulated molecules—both monomer and aggregate. J-aggregated TDBC occluded within SBA-15 represents a robust, new superradiant fluorescent nanomaterial.

ACKNOWLEDGMENT

First of all I am very lucky and grateful to meet and have my great mentor, Dr. Daniel L. Akins. His advice and guidance during all my graduate studies were beneficial, enriching and very useful. It should be emphasized that Dr. Akins' s scientific attitude and integrated personality greatly inspired me and will benefit me for my future development. Also he has always been friendly and very understanding. I would like to express special thanks to Dr. Ronald H. Brown and Ms. Smith Sandra for their unselfish assistance and advice in my graduate study and campus life. I appreciate the help from Dr. Chu Guo, Hanru Zhu, Haiquan Guo, Fleumingue Jean-Mary for their valuable discussion, suggestions and assistance in carrying out the experiments. Doing research wouldn' t have been enjoyable without the presence of my colleagues and friends, Yanting liao, Phillipe Mercier, Dionne Miller, Metin Aydin, Nathan Stevens and Sheuli Zakia. I also appreciate the great help from Dr. Maria Tamargo and Dr. Teresa Bandosz of the Chemistry Department at City College of New York, and Dr. Ruth Stark, Dr. Hsin Wang, Dr. James Batteas and James Saccardo of the Chemistry Department at College of Saten Island who made their instruments available to us.

I really could not have done it without my family and friends behind me. Especially my wife Jun zhang for her encouragement, support and most of all she has never failed to be there for me. My parents, Defeng Xu and Yufang Liu, and my brother and sisters for their unconditional love and continuous blessing at any time. My close friend, Mr. Jian Huang, for his unceasing help in the past 20 years. My previous mentors, Prof. Quanzhi Li and Prof. Zuzhan Yu from Fudan University, for their great guidance that had helped me achieve my goal.

TABLE OF CONTENTS

Bibliography

LIST OF TABLES

LIST OF DIAGRAMS AND FIGURES

concentration of 5×10^{-5} M and pH =1.5, excitation wavelength λ_{ex} = 488 nm, integrating time 10 second, repeating time 100. (C) TSPP-A/3DMA, excitation wavelength λ_{ex} = 488 nm, integrating time 30 second, repeating time 1. (D) TSPP-5-M/MCM-41,excitation wavelength λ_{ex} = 457 nm, integrating time 3 second, repeating time 1. (E) Solution phase protonated TSPP with concentration of 5×10^{-5} M and pH =4.0, excitation wavelength λ_{ex} = 457 nm, integrating time 10 second, repeating time 1.

CHAPTER 1

AGGREGATION OF TETRAKIS(*P*-SULFONATOPHENYL)PORPHYRIN (TSPP) WITHIN MODIFIED MESOPOROUS MCM-41

1.1 Introduction

Porphyrin aggregates formed from monomers that are initially dispersed in a medium and spontaneously align themselves (i.e., self-assemble), without the formation of covalent linkages, are of considerable scientific interest. Such aggregates are model composite structures for gaining insight into the roles that optically induced transient structural changes and photon dynamics play in photosynthesis [1,2]. Additionally, through the study of spectral properties and photodynamical behaviors of aggregated porphyrin structures, an important outcome sought is the translation of the electron transfer specificities and speeds often found for biological reactions to the realm of molecular photonic devices (i.e., biomimetics) or photonic materials; enormous interest in the applications area has been evidenced [3,4]. Thus, studies of structures and optical dynamics of porphyrin aggregates have both scientific and technological importance.

Research efforts involving porphyrin aggregates dealing with homogeneous solution entities as well as adsorbates on electrode surfaces have been reported. Akins and his coworkers have, In particular, conducted solution studies dealing with aggregate formation by porphyrins with negatively charged aryl-substituents at *meso* positions (for example, tetrakis(*p*-sulfonatophenyl)porphyrin (TSPP); see Fig. 1-1 for structure) [5-7]. Their heterogeneous, electrode studies have dealt with TSPP [8] as well as selected

metallo-TSPP complexes [9]. In the present dissertation, we make our efforts and report the formation of aggregated TSPP encapsulated within an aluminosilicate mesostructure, specifically MCM-41 (a Mobil Crystal Material), which we have synthesized as a one-dimensional, highly uniform pore size, hexagonal, mesoporous powdered material. The schematic synthesis mechanism is shown in Fig. 1-2[10]. By using different surfactants, the pore size of the synthesized MCM-41 can be tailored to have almost uniform dimension ranging from 2 to 6 nm. The porphyrin aggregate formed within the pores of the MCM-41 has been shown to be the so-called J-aggregate. The composite structure (aggregated TSPP within the pores of MCM-41) represents a new "ship-in-a-bottle-type" nanomaterial whose properties derive from exciton energies and dynamics that result from quantum confinement. This quantum confinement is associated with both the restricted growth region available to the spontaneously self-assembled molecular aggregate, which forms when TSPP monomers are protonated (and form the dianion) under sufficiently acidic conditions, and the inherent confinement (characterized in terms of a coherence length [11-13] of the exciton's movement among a subset of coherently responding molecules within the physical aggregate.

To stabilize the synthesized MCM-41 and allow formation of aggregated TSPP from the occluded monomers, we found it necessary to modify the interior structure of the mesoporous silica through use of an alkoxysilane silylation reagent. Specifically, we used aminopropyltriethoxysilane (APTES: NH_2-$(CH_2)_3$-Si-$(C_2H_5O)_3$), which satisfies guest-host intermolecular and/or electrostatic interactions and links oxygens at the interface, thus rigidifying it. The positive electrostatic interaction derives from functionalizing the surface with NH_2, which under pH control can be converted to NH_3^+,

thus providing a strong attractive interaction with the sulfonato groups of the porphyrin. Various MCM-41/TSPP assemblies were obtained through ion exchange mixing of the modified MCM-41 with TSPP monomer in different ratios. Upon acidifying filtered residues containing various assemblies in a programmed way, thereby changing the pH of the microenvironment within the cavity of the mesoporous material, conditions were attained where first the occluded protonated monomer (i.e., the dianion) and then the J-aggregated TSPP were formed. Specifics of the chemical and spectroscopic techniques are provided below.

1.2 Experimental

1.2.1 Synthesis of MCM-41

Polycrystalline powders of the mesostructural aluminosilicate MCM-41 were prepared by using cetyltrimethylammonium bromide (CTAB) as the template [10,14]. Briefly, Na_2SiO_3 (Aldrich, ~27% SiO_2) solution and a calculated amount of $NaAlO_2$ (Alfa) solution (Si/Al = 20) were added to CTAB (Aldrich) solution according to the molar composition ratio $5SiO_2$:$0.4Al_2O_3$:CTAB:$610H_2O$. The pH was lowered to 11 with 2 M H_2SO_4 and the mixture was stirred for >3 hrs at about 318 K. Then the temperature was raised to 373 K, and the reaction allowed for 72 hrs in a teflon-lined autoclave. The resultant precipitate was filtered, washed thoroughly with distilled water, and calcined in air at 773 K to obtain the final product MCM-41 (see below for XRD patterns and their interpretations).

1.2.2 Modification of MCM-41

Several detailed reports have been recently published describing MCM-41 surface modifications using alkoxysilane-coupling agents [15-22]. For our studies, the modified MCM-41 was prepared according to a procedure detailed in Ref. 15. Briefly, about 1.5 g of the calcined MCM-41 was mixed with a chloroform solution of APTES (100 ml, 0.2 M) and stirred overnight at room temperature. The precipitate was filtered and washed with chloroform and dichloromethane.

1.2.3 Formation of TSPP/MCM-41 Composites

A typical ion-exchange preparation of a TSPP/MCM-41 composite involved stirring a mixture of 300 mg of modified MCM-41, 5 mg TSPP, and 25 ml of distilled water for over 24 hrs at room temperature with the pH held at about 5, using 2 M H_2SO_4. The solution was then centrifuged, and the supernatant aqueous solution decanted. The filtrate was washed several times with pH/5 water to remove TSPP monomers at the external surface and then dried in air; no conversion of occluded monomer to surface monomer occurred with time, as evidenced by absence of TSPP in subsequent wash solutions. The resultant residue is here designated TSPP-X-M/MCM-41, where TSPP-X-M indicates that monomeric TSPP is encapsulated within the modified MCM-41and X is the amount of TSPP used by weight: absorption and emission studies (see below, section III) have confirmed the presence of monomer under the above conditions. The final step in forming occluded, aggregated TSPP involves adding 2 M H_2SO_4 to the solid residue. An immediate color change occurs in which the residue changes color from dark yellow to olive. The powdered residue was then spectroscopically investigated (see below.

section III) and identified as the occluded J-aggregated form of TSPP, designated here as TSPP-A/MCM-41.

1.2.4 Instrumentation

Nitrogen isotherm was measured using an ASAP 2010 (Micromeritics) at 77 K. Before the experiment the sample was heated at 573 K and then outgassed at this temperature under a vacuum of 10^{-5} torr to constant pressure. The isotherm was used to calculate the surface area, pore size distribution and pore volume. These studies were conducted in the laboratory of Dr. Teresa Bandosz of the Chemistry Department at City College of New York.

Absorption spectra were recorded using a Perkin-Elmer, Lambda 18, UV-vis-NIR spectrometer. Steady-state fluorescence spectra were acquired using a SPEX, Fluorolog-τ2 spectrofluorometer. The x-ray diffraction (XRD) instrument used was a Rigaku diffractometer using Cu $K_{\alpha 1}$ (0.154 nm) x-rays: typically run at a voltage of 40 kV and current of 30 mA. The latter instrument was made available to us by Dr. Maria Tamargo, also of the Chemistry Department at the City College of New York. Solid state ^{29}Si MAS NMR spectra were obtained on a Varian 300 spectrometer. Samples were spun at a frequency of 4 kHz in a MAS zirconia rotor. Cross-polarization MAS was done with ^{29}Si in the low power mode with frequency of 63 MHz and a 90° pulse of 5 μs, and ^{1}H in high power mode with power of 59 MHz and a 90° pulse of 5 μs. The contact time used in this study was 8 ms, which has been proven to be long enough to permit full cross polarization for different silicons. Spectral contributions from silicons deeper in the

lattice are strongly discriminated against in the CP experiment due to their prohibitively long Si — H distances, which will be discussed in the following section. As a consequence, the intensities of the signals from the isolated and geminal silanols and the attached silane groups are believed to be reliable and valid. MAS without CP was done with low power ^{29}Si at 57 MHz and relaxation delay 2 second. The reference sample used is tetramethylsilane (TMS). These latter experiments were conducted at the College of Staten Island in the laboratory of Prof. Ruth Stark.

Time-dependent emission measurements utilized a Hamamatsu streak camera, Model C4334, optically coupled to a charge-coupled-device (CCD) array detector. This system allowed the measurements of both the emission decay rate and the time-resolved emission spectrum. As shown in Diagram 1-1,the exciting light source was a Spectra-Physics all-solid state laser system. A Millennia V laser with 5 watt of green 532 nm pumps a mode-locked Ti: sapphire oscillator (Tsunami), which produces approximately 500 mW of 800 nm with pulse width less than 2 ps. These pulses are directed to the Spitfire to be stretched, amplified and then recompressed. The Spitfire is pumped with a frequency doubled Nd : YLF laser. The output power from the Spitfire ca. 1 watt, with wavelength of 800 nm laser and pulse duration of 1 ps, at a repetition rate of 1 KHz, was used to create tunable optical parametric emission through use of OPA-800 Ultrafast Optical Parametric Amplifier, made by Spectra Physics. As Shown in Diagram 1-2, the input laser of 800 nm is first reflected off two mirrors that flip the polarization from horizontal to vertical, then is splitted int two legs. In the first leg, approximately 96% of the energy is transmitted and used for pumping the OPA. The remaining <4% is reflected by beam splitter to produce a white light continuum that provides seed for OPA. A half

waveplate and a cubic polarizer control the beam energy, and a lens focuses the beam into a solid-state material where the continuum is generated. It is re-collimated and relayed to BBO crystal through the variable delay stage. In the second leg, the major portion of the amplified beam is split into two pump beams, each of which are down-collimated to pump the BBO crystal. About 15% of the beam is used to pump the first pass or pre-amplification stage, and the remainder is used to pump the second pass or power ampfifier stage.In the pre-amplification stage, the pump beam is steered to the BBO crystal. This dichroic mirror combines the pre-amplification pump beam with the white light that is generated in the white light arm. The white light is temporarily overlapped and amplified by the pre-pump beam. The signal and idler beams in the BBO crystal is generated in the pre-amplification stage. In the power amplifier stage, the pump beam is directed to the crystal by five mirrors and the 800 nm dichroic mirror, where it is overlapped with the returning idler and signal beams in the BBO crystal for final amplication. The amplified signal and idler output wavelengths are determined by both of the phase-matching angle of the BBO crystal and the grating angle. The residual 800 nm beam is separated from the amplified signal and idler beams by dichroic mirror, and the signal and idler are then either separated and made available through difference exit ports or are sent to the harmonic generation leg for wavelength extension through second and fourth harmonic generation. The output laser wavelengths are available in the range from 400 to 1000 nm with pulse width of 1 ps. HPD-TA 3.1.0 software was used to process the data.

1.3 Results and Discussion

The adsorption-desorption isotherm of calcined MCM-41 is shown in Fig. 1-3. From the adsorption branch of the N_2 adsorption/desorption isotherm and Barrett-Joyner-Halenda (BJH) formula [23], the pore size distribution, the cumulative surface area, A_{BJH}, and the cumulative pore volume are obtained, as shown in Fig. 1-4. This method gives a remarkably narrow pore size distribution with a pore size of ca. 29 Å and high pore volume and surface area with 0.80 cm^3/g and 953 m^2/g, respectively.

XRD patterns of pristine calcined MCM-41, modified MCM-41, the monomer-incorporated composite (TSPP-5-M/MCM-41), and the aggregate-incorporated composite (TSPP-5-A/MCM-41) are shown in Fig. 1-5. The XRD patterns of all other monomeric and aggregated TSPP/MCM-41 composites are similar to those of TSPP-5-M/MCM-41and TSPP-5-A/MCM-41, respectively(not shown).It is found that, after the silylation reaction and likely formation of a monolayer of silyation product on the surface walls, the XRD pattern of the modified MCM-41 is essentially identical to that of the original calcined MCM-41. Using Bragg's equation and comparison with reference studies [16,24], the pore size of calcined MCM-41 is estimated to be ca. 30 Å in line with the result of nitrogen isotherm. Additionally, we find, upon attachment of the (putative) monolayer of silylation product to the internal channels of the calcined MCM-41, that the pore size is narrowed to ca. 21 Å again through the use of the Bragg equation. An opening of 21 Åis sufficiently large to allow TSPP, of approximate dimensions (14×14) $Å^2$, to be incorporated into the modified MCM-41.

The XRD patterns of TSPP-5-M/MCM-41 and TSPP-A/MCM-41 show strong (100) peaks and proportional (110) and (200) peak intensities, suggesting that a high

framework stability is maintained for the modified MCM-41 when either monomeric or aggregated TSPP is incorporated. What differences in relative intensities that occur, likely are attributable to electrostatic interaction between sulfonato groups of TSPP and the interior walls of the cage as well as with the aggregate's transverse dimension as it grows along the channel length of the mesoporous material.

The ^{29}Si MAS NMR spectra of calcined MCM-41, modified MCM-41 and monomeric TSPP-5-M/MCM-41 are shown in Fig. 1-6 and Fig. 1-7. It is to be noted that the difference between ^{29}Si MAS NMR and CP/MAS NMR MAS spectra is obvious. For ^{29}Si MAS NMR, it just reveals the information of bulk samples. For all three samples, three peaks at ~-110 ppm, ~-100 ppm and ~-92 ppm, corresponding to Q^4, Q^3 and Q^2 which will be discussed in detail below, are observed by multi-peak fitting. But almost no change in their relative peak intensities is illustrated from their spectra, regardless of different samples. In the present studies, with the modification of calcined MCM-41 using APTES and monomeric TSPP encapsulation within the modified MCM-41, we are interested in understanding the change in the surface structures. The structure of the functionalized MCM-41 and TSPP/MCM-41 composite and the chemical bonding can be studied by solid-state NMR experiments [25a]. The ^{1}H and ^{29}Si cross-polarization experiment restricts detection of an NMR signal to silicon nuclei that are near protons, i.e, at or near the surface. The results suggest that the replacement of regular MAS NMR with CP MAS NMR is necessary. Therefore, ^{29}Si CP/MAS NMR is a sensitive and reliable technique for qualitative and quantitative determination of SiOH group on solid surfaces. Fig. 1-7 shows the ^{29}Si CP/MAS NMR spectra for calcined MCM-41(A), modified MCM-41(B) and monomeric TSPP-5-M/MCM-41(C) samples. For the

calcined sample without silylation, three peaks can be observed near ¨ €00 ppm. According to Maciel et al. [25b], the low-intensity peak at -92 ppm corresponds to surface silicon atoms with two siloxane bonds and two silanol groups, i.e., geminal silanol sites, $(SiO)_2$*$Si(OH)_2$ (Q^2), which may be either single or hydrogen-bonded, and similarly the resonance at -100 ppm is attributed to surface silicon atoms with three siloxane bonds and one silanol group, i.e., isolated silanol sites, $(SiO)_3$*SiOH (Q^3), while the resonance at -110 ppm is ascribed to surface silicon atoms with four siloxane bonds, i.e., $(SiO)_4$*Si (Q^4) [21b]. For two silated samples, modified MCM-41 and monomeric TSPP-5-M/MCM-41, the intensity for Q^3 silicon resonance is significantly decreased while the Q^4 silicon resonance is substantially increased. The intensity redistributions of these silicon sites are thought to be due to the reactions of surface SiOH groups with APTES. For TSPP-5-M/MCM-41 sample, the relative intensity of Q^3 resonance slightly increases compared with modified MCM-41. The result suggests that during the mixing of TSPP and modified MCM-41 and with water solvent, some new isolated silanol sites are created on the surface walls.

In part B and C of Fig. 1-7, three additional peaks from ¨ €0 to ¨ €0 ppm correspond to three different environments for the siloxane groups in the functionalized monlayers. Similar to monolayers formed by using (methoxyl) mercaptopropylsilane (TMMPS) as the silylation reagent [17a], these three peaks are assigned as following: (a) isolated groups that are not bound to any neighboring siloxanes, (b) terminal groups that are only bound to one neighboring siloxane, and (c) cross-linked groups that are bound to two neighboring siloxanes. It is to be noted that among the three, the most dominant peak comes from cross-linked siloxane group. Comparing with the reference [17a], we

deduce that the surface coverage of functionalized monolayers on mesoporous MCM-41 is over 50%. Almost no changes in their relative intensities for modified MCM-41 and TSPP-5-M/TSPP are illustrated, indicating that the monolayers formed by silylation are very stable. Therefore, the monolayers can be used to rigidify the framework of MCM-41, in line with the XRD results. To assign the peaks corresponding to different silicon sites, the CP MAS NMR spectrum of the modified MCM-41 is used for multipeak fitting, and the fitting result is illustrated in Fig. 1-8. One finds that the peaks from fitting (both part A and B) are well assigned by the above. The schematic representation of monolayer with different conformations is shown in Fig. 1-9.

It is to be noted that all attempts to intercalate TSPP into either the calcined or modified forms of MCM-41 under basic condition were unsuccessful. We believe that unfavorable surface electrostatics prevent ion exchange in the calcined material. And we suspect that only in acidic medium, where the surface attached amino groups arising from silylation with APTES are protonated, and the interface is positively charged, is TSPP with its negatively charged sulfonato groups capable of incorporation into modified MCM-41.

Diffuse reflectance (DR) UV-vis spectra of the residues designated TSPP-5-M/MCM-41 and TSPP-5-A/MCM-41 are shown in Fig. 1-10. Also included in this figure, for comparison purposes, are transmission UV-vis spectra of TSPP in solution under pH conditions that have been shown to create either free-base or aggregated TSPP solution species.

The existence of aggregates of TSPP (i.e., the so-called J-aggregate) in homogeneous solution is indicated by the presence of a sharp J-type absorption band at 490 nm (B-band or Soret band) accompanied by a weak band at 705 nm (Q-band) [5-7,26]. The J-aggregate has been shown to be composed of protonated TSPP (i.e., dianionic $H_4^{+2}TSPP^{-4}$) as the monomeric unit, as indicated by spectral titration-type studies that reveal the growth of the aggregate band intensity at the expense of intensity of the dianion 432-nm band [5]. Additionally, based on comparison with the earlier observations with the cyanine dyes by Akins, et al., aggregation is also indicated by the enhancement of low frequency Raman bands (at 241 and 317 cm^{-1} in the case of TSPP) when resonance excitation (e.g., radiation in resonance with the 490 nm absorption) is used to excite the Raman spectrum [27,28]. In this latter regard, Raman spectra for the composite materials have also been acquired and clearly indicate the presence of either occluded monomer or aggregate. These latter studies will be discussed in chapter 2.

It has also been shown earlier by Akins, et al. that through a conflation of electronic absorption, fluorescence, fluorescence-excitation, and vibrational Raman spectra of selected homogeneous solution phase tetraaryl-substituted porphyrins (free-base and protonated), N-protonation induces structural changes that promote aggregation [6]. Foremost, the porphyrin is converted from a configuration in which the aryl moiety is twisted relative to the macrocycle plane to one in which it is nearly coplanar. It was also deduced that a basic requirement for aggregation is that the protonated species be zwitterionic [6]. Akins et al. suggested that the molecular subunits in the tetraaryl-substituted porphyrin aggregates are arranged in a cofacial fashion with a displacement between next nearest neighbors such that oppositely charged sites (positively charged

central nitrogens and negatively charged sulfonato groups) are positioned close to one another, giving rise to J-aggregate type arrangements (specifically, spread "deck-of-cards" and/or "zigzag," both corresponding to head-to-tail alignments of the transition dipole moments) [29].

Returning to Fig. 1-10, it is observed that the encapsulated free base monomer exhibits a blue shift for its Soret-region band (396 nm) when compared to the Soret band (413 nm) of the solution monomeric species. A blue shift for the absorption is also found for the encapsulated aggregate when compared to the solution aggregate: 487 nm vs. 490 nm, respectively. Such shifts can be explained in terms of intramolecular charge-transfer caused by host-guest interaction, which is connected to steric effects associated with the pore structure within modified MCM-41.

Additionally, the broad structure for the Soret-type band for TSPP-5-M/MCM-41 (in Fig. 1-10) can be interpreted as site specific absorptions for encapsulated TSPP; suggesting that the monomeric species is distributed at various positions within the cage and experience, as a result, a range of perturbations. By the same argument, the similarity between the spectrum of TSPP-5-A/MCM-41 and solution phase aggregate, both in terms of band positions and widths, can be interpreted as indicating that upon formation of the aggregate the molecules are coupled and realigned such that site specific perturbations to the exciton absorption energy, line width, and possibly other properties are diminished. Molecular structure calculations will be conducted in the future to shed light on these issues.

To obtain maximum monomeric TSPP occluded into channels of modified MCM-41, it is necessary to allow the mixture of monomeric TSPP, modified MCM-41 and water to equilibrate under stirring. The effect of time on absorption spectrum of the mixture consisting of 30 mg of TSPP and 300 mg of modified MCM-41 is shown in Fig. 1-11. one observes that after 18 hrs, there was a large amount of aggregated TSPP at external surface of modified MCM-41. With the increasing of stirring time, more TSPP at the external surface diffuses into the channels and are attached to the active sites by strong electrostatic interaction through ¨ SO^{3-} groups and ¨ NH_3^+. The attached TSPP inside the channels is formed at the expense of aggregated or monomeric TSPP at the external surface and was in the form of monomeric species at ca. pH = 5. Therefore, as illustrated in Fig. 1-11, aggregate TSPP greatly decreased after 23 hr and finally disappeared after 89 hrs. The incorporation of monomeric species inside the channels is also demonstrated by the blue shifts of free-base form caused by the host-guest interaction: 412 vs 410 vs 408 vs 408 nm for mixing time of 18, 23, 41 and 89 hrs, respectively.

The composites with different ratios of TSPP over modified MCM-41 were prepared and their monomeric and aggregated diffusion reflectance UV-vis spectra are illustrated in Fig. 1-12 and Fig. 1-13, respectively. For all monomeric composites, more dramatic blue shifts for low-loading TSPP/MCM-41 composites are observed because of stronger interaction between negative SO^{3-} groups and greater abundance of active sites provided by ¨ NH_3^+ (Fig. 1-12). In our study, the blue shift is in the range from 402 nm (TSPP-30-M/MCM-41) to 392 nm (TSPP-2.5-M/MCM-41). The J-aggregate absorption for all aggregated composites is at 486 to 488 nm (Fig. 1-13), indicating that the J-aggregated TSPP formed within the core of modified MCM-41 is more integrated, thus less blue

shift is observed, compared with monomeric composites. It is to be noted that for both monomeric and aggregated composites, the Soret bands are broadened with the increase of amount TSPP loaded, which can be explained by the same argument above, i.e., a wider range of perturbations for more amount of TSPP occluded.

Fluorescence spectra for solution phase and composite systems were also acquired (see Fig. 1-14). As shown in Fig. 1-14, parts A and B, which were acquired with excitation at 410 nm, the Q-band emission from monomeric TSPP in solution and the composite TSPP-M/MCM-41 are essentially identical, except for the small shift between emission peaks, indicating that the monomer chromophore is the emitting species in the composite. One finds in this case two emission peaks, Q(0,0) and Q(0,1), which are essentially the mirror images of their respective absorption bands (see Fig. 1-13) at Q(0,0) and Q(1,0) [6].

In the case of aggregated TSPP in solution and the composite TSPP-5-A/MCM-41, the fluorescence spectra excited at 490 nm, are shown in parts C and D of Fig. 1-14, respectively. One emission band at ca. 715 nm is observed for each sample, which is exactly what is to be expected for mirror emission associated with the corresponding absorption shown in Fig. 1-10.

The decay curves and time-resolved fluorescence spectra foraggregated TSPP within both modified MCM-41 and in solution have been measured. Fig. 1-15, Fig. 1-16 and Fig. 1-17 show, respectively, decay curves for aggregated TSPP in MCM-41 and solution; time-resolved fluorescence of TSPP in solution and time-resolved fluorescence of TSPP in MCM-41.

For laser excitation at 488 nm, the emission decay envelopes for both aggregated TSPP-5-A/MCM-41 composite and solution aggregate are similar (see Fig. 1-15). The fluorescence decays follow single exponential law with lifetimes, τ_0, of ca. 179 and 151 ps, respectively, for TSPP-5-A/MCM-41 and solution aggregate, in good accord with aggregated porphyrins reported earlier [30]. The result suggests the similar exciton emission behaviors for both samples, thus the aggregate formed within the MCM-41 is more integrated, in line with the absorption results above, which showed less shifts of aggregate absorption.

From the time-resolved emission spectra (Fig. 1-16 and Fig. 1-17), the broader emission bands for TSPP-5-A/MCM-41, compared with those of aggregated solution. It demonstrates that there exists more microenvironment purturbation to the formed aggregate within solid sample because of heterogeneous effect, than that to the aggregate in homogeneous solution.

The combination of studies above clearly indicates that we have formed aggregated TSPP dianion within the pore of our modified MCM-41. It is also of note that we have been able to load as much as 10% by weight of TSPP into the mesoporous material, undoubtedly because of the large internal surface area of the mesoporous material, which is one of its intrinsic properties.

Two possible TSPP J-aggregates are shown in Fig. 1-18. These are designated, as mentioned earlier, the zigzag (labeled **A** in Fig. 1-18) and "spread-deck-of-cards" (labeled **B** in Fig. 1-18) conformations. Such aggregates, presumably, would form along the 1-dimensional cylindrical channels of the modified MCM-41 aluminosilicate.

1.4 Conclusions

Our studies lead us to the following conclusions:

1. Surface silylation, using an alkoxysilane reagent, which thickens and functionalizes the walls of the aluminosilicate, facilitates the formation incorporated J-aggregated TSPP by maintaining the integrity of the walls.

2. CP MAS ^{29}Si NMR measurements show that for modified MCM-41 and TSPP-5-M/MCM-41 a large peak attributable to the aluminosilicate support occurs. Three additional peaks from the functionalized monolayer are identified, i.e., isolated groups, terminal groups and cross-linked groups, which are formed at the expense of surface geminal silanol sites, $(SiO)_2*Si(OH)_2$ (Q^2), and isolated silanol sites, $(SiO)_3*SiOH$ (Q^3).

3. The conflation of XRD, UV-vis absorption, fluorescence measurements for TSPP in solution and post-formation addition to an MCM-41 aluminosilicate results in the selective formation of either monomeric or aggregated TSPP occluded in the core.

4. Spectral properties of the occluded aggregate indicate that formation of the aggregate within MCM-41 increases the isolation of constituent monomers from site specific interactions that cause the broadening of spectral features, and shortens the fluorescence lifetime as well.

Bibliography

[1] Okamura, M. Y.; Feher, G.; Nelson, N. In *Photosynthesis*, Govindjee, Ed.; Academic Press: New York, **1982**, pp. 195-272.

[2] Pearlstein, R. M. In *Photosynthesis*, Amesz, J., Ed.; Elsevier: Amsterdam, **1987**, pp 299-317.

[3] O'Neil, M. P.; Niemcyzk, M. P.; Svec, W. A.; Gosztola, D.; Gaines III, G. L.; Wasielewski, M. R. *Science* **1992**, *257*, 63.

[4] Wagner, R. W.; Lindsey, J. S.; Seth, J.; Palaniappan, V.; Bocian, D. F. *J. Am. Chem. Soc.* **1996**, *118*, 3996.

[5] Akins, D. L.; Zhu, H.-R.; Guo, C. *J. Phys. Chem.* **1994**, *98*, 3612.

[6] Akins, D. L.; Zhu, H.-R.; Guo, C. *J. Phys. Chem.* **1996**, *100*, 5420.

[7] Akins, D. L. In *J-Aggregate*; Kobayashi, T., Ed.; World Scientific: Singapore, 1996, pp 67- 94.

[8] Guo, C.; Ren, B.; Akins, D. L. *J. Phys. Chem. B.* **1998**, *102*, 8751.

[9] Guo, C.; Ren, B.; Akins, D. L. *J. Phys. Chem.* In revision, **2000**.

[10] Beck, J. S.; Vartuli, J. C.; Roth, W. J.; Leonowicz, M. E.; Kresge, C. T.; Schmitt, K. D.; Chu, C. T.-W.; Olsen, D. H.; Sheppard, E. W.; McCullen, B.; Higgins, J. B.; Schlenker, J. L. *J. Am. Chem. Soc.* **1992**, *114*, 10834.

[11] Grad, J.; Hernandez, G.; Mukamel, S. *Phys. Rev. A.* **1988**, *37*, 3835.

[12] Spano, F. C.; Mukamel, S. *J. Chem. Phys.* **1989**, *91*, 683.

[13] Spano, F. C.; Kuklinski, J. R.; Mukamel, S. *J. Chem. Phys.* **1991**, *94*, 7534.

[14] Kresge, C. T.; Leonowicz, M. E.; Roth, W. J.; Vartuli, J. C.; Beck, J. S. *Nature* **1992**, *359*, 710.[15] Liu, C. -J.; Li, S. -G.; Pang, W. -Q.; Che, C. -M. *Chem. Commun.*, **1997**, *65*, 78.

[16] Mercier, L.; Pinnavaia, T. J. *Adv. Mater.* **1997**, *9*, 500.

[17] (a) Feng, X.; Fryxell, G. E.; Wang, L. Q.; Kim, A. Y.; Liu, J.; Kemner, K. M. *Science* **1997**, *276*, 923. (b) Liu, J.; Feng, X.; Fryxell, G. E.; Wang, L. Q.; Kim, A. Y.; Gong, M. *Adv. Mater.* **1998**, *10*, 161.

[18] (a) Cauvel, A.; Renard, G.; Brunel, D. *J. Org. Chem.* **1997**, *62*, 749. (b) Brunel, D.; Cauvel, A.; Fajula, F.; DiRenzo, F. *Stud. Surf. Sci. Catal.* **1995**, *97*, 173.

[19] Sutra, P.; Brunel, D. *Chem. Commun.* **1996,** 2485.

[20] Bellocq, N.; Brunel, D.; Lasperas, M.; Moreau, P. *Stud. Surf. Sci. Catal.* **1997**, *108*, 485.

[21] (a) Subba Rao, Y. V.; De Vos, D. E.; Bein, T.; Jacobs, P. A. *Chem. Commun.* **1997**, 355. (b) Subba Rao, Y. V.; De Vos, D. E.; Jacobs, P. A. *Angew. Chem., Int. Ed. Engl.* **1997**, *36*, 2661.

[22] Diaz, J. F.; Balkus, K. J., Jr.; Bedioui, F.; Kurshev, V.; Kevan, L. *Chem. Mater.* **1997**, *9*, 61.

[23] Barrett, E. P.;Joyner, L. G.; Halenda, P. P. *J. Am. Chem. Soc.* **1951,** *73*, 373.

[24] (a) Sung-Suh, Hyung Mi; Luan, Z.; Kevan, L. *J. Phys. Chem. B.*, **1997**, *101*, 10455. (b) Stucky, G. D.; Monnier, A.; Schuth, F.; Huo, Q.; Margolese, D.; Kumar, D.; Kridhnamurty, M.; Petroff, P.; Firouzi, A.; Janicke, M.; Chmelka, B. F. *Mol. Cryst. Liq. Cryst.*, **1994**, *240*, 187.

[25] (a) Sindorf, D.W.; Macier, G.E. *J Am. Chem. Soc.* **1983**, *105*, 3769. (b) Sindorf, D. W.; Maciel, G. E. *J. Am. Chem. Soc.* **1981**, *103*, 4263.

[26] (a) Akins, D. L.; Özçelik, S.; Zhu, H. -R.; Guo, C. *J. Phys. Chem.* **1996**, *100*, 14396. (b) Ohno, O.; Kaizu, Y.; Kobayashi, H. *J. Chem. Phys.*, **1993**, *99*, 4128.

[27] Akins, D. L. *J. Phys. Chem.* **1986**, *90*,1530.

[28] Akins, D. L.; Akpabli, C. K.; Li, X. *J. Phys. Chem.* **1989**, *93*, 1977.

[29] Kasha, M. *Radiat. Res.* **1963**, *20*, 55.

[30] Khairutdinov, R. F.; Serpone, N. *J. Phys. Chem. B* **1999**, *103*, 761.

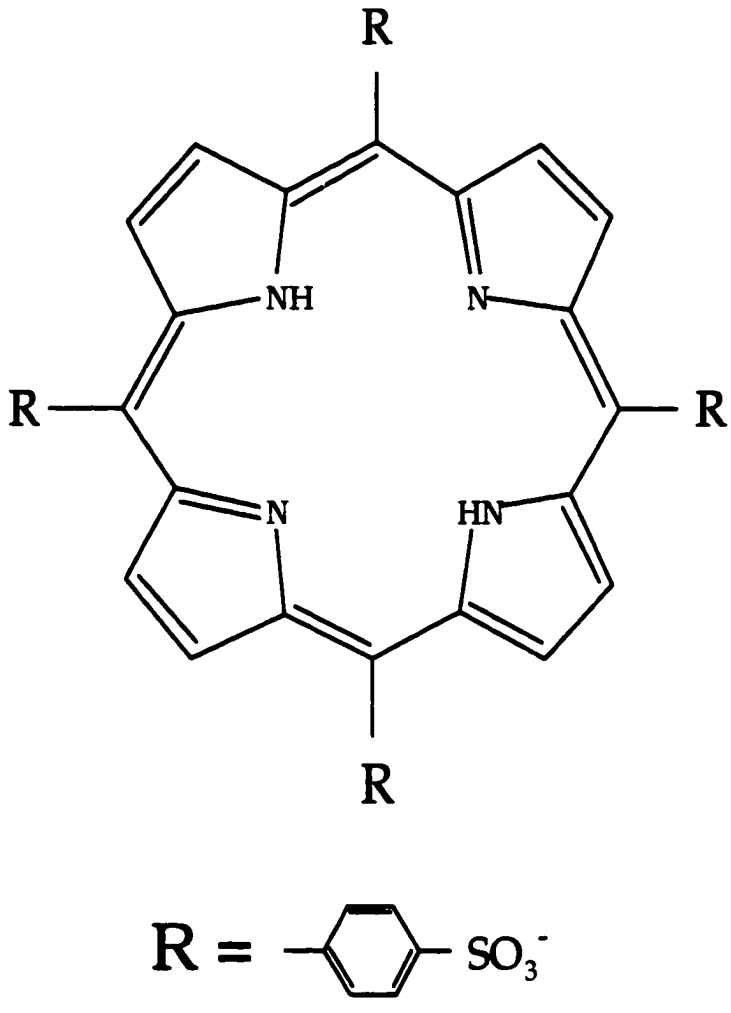

Fig. 1-1

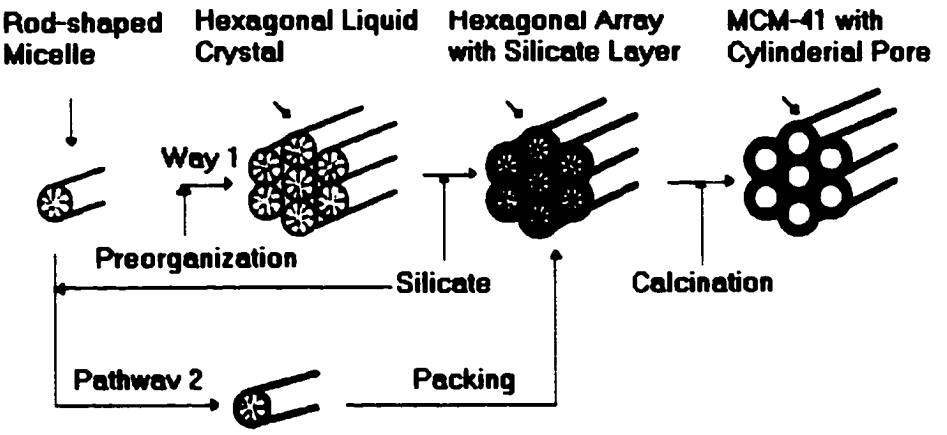

Fig. 1-2

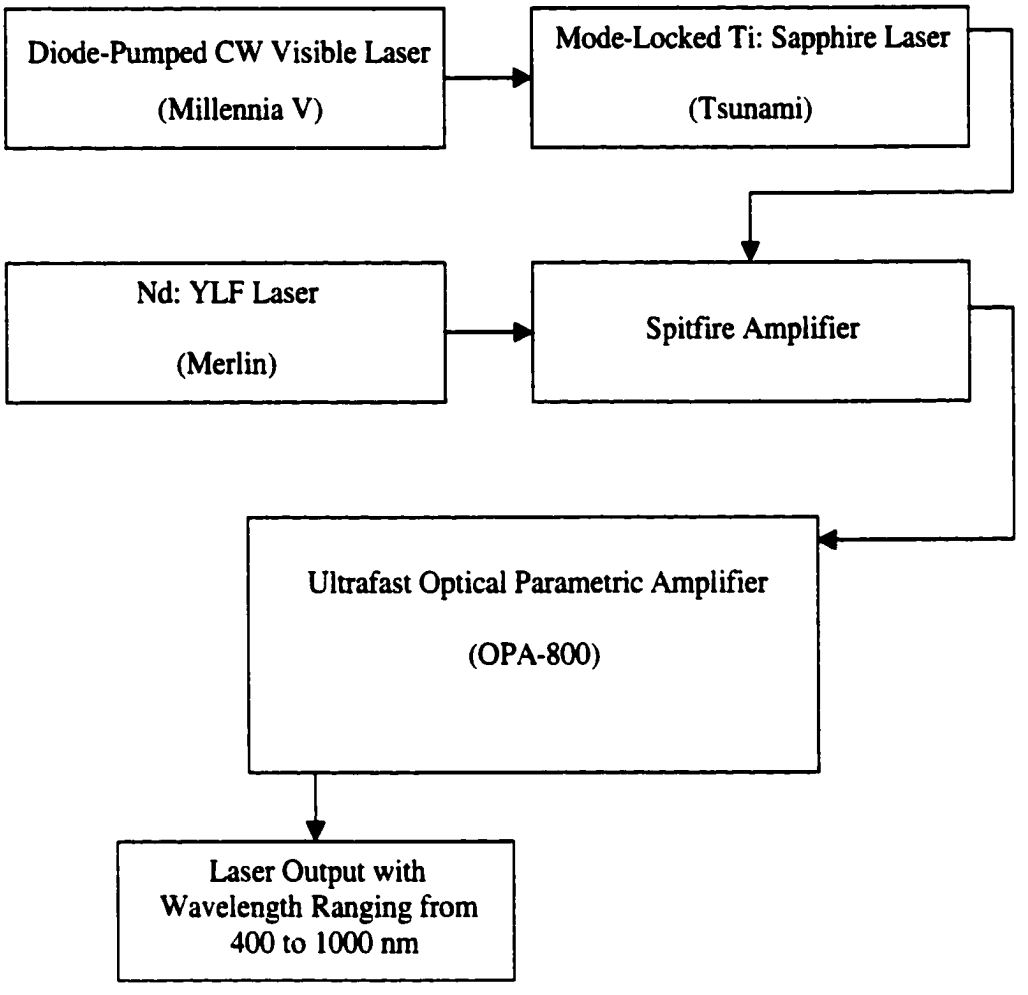

Diagram 1-i

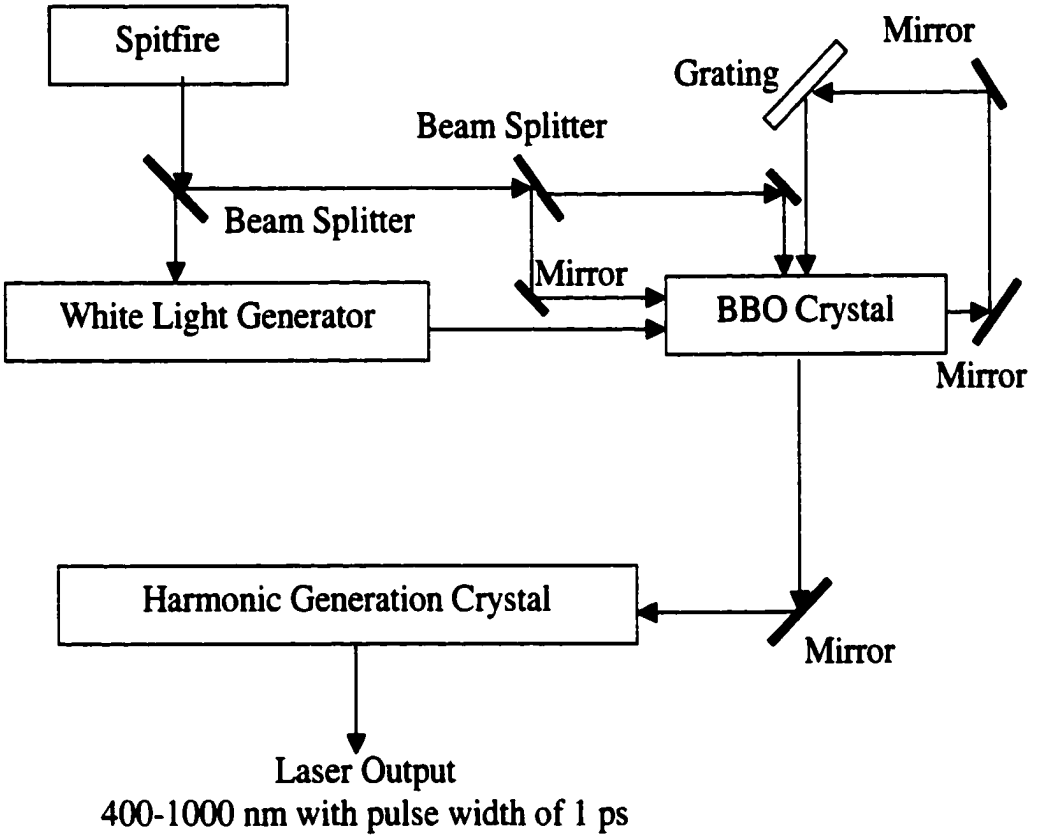

Diagram 1-2

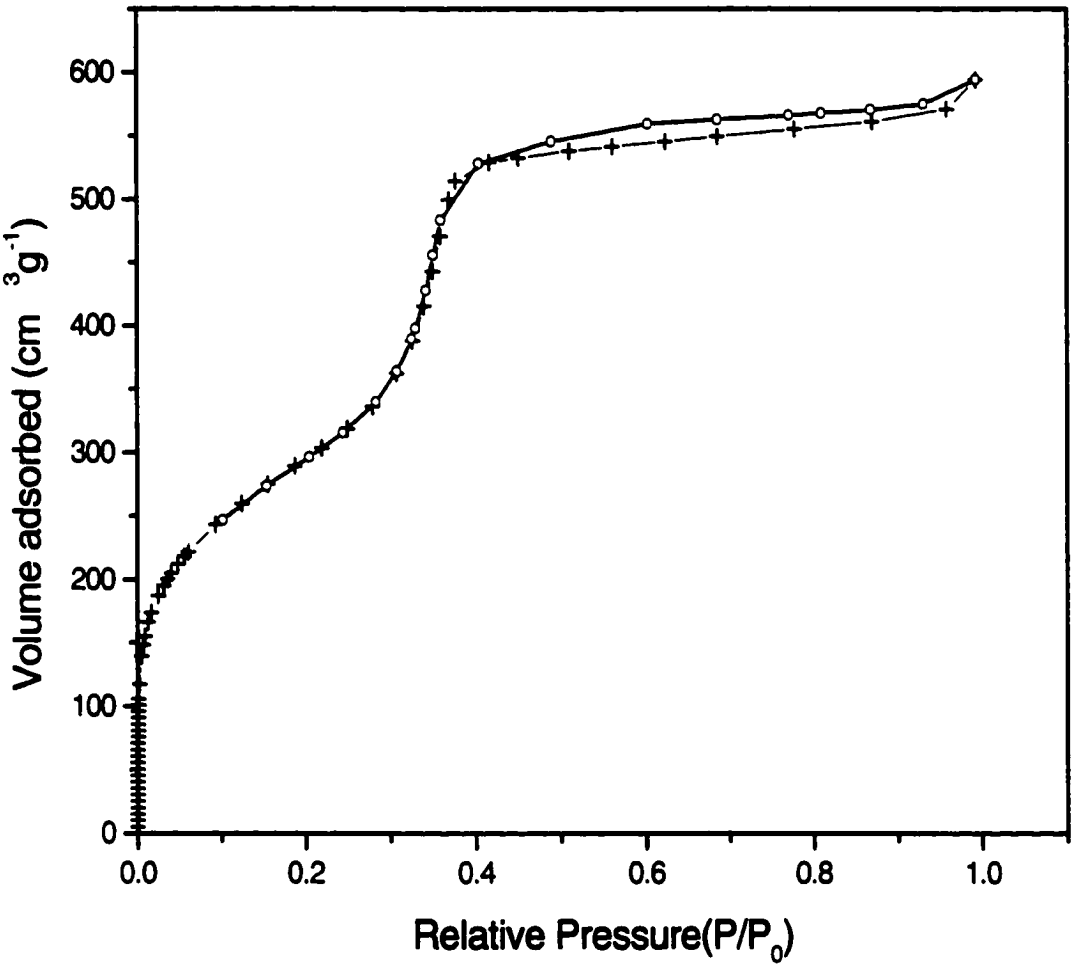

Fig. 1-3

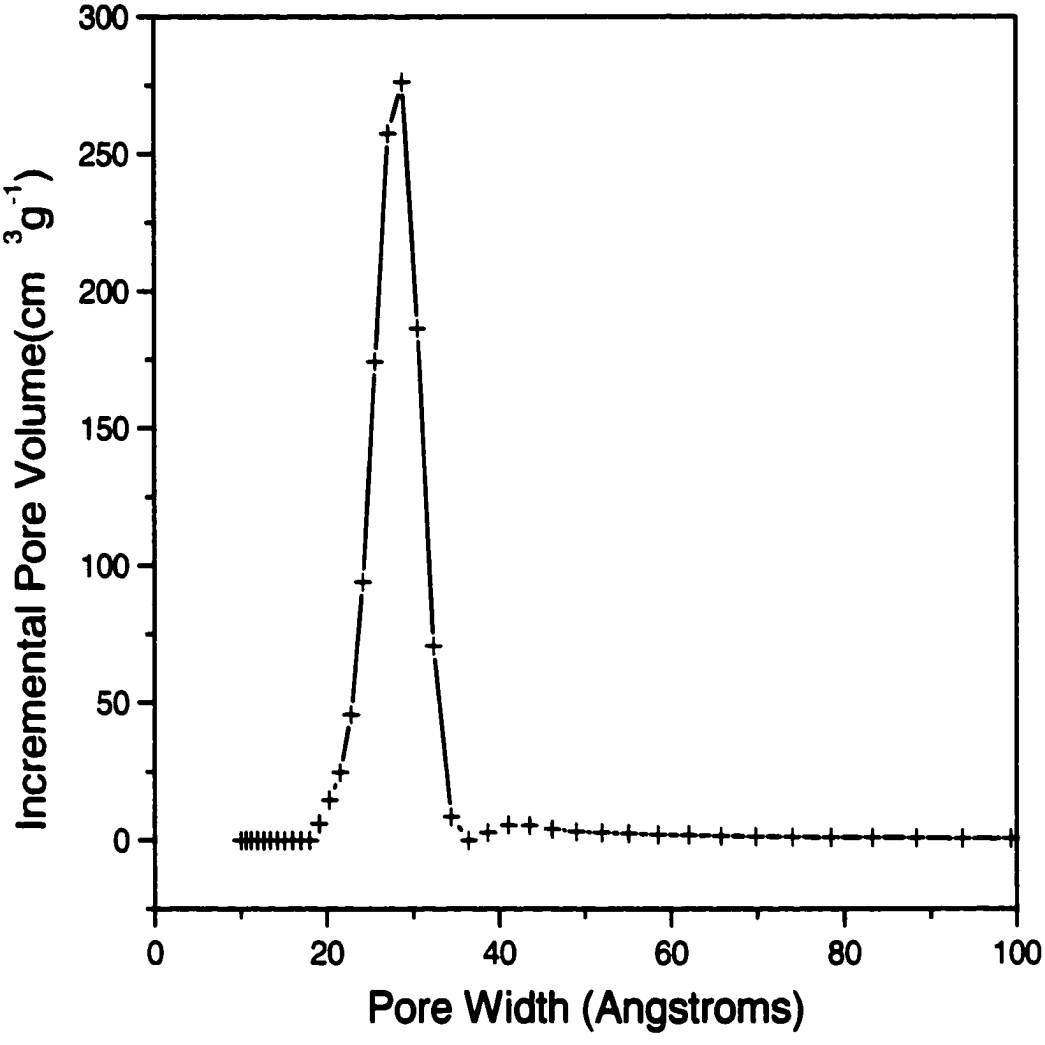

Fig. 1-4

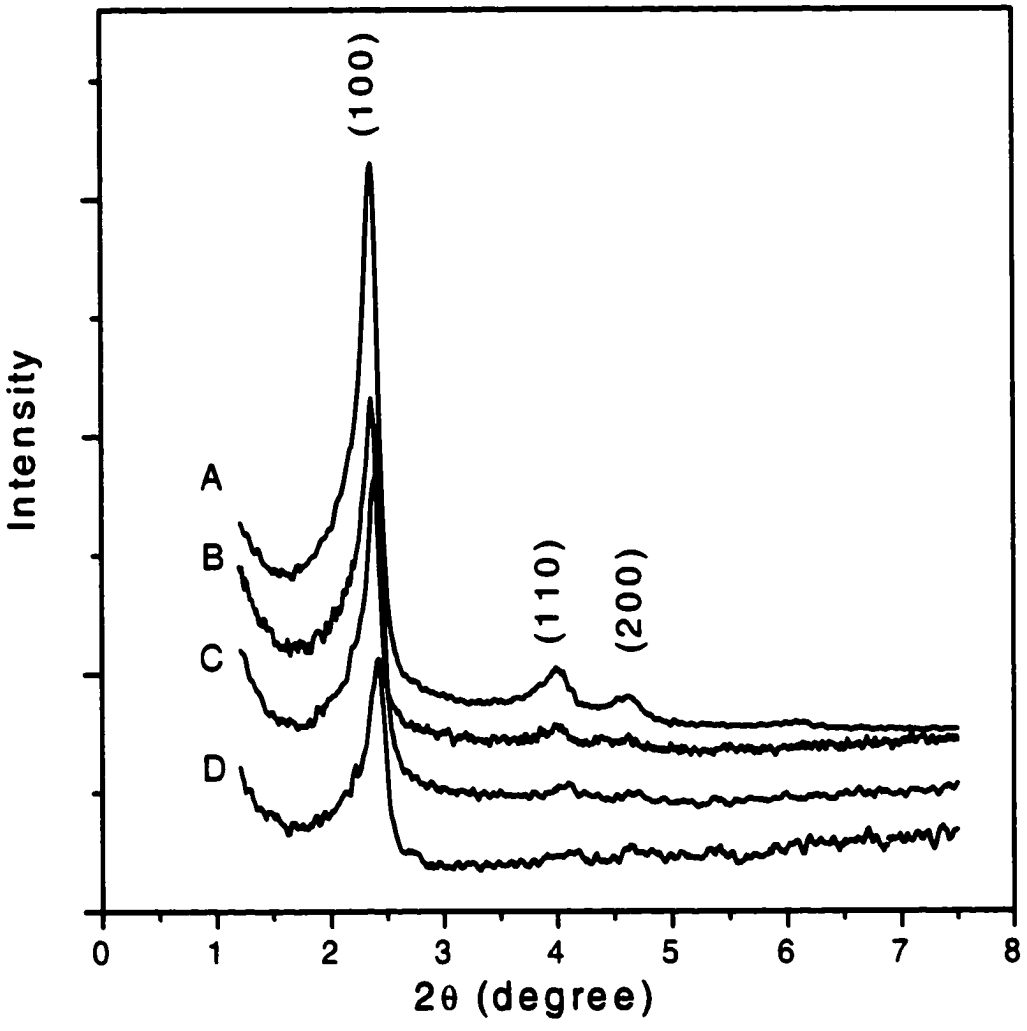

Fig. 1-5

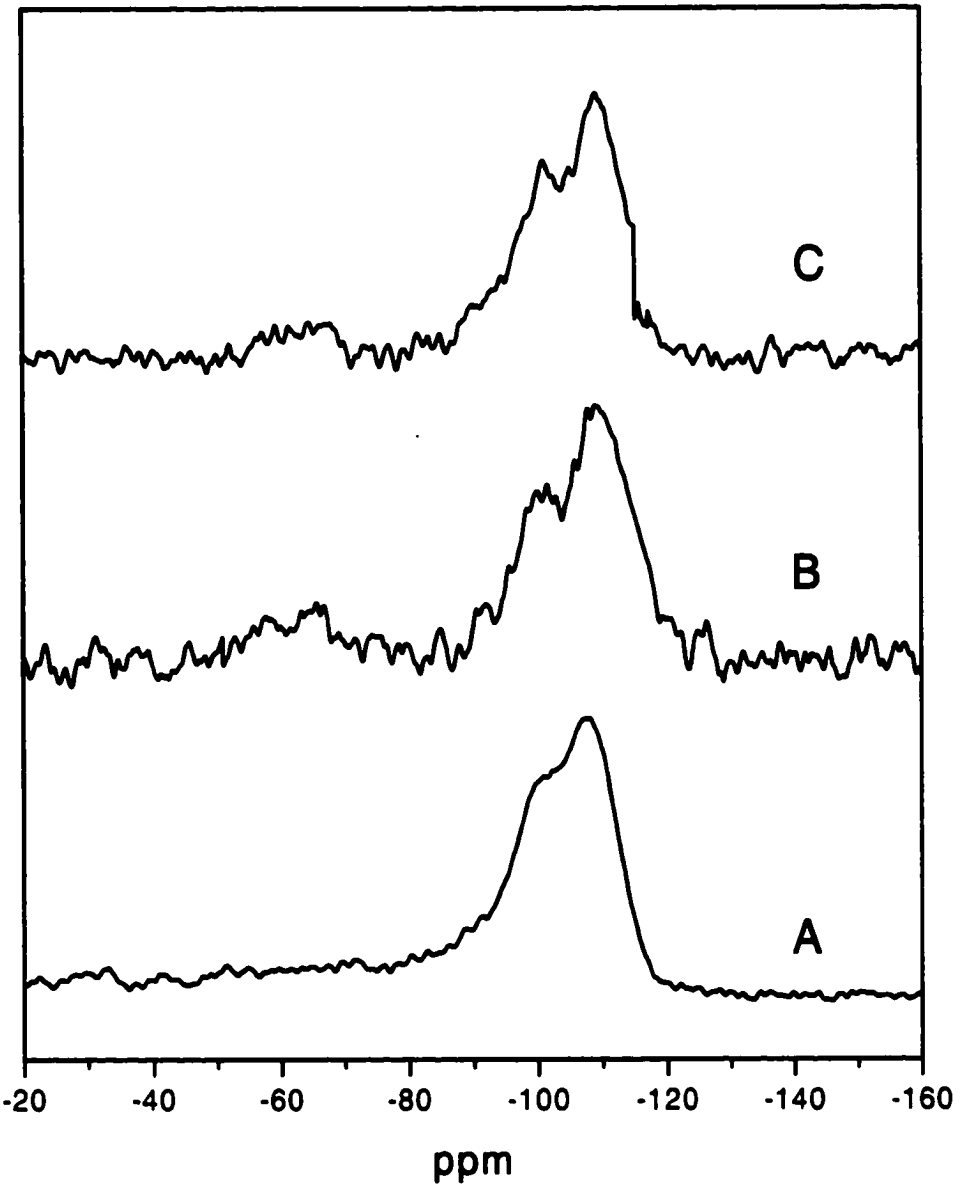

Fig. 1-6

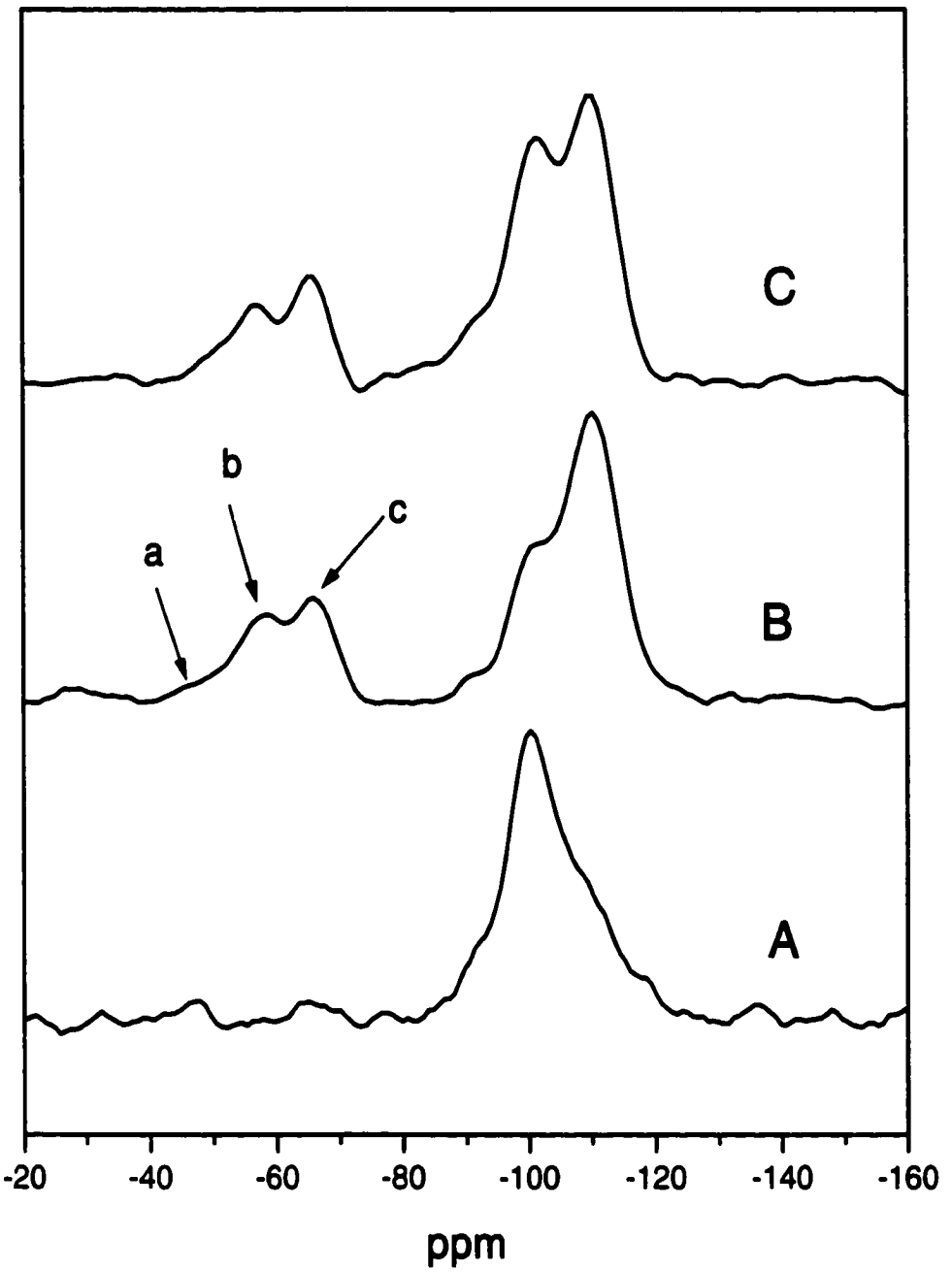

Fig. 1-7

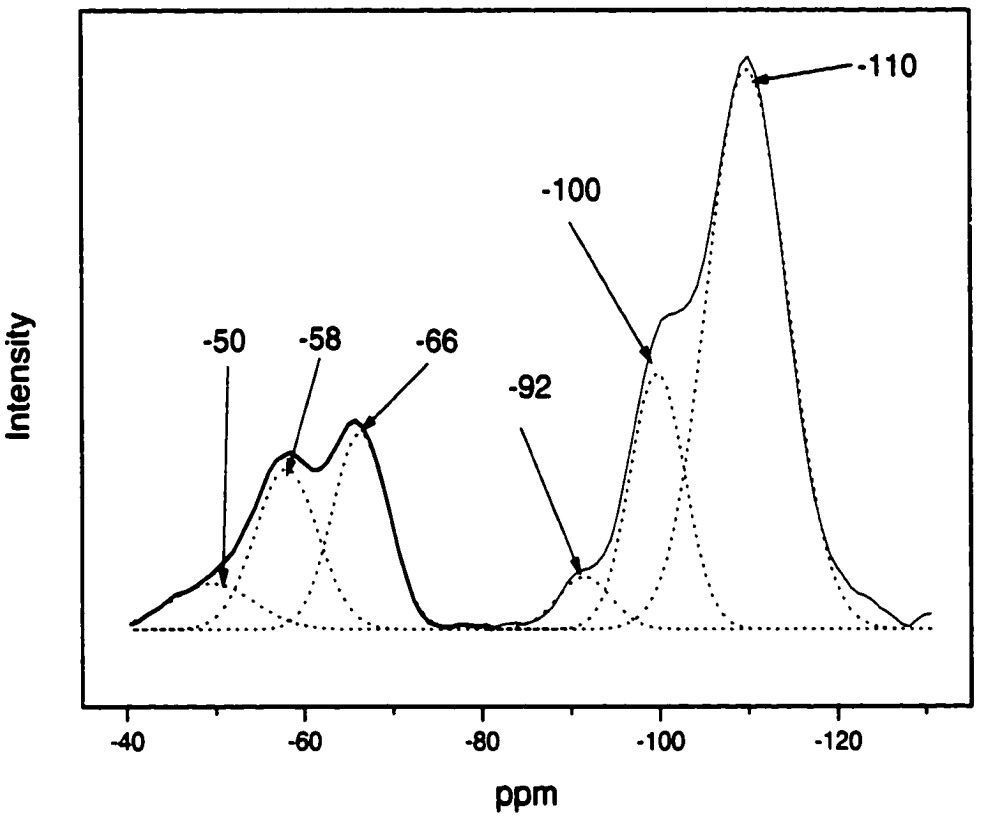

Fig. 1-8

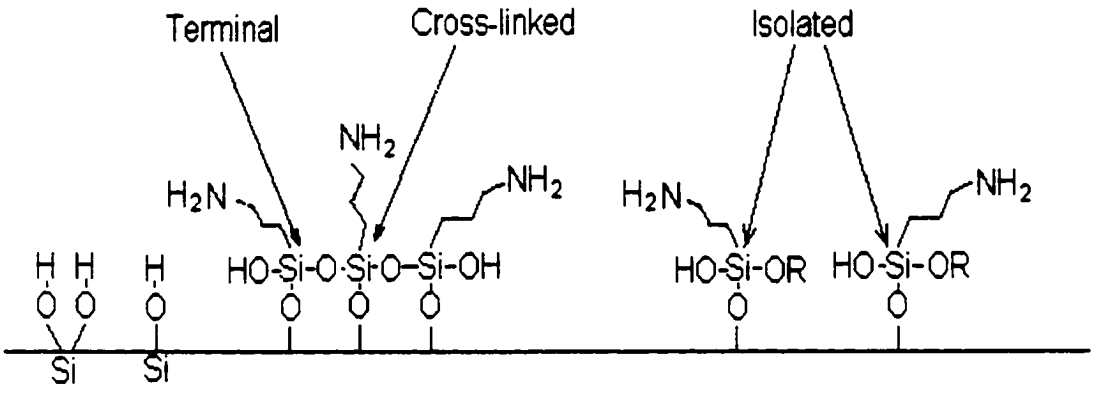

Fig. 1-9

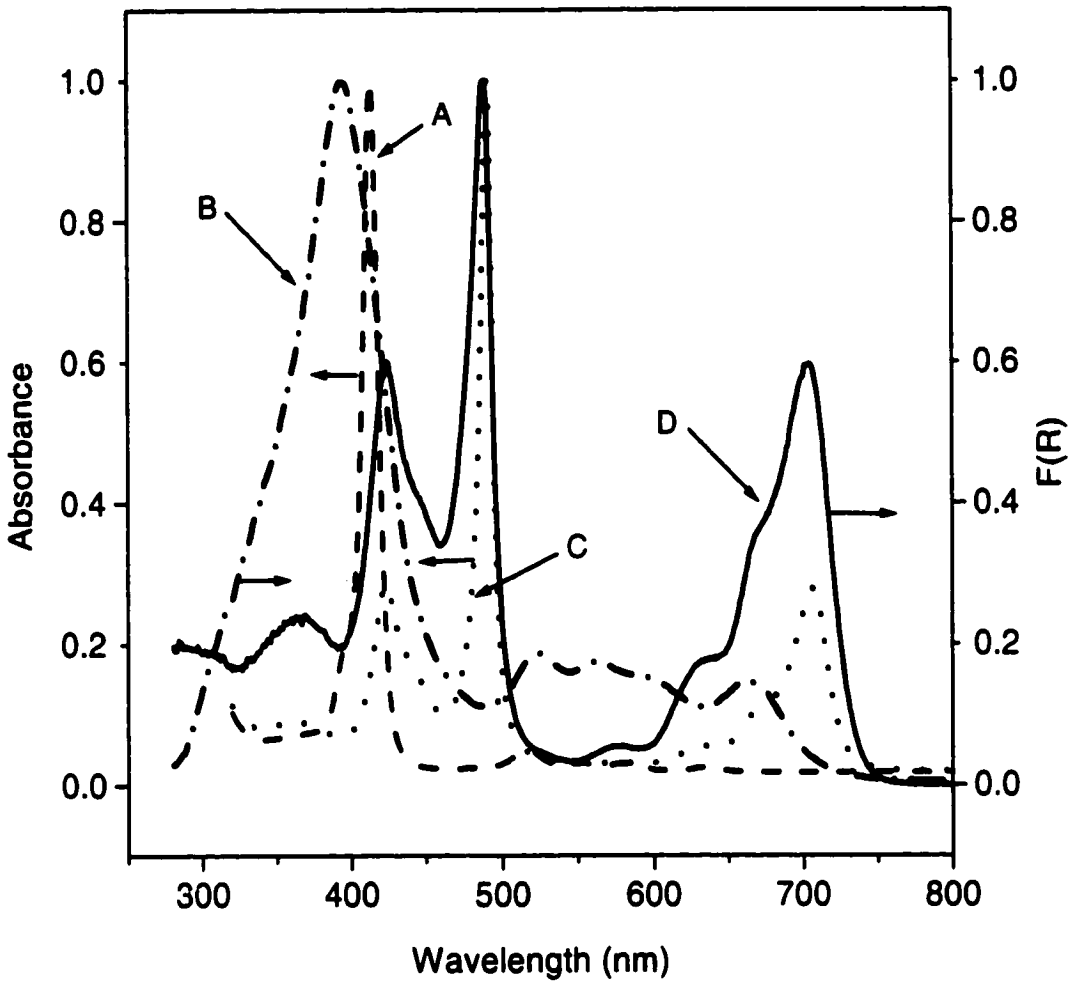

Fig. 1-10

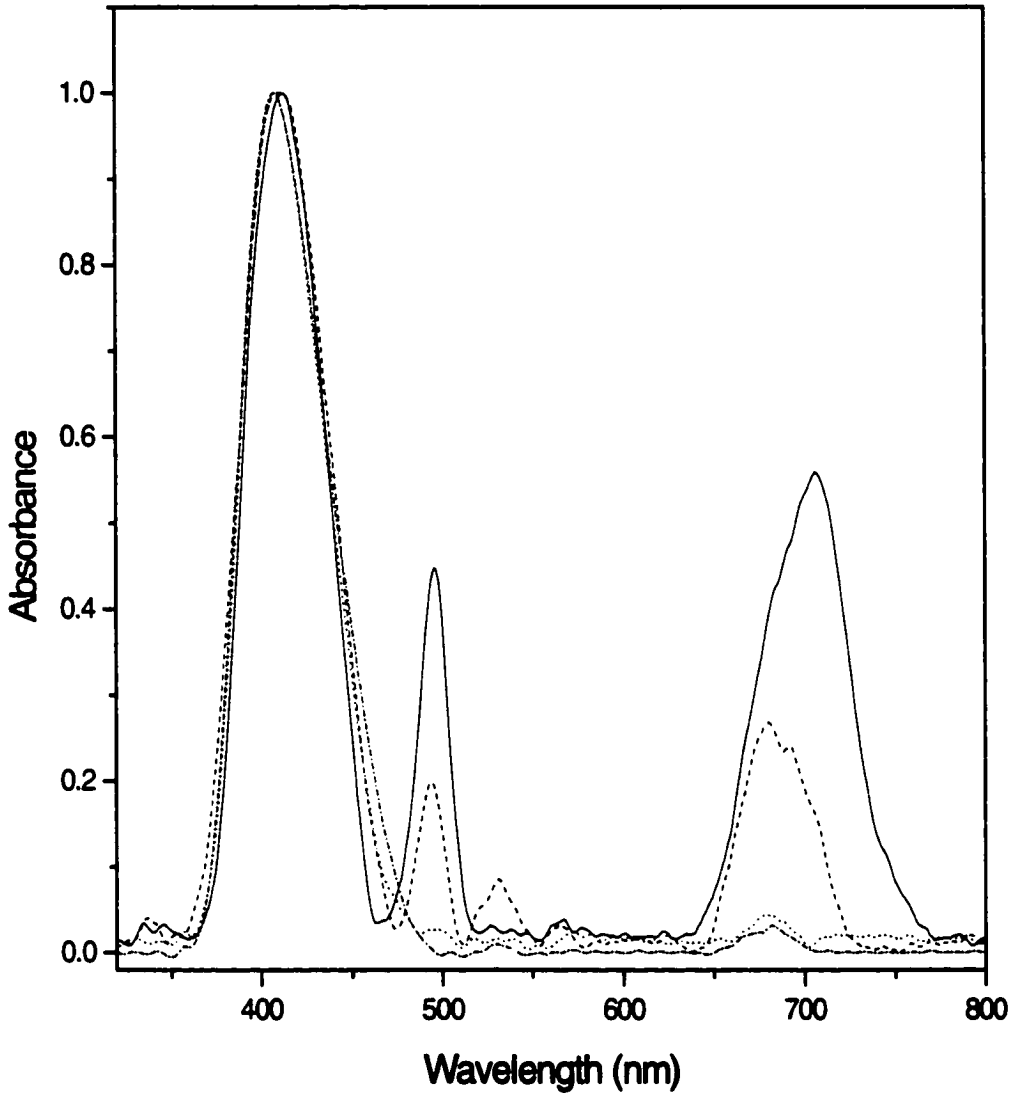

Fig. 1-11

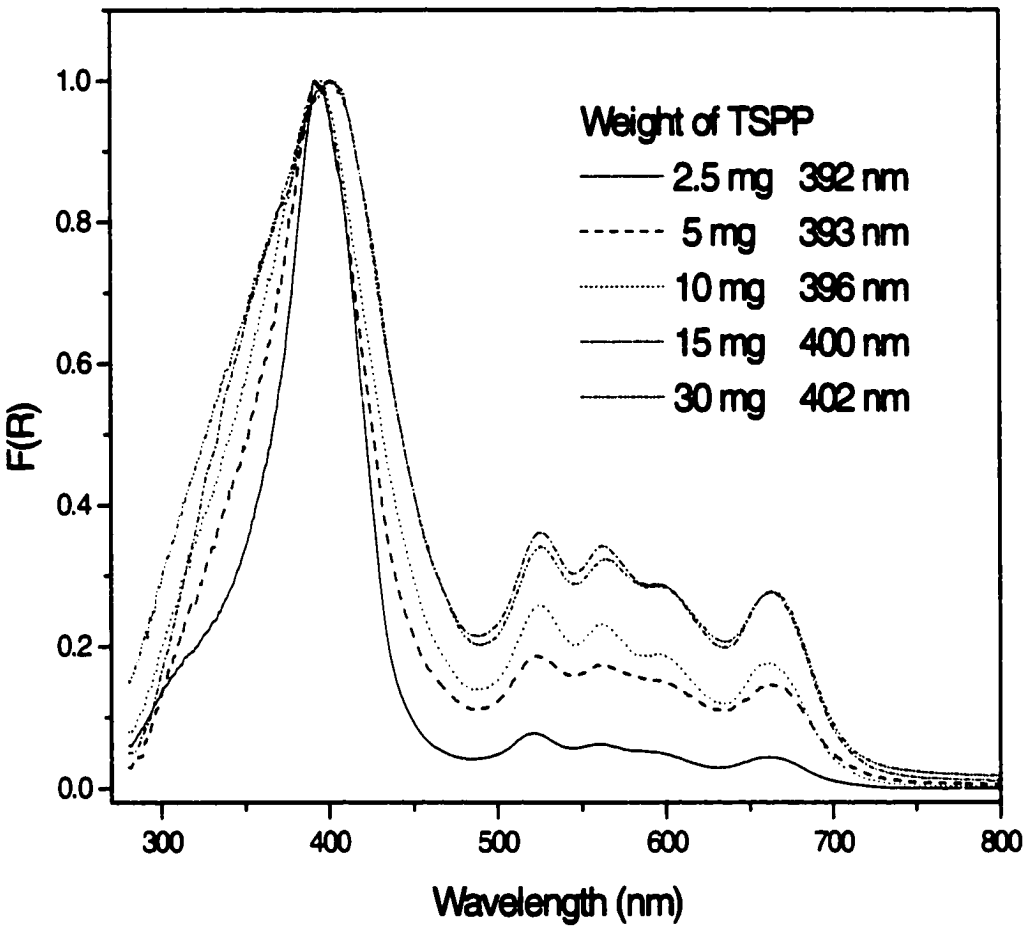

Fig. 1-12

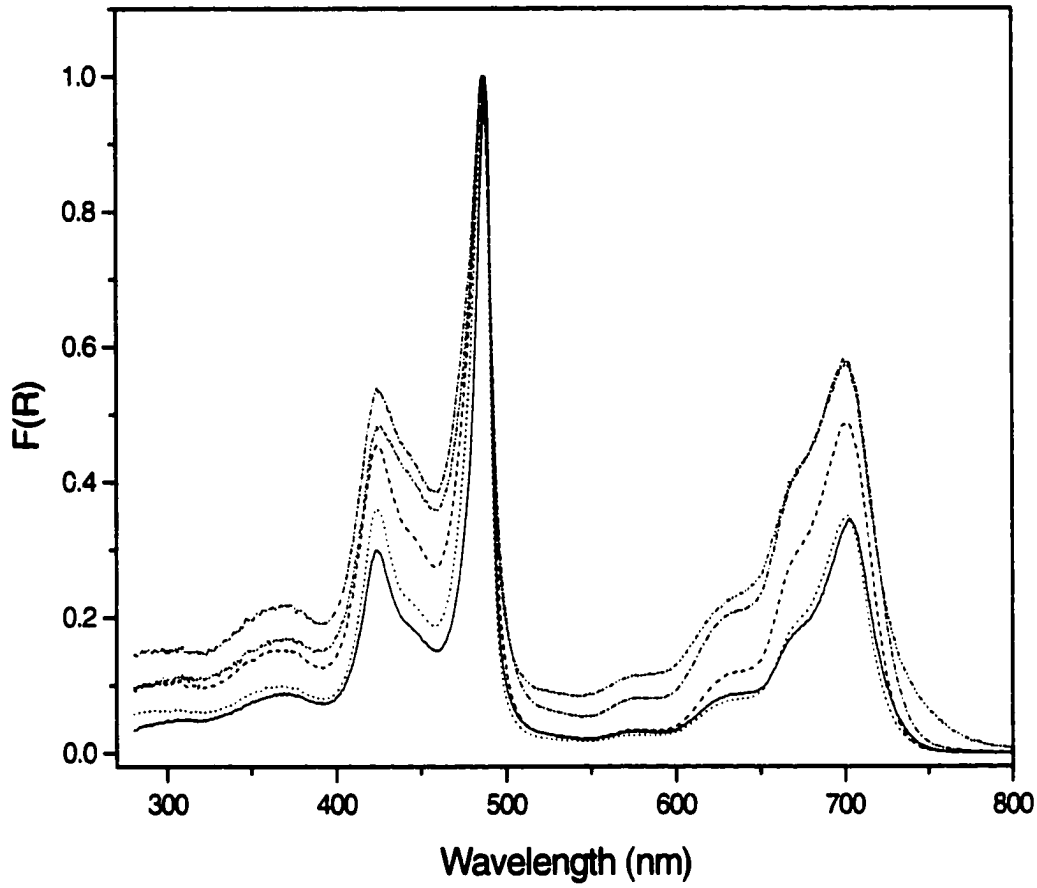

Fig. 1-13

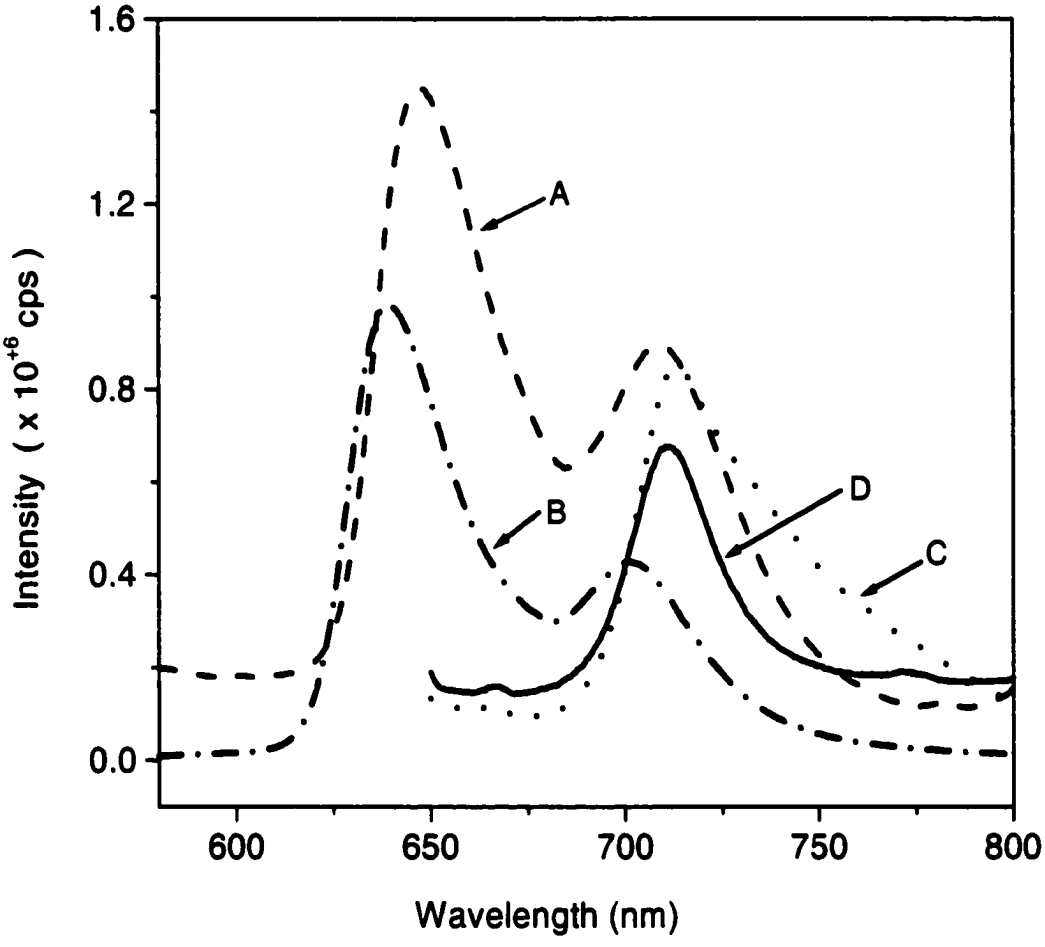

Fig. 1-14

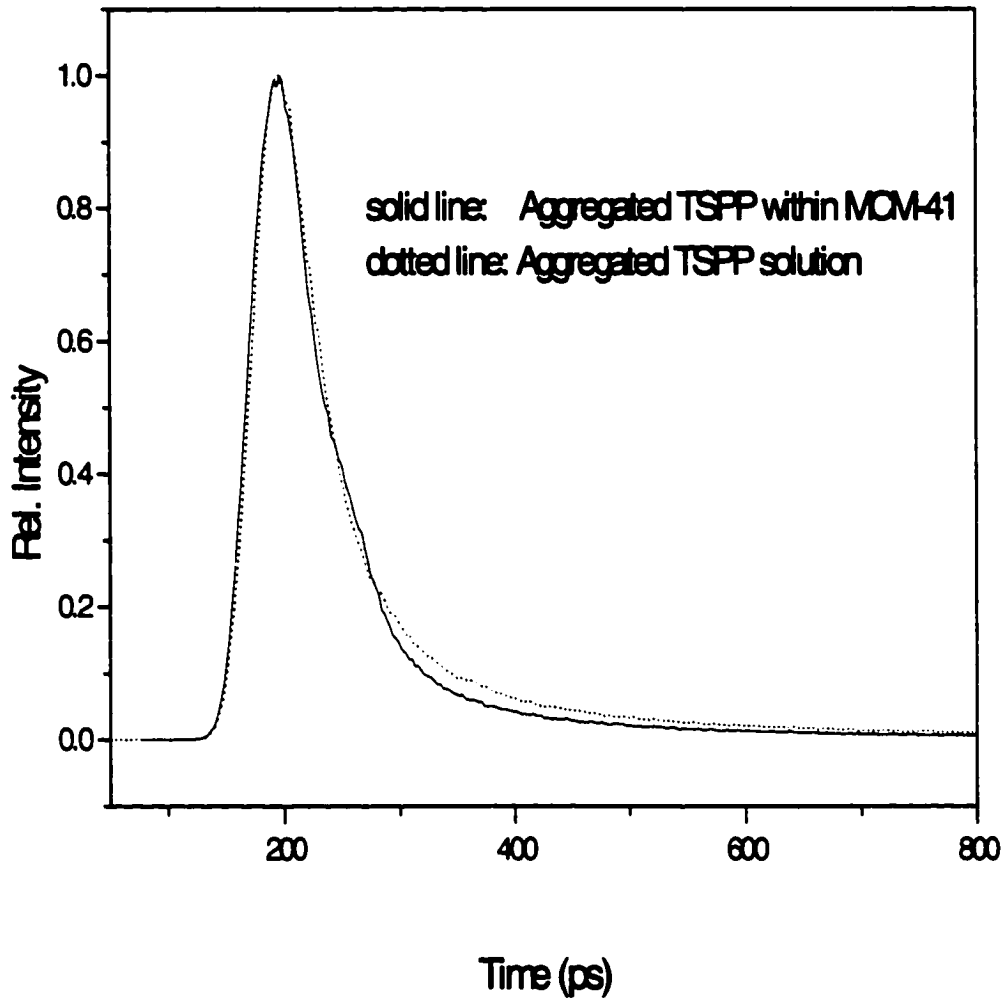

Fig. 1-15

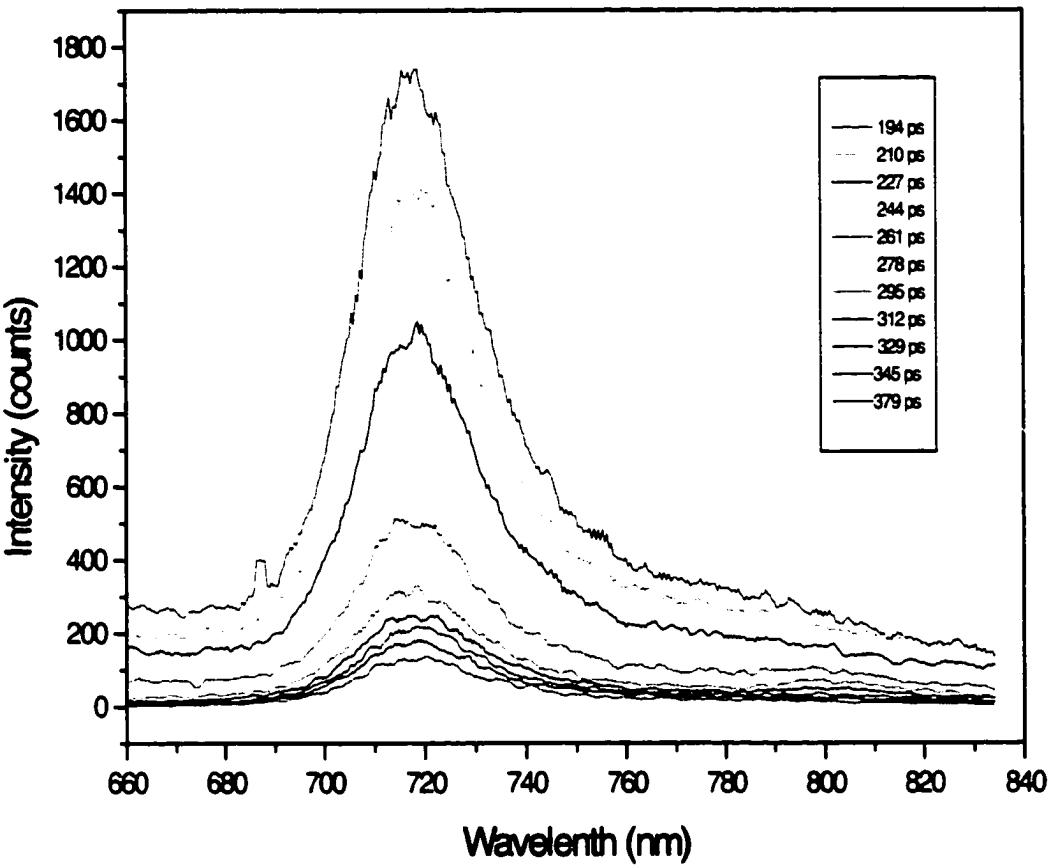

Fig. 1-16

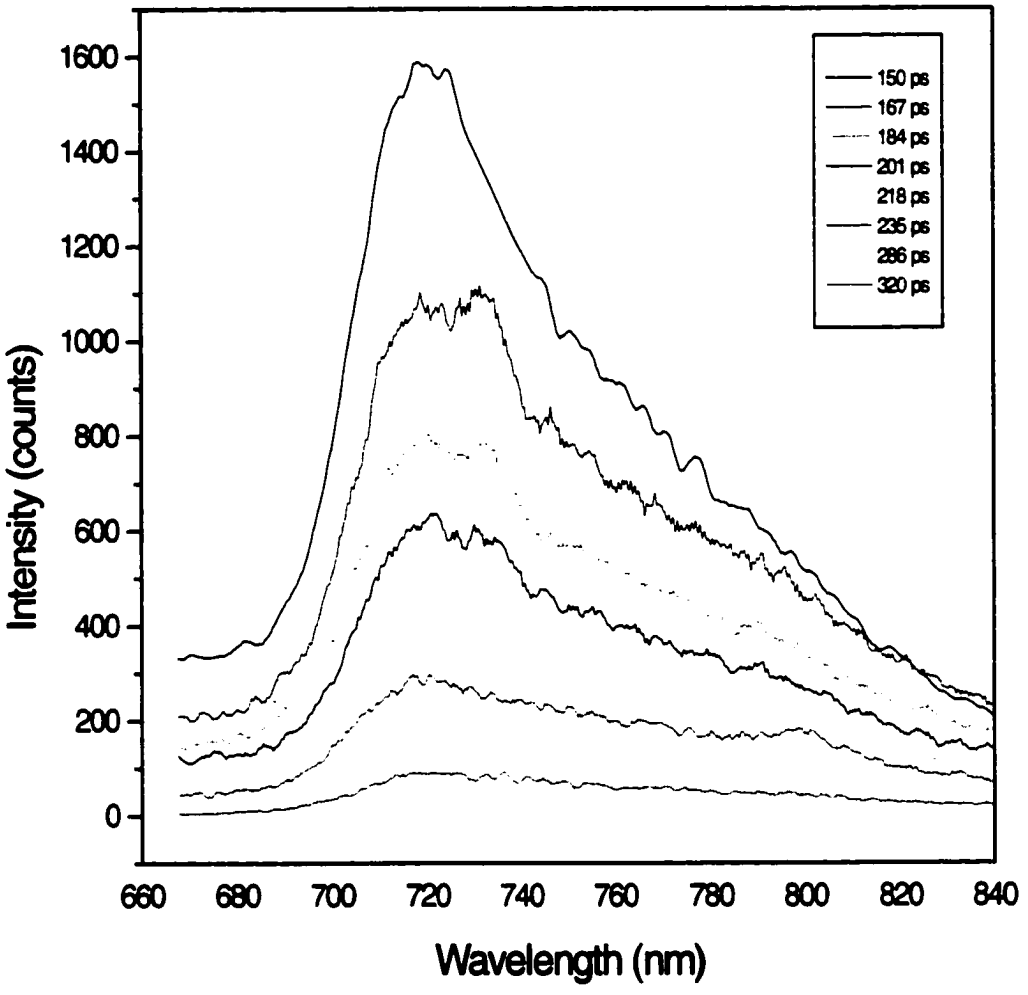

Fig. 1-17

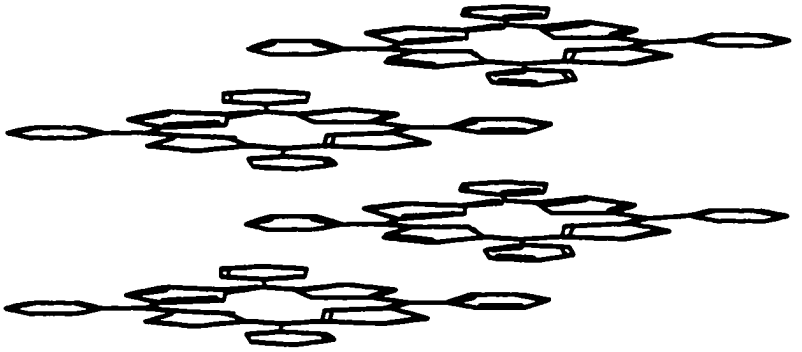

A

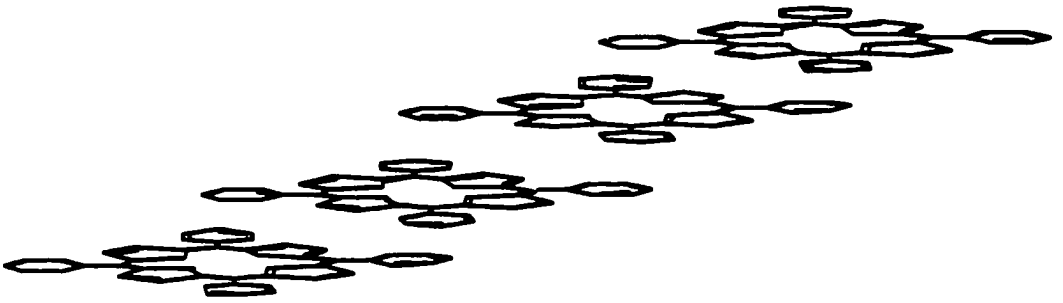

B

Fig. 1-18

CHAPTER 2

SPECTROSCOPIC COMPARISON OF TETRAKIS(*P*-SULFONATOPHENYL)PORPHYRIN FORMED WITHIN MODIFIED MCM-41 AND IN THE PRESENCE OF AN IONIC VESICLE

2.1 Introduction

Many research efforts in self-assembling processes of molecular components into large supramolecular structures have been carried out greatly because of their involvement in many fundamental physicochemical as well as biological processes. The possibility of changing the mesoporous structurof the resultant species through a proper choice of the molecular components and matrixes provides the methods to the design and synthesis of materials capable of exhibiting specific properties and functions [**1-3**]. Many molecules with large conjugated system are well suited building blocks for self-assembling [4].

Molecules that are widely investigated because they can be easily induced to aggregate include dyes such as the cyanines [6-17] and the xanthenes [18-20], some polycyclic aromatics [21-26], as well as several synthetic porphyrins [27-34]. These molecules have been found to form J- and/or H-aggregates in homogeneous solution, on surfaces (such as on electrodes and colloidal particles), as well as on interfaces of artificial bilayers and native membranes, through noncovalent interactions.

Beyond attempts to just understand how molecular aggregates are formed and how they function, are several efforts aimed at exploiting their sometimes-unique properties. And, in fact, molecular aggregate structures find important current technological applications. For example, aggregates formed of molecular dyes have been used as spectral sensitizers (especially for silver halide semiconductor materials) [35]; as organic photoconductors [36]; as optical probes in biological and synthetic membrane systems [37]; as photopolymerization initiators [38]; and, because of their enhanced nonlinear optical susceptibilities [39,40], as materials for use in nonlinear optical devices [41-43]. Many relevant physicochemical properties of this class of compounds, including spectroscopic and photophysical features, are strictly dependent on their aggregation state. Aggregates involving porphyrins, which historically have served as model structures for gaining insight into the roles that optically induced transient structural changes and photon dynamics play in photosynthesis [1,44], have a unique promise. For, through the study of spectral properties and photodynamical behaviors of aggregated porphyrin structures, an important outcome that is sought is the translation of the electron transfer specificities and speeds often found for biological reactions to the realm of molecular photonic devices (i.e., biomimetics) or photonic materials [45,46].

In Chapter 1, we reported a system based on the formation of encapsulated nanoscale molecular aggregates in mesoporous aluminosilicate cage compounds (i.e., Mobil Crystalline Materials -41; referred to as MCM-41). These composites represent a new type of nanostructural material with useful optical properties, including, in some cases, high luminescence cross-sections (resulting from superradiance, which will be discussed in Chapter 3 and Chapter 4) and controllable strong attenuation of incident

radiation. Such properties represent functionalities that are useful in photonic and optoelectronic devices and can be directly exploited in defining high intensity pixels in display systems [47].

Continuing from the previous work, in the present chapter, it is necessary to investigate the aggregation behaviors of TSPP in different environments, i.e., in the presence of an ionic vesicle, within the nano-sized cavity of modified MCM-41, and in homogeneous solution by electronic and Raman spectroscopies. The aqueous cationic vesicle microglocules (which represent a reasonable model of a lipid membrane was formed from didodecyldimethylammonium bromide (referred to hereinafter as 3DMA; with chemical formula $(CH_3)_2(C_{12}H_{25})_2N^+Br^-$).

We have found, as is discussed in more detail later, that a key factor in leading to formation of aggregates in 3DMA is the increase in the site concentration of the monomers promoted by the electrostatic attraction between the anionic porphyrin substituents and the positively charged binding sites of the vesicle. We have surmised that aggregation of TSPP monomers, which anchor to the vesicle, proceeds through a similar mechanism as occurs in other environments (e.g., in homogeneous solutions and on electrode surfaces), with protonation of TSPP monomers an indispensable prerequisite step. To form occluded, aggregated TSPP inside the channels of modified MCM-41, a "ship-in-bottle technique" was applied. The monomeric TSPP was first delivered into the channels of the molecular sieves by host-guest interaction, and then upon acidifying filtered residue, the occluded aggregate TSPP was formed. Although the microenvironments are different, the process of forming aggregated TSPP within MCM-

41 is somewhat similar to that for formation in homogeneous solution, i.e., self-alignment of protonated monomers.

2.2 Experimental

2.2.1 Preparation of TSPP/vesicle samples

TSPP was purchased as the sodium salt from Mid-Century Chemical Co. (Posen, IL) and used without further purification. Double-distilled, deionized water was used as the solvent. The pH of a solution was adjusted with either 0.1 M H_2SO_4 or 0.1 M NaOH, using a Marrison Science, Inc., Model 90 pH/temperature meter. Spectroscopic grade KCl was used to regulate the ionic strengths of solutions. Solutions were freshly prepared, but measurements were made only after an equilibration period of ca. 30 min. All measurements were made at ambient temperature.

Vesicle samples can be prepared by sonication of either monomeric 3DMA in water or of a mixture containing a 3DMA agglomerated film and water. In our experiment, the 3DMA vesicle was prepared by sonicating the mixture of 3DMA and water with certain ratio. The obtained vesicle solution is transparent. TSPP-vesicle aqueous samples were prepared by dropwise addition of 3DMA vesicle solution into the solution containing TSPP to a predefined molecular ratio of [3DMA] to [TSPP]. The aggregated TSPP on vesicle surface used for UV-vis and Raman measurements in this paper was obtained according to the molecular ratio of 2.5, and is designated here as TSPP-A/3DMA.

To insure that spectral signals were due only to TSPP aggregate entities that were bound to vesicle substrates, all spectroscopic measurements were conducted with the solution concentration below a "threshold value" where TSPP does not self-aggregate in homogeneous solution (specifically, $<10^{-5}$ M in solution of pH = 2.5).

For either UV-vis or Raman measurements, both free base TSPP with pH=10 and concentration of 5×10^{-6} M, and protonated TSPP solutions with pH=4.0 and concentration of 5×10^{-6} M were prepared using deionized water, and they are denoted NaTSPP and HTSPP, respectively.

2.2.2 TSPP/MCM-41 composites preparation

The preparation of TSPP/MCM-41 composites was described in detail by chapter 1. Briefly, 5 mg of TSPP was incorporated in 300 mg of modified MCM-41 by ion-exchange method. Upon acidifying filtered residue of the above assembly, thus changing the pH of the microenvironment within the cavity of MCM-41, the aggregated TSPP was formed. The occluded monomeric and J-aggregated forms of TSPP are designated here as TSPP-5-M/MCM-41 and TSPP-5-A/MCM-41, respectively.

2.2.3 Instrumentation

Electronic absorption spectra were recorded using a Perkin-Elmer Lambda 18, UV-vis-NIR spectrometer. The accessory, RSA-PE-18, with a six-inch diameter integrating sphere, was used for diffuse reflectance spectrum measurements.

Raman spectra of the aggregate (i.e., TSPP solution sample, TSPP-A/3DMA and TSPP-5-A/MCM-41 composite) were resonantly excited with laser radiation of

wavelength 488 nm, in order to enhance scattering signals for the corresponding species. The protonated TSPP and monomeric TSPP-5-M/MCM-41 composite were excited with laser radiation of wavelength 457 nm. Excitation was provided by a Coherent Innova 200 argon-ion laser. The excitation power was maintained below 50 mW, and Raman scatterings were collected and dispersed by a Spex 1877, 0.6-meter spectrometer. A Spex Spectrum-1 CCD camera was coupled to the spectrometer and maintained at 140 K by liquid nitrogen. Raman spectra reported here were obtained with different exposure time and repeating time (see Fig. 2-5), and have been refined by background subtraction using Microcal Origin software (version 5.0). The smoother curves were observed by increasing the repeating time, thus the higher resolution was reached. The estimated spectral resolution is ca. 2 cm^{-1}.

2.3 Results and Discussion.

A. Absorption spectra of TSPP/vesicle suspensions and TSPP/MCM-41 composites

The formation of aggregated TSPP in acidic solution in the presence of 3DMA can be quantitatively assessed, using visible absorption spectroscopy, through the existence of an absorption band near 490 nm. A second, weaker absorption band near 710 nm is also an indicator of the presence of the aggregate, but was not made use of for determining the concentration of aggregate. Both aforementioned absorption bands have been attributed to the aggregate as a result of homogeneous solution studies [48].

We examined the pH dependence of the absorption spectrum of 3.3×10^{-6} M TSPP in aqueous solution, in the presence and absence of 3DMA. For pH values in the range greater than ca. 7, an unchanged absorption spectrum is found (as represented in Fig. 2-1 by the single spectrum labeled as pertaining to the pH range 7.5 to 10.3) that corresponds to that of the free base, with its Soret band at 413 nm. At pH = 4.5, one finds in the Soret region a band at ca. 433 nm, with a shoulder at ca. 413 nm. These two features are attributable to the protonated monomer and the free base, respectively. At pH = 2.5, for the porphyrin concentration used, essentially only protonated TSPP is shown to be present.

Presented in Fig. 2-2 and Fig. 2-3 are the absorption spectra and kinetic profile for the conversion of the diacid monomeric form of the H_4TSPP^{2-} poyphyrin to a J-aggregate. Aggregated formation was initiated by addition of 3DMA to the TSPP solution. The final solution condition is 4.0 ml of 5.0×10^{-5} M TSPP and 2.0 ml of 1.0×10^{-4} M 3DMA at pH = 3.0. It was observed that the time approaching equilibrium is approximately 25 minutes. It is explained by the process that the monomeric TSPP diffuses to the vesicle surface and then the aggregated species is formed on the surface due to the increased local concentration of diacid TSPP. We found from Fig. 2-3 that after the equilibrium was reached, the absorption intensity of aggregated TSPP, i.e., peak position at ca. 490 nm, was remained unchanged within the next 3 hrs. The results showed that the equilibrium position was slowly approached after rapid formation of aggregate. To make sure that the equilibrium was reached for all samples, the absorption spectra were acquired 30 minutes after the addition of 3DMA to TSPP solution.

As regards the preparation of TSPP/vesicle suspensions, the approach that was typically used was to add vesicle solution to a solution of the chromophores under vigorous oscillation, leading to formation of TSPP aggregate. It thus follows that addition of 3DMA vesicle promotes increasing the "local concentration" of protonated TSPP above a self-aggregation concentration threshold, likely as a result of electrostatic induced adsorption. One might suspect that this self-aggregation could be promoted through the change of ionic strength of the solution derived from the addition of the ionic vesicles, but the replacement of vesicle by KCl to the same ionic strength does not lead to aggregate formation (as shown in Fig. 2-1). Thus the influence of ionic strength of the solution in promoting self-aggregation, at the low concentration used, is not a dominating one, though the overarching role of electrostatics in facilitating aggregation is suggested by the observation that a negatively charge vesicle suspension, for example an L-x-dimistoylphosphatidy-cholone (DPPC)-dicetylposphate (DCP) vesicle suspension (of molecular ratio from DPPC : DCP = 1:0 to 2:3) in water does not promote TSPP aggregation.

Significant changes in absorption spectra for TSPP in solution of pH = 2.5 induced by successive additions of aliquots of a 3DMA vesicle suspension were observed. The dependence of the amount of aggregated TSPP on the amount of vesicle added is shown in Fig. 2-4. From such spectral measurements it is evident that, upon increasing the relative amount of vesicle, the intensity of the 490nm absorption band increases at the expense of the 433-nm absorption band. This finding and an observed isobestic points near 450 nm and 660 nm suggest that TSPP aggregation is accomplished via an intermediate step of protonation of the free base; i.e., protonated TSPP forms the

aggregate. It is also found, for a given initial concentration of TSPP (i.e., $[TSPP]_o$), that increasing the stoichiometric molecular concentration ratio of 3DMA relative to TSPP, i.e., $R_o = [3DMA]_o/[TSPP]_o$, results in the aggregate absorption going through a maximum while the absorption due to protonated TSPP (at 433 nm) attains a minimum value at the same concentration ratio. Further examination of the system reveals that after the maximum in aggregate absorption is attained, addition of more vesicle results in an increase in the absorption at 412 nm. Hence, "excess" 3DMA leads to deprotonation and deaggregation.

At molecular concentration ratio of R_0=2.5, the maximum TSPP aggregate was formed on the 3DMA vesicle surface, and the absorption spectrum is shown in Fig. 2-4.

The spectral patterns and their variations for TSPP in the presence of the cationic vesicle are similar to those observed for homogeneous solution systems; however, in the former case, the aggregate band is substantially wider than that for the latter case (i.e., ~1300 vs ~380 cm^{-1}, respectively). This contrast is likely attributable to a structural difference between aggregates that form in the two environments (with possibly the vesicle system possessing more than one type of aggregate), as well as to an increased vibrational dephasing associated with the vesicle environment.

Based on accumulated studies of the present vesicle system, we have deduced, as mentioned earlier, that TSPP aggregation involves an initiation step in which the monomer is protonated, followed by a propagation step in which the diacid is incorporated into the vesicle. This incorporation likely involves the anchoring of one or more molecules onto the vesicle surface via electrostatic attraction between the end-

group of TSPP (i.e., SO_3^-) and the positively charged head-group $N^+(CH_3)_2$ of the vesicle-forming species.

The absorption spectra of TSPP/MCM-41 composites and aqueous TSPP solutions have been illustrated in the previous chapter. The UV-vis absorption bands of various samples are shown in Table 2-1. One finds that for aggregate samples, both Soret band and Q-band shifts are illustrated, i.e., Soret bands at 490, 487, 495 nm for aggregated solution TSPP, TSPP-A/MCM-41, and TSPP-A/3DMA, respectively; with corresponding Q-bands at 706, 704 and 710 nm. The differences observed can be explained by considering different environments in which the aggregates are formed.

Our model for formation of aggregated porphyrin in the presence of an organic vesicle is to consider the threshold phenomenon as being an activation process in which the vesicle surface is coated by adsorbed diacid monomers. The alignment of molecules in this foundation layer would likely be defined by electrostatic interaction between the vesicle head-groups and the diacid's negatively charged centers. We then suggest that the resultant foundation structure would lead to aggregate chains attached as pendants onto the coated vesicle. Such a model probably promotes the aggregation between protonated TSPP molecules. Therefore, when compared with aggregated aqueous TSPP solution, more red-shift Soret band for TSPP-A/3DMA sample might be expected; which is reflected by the results in Table 1(shift from 490 to 495 nm). As discussed previously in chapter 1, the shift from 490 to 487 nm for encapsulated aggregate (TSPP-5-A/MCM-41 sample) can be explained in terms of intramolecular charge-transfer caused by host-guest interaction, which is connected to steric effects associated with the pore structure within

modified MCM-41. Such effect is also noted from the occluded monomeric TSPP (TSPP-5-M/MCM-41 sample). These electronic structure differences will be studied and illustrated in the Raman spectra.

B. Raman spectra of TSPP/vesicle suspension and TSPP/MCM-41 composites

Resonance Raman spectra for various aggregated TSPP samples, i.e., aqueous solution, TSPP-5-A/MCM-41 and TSPP-A/3DMA, are shown in Fig. 2-5. Also included in Fig. 2-5 are protonated TSPP solution and TSPP-5-M/MCM-41. We found that no Raman signals of TSPP (not shown) occur in aggregated homogeneous solution of pH=1.5 at 3.3×10^{-6} M under the same experimental condition, however a Raman spectrum of aggregated TSPP (Part C) results when the 3DMA vesicle suspension is added to the TSPP solution of pH=2.5 with final concentration of 3.3×10^{-6} M. At very low concentration ($< 10^{-5}$ M), the concentration of the aggregated TSPP in the homogeneous solution, even under stronger acidic condition (pH=1.5), is much lower than that in TSPP-A/vesicle suspension. The reason is that the cationic vesicle attracts more negatively charged TSPP to the surface, thus resulting in the local concentration increase of TSPP at the vesicle surface. As we observed above from absorption spectrum, although less acidic (pH=2.5), a large amount of aggregated TSPP was formed in TSPP-A/3DMA suspension. It is reasonable that for TSPP-A/3DMA, the dramatic increase in Raman signals should be experimentally demonstrated, as seen from Part C in Fig. 2-5. In this experiment, surface-enhancement effect associated with the resonant excitation of laser radiation provides an appropriate approach for the investigation into

the system with very low concentration, which was previously implemented mainly by taking advantage of electrode surfaces [49].

It is to be noted that for solid composite sample TSPP-A/MCM-41, relatively strong Raman signals and good spectral pattern are observed (Part A of Fig. 2-5). The resonance Raman spectra, are distinguished by two enhanced low-frequency bands (at ca. 241 and 317 cm^{-1}, characteristic of aggregated species), and the spectral patterns in the frequency region above ca. 1000 cm^{-1} are the same as that of protonated TSPP monomer in acidic solution (see Fig. 2-5). The shifts and relative intensities in two enhanced bands: 240 (6.3) vs 241 (5.9) vs 246 (7.8) cm^{-1} for TSPP aggregated in solution, TSPP-A/MCM-41 and TSPP-A/3DMA, respectively, and 317(6.3) vs 315 (4.6) vs 319 (6.8) cm^{-1} as well, are reflective of different environments.

As we mentioned above, for TSPP-A/3DMA suspension sample, the much stronger electrostatic interaction between the end-group of TSPP (i.e., SO_3^-) and head-group $N^+(CH_3)_2$ of the vesicle-forming species caused by the highly positive-charged vesicle surface. Such interaction induces the electron redistribution of four nitrogen atoms on the porphyrin ring, and thus strongly influences the dipole-dipole interaction. As a result, compared with homogeneous solution aggregate, the Raman shifts to higher wavenumbers, caused by difficult ruffling motion and doming motion (which are defined by Akins, et al. previously [48]) are expected to observe, which are illustrated above. Kano and his co-workers also observed the 244 cm^{-1} frequency by sub-5-fs spectroscopy, which reveals a coherent molecular vibration coupled to the Frenkel exciton [50].

After silylation and under acidic condition, the positve-charged sites on the surface wall of modified MCM-41 are not as concentrated as that on the cationic vesicle surface. In the meantime, the pore size of 20 Å for the modified MCM-41 is sufficiently large to allow aggregate alignment inside the channels without considerable steric effect. Thus the aggregates formed within the channels are probably more integrated than those formed on vesicle surface. Therefore, as seen in Table 2-2, the changes in corresponding peak positions of two low bands for TSPP-5-A/MCM-41 are smaller. In addition, the data of Raman spectra (Table 2-2) for TSPP-5-A /MCM-41 and TSPP-5-M/MCM-41 suggest that the formation of TSPP aggregate results in the detachment of most of monomeric TSPP molecules at the MCM-41 surface wall.

Although the small shifts and changes in relative intensities (Table 2-2) are illustrated, the Raman spectra that are found, for TSPP-5-A/MCM-41 and TSPP/3DMA samples, are almost identical to that for aggregated TSPP in homogeneous solution [48,51] and for aggregated TSPP formed on an electrode surface. The similarity of Raman spectra for the vesicle system, MCM-41 composite system and the homogeneous system is consistent with our conjecture that the TSPP aggregate is formed in these three cases through the self-assembly of the protonated TSPP monomer—which is expected to have essentially the same structure in the different environments. Comparison with homogeneous solution reveals, however, that for the vesicle system the relative intensities of the low frequency doublet bands when compared to the intensities of bands attributable to the macrocycle structure (above ca. 1000 cm^{-1}) do not exhibit the same level of relative enhancement intensity as found for homogeneous solution resonance Raman spectra.

When excited at 457 nm, the spectral pattern (Part D) for TSPP-5-M/MCM-41 is much different from that of protonated solution TSPP (Part E). The dramatic changes in Raman shifts are shown in Table 2-2. The result suggests that the occluded protonated TSPP monomer is present in the composite, although the amount of protonated TSPP monomer is much less than that of the free base form TSPP (seen from the UV-vis spectrum in Chapter 1). Thus the investigation into Raman spectrum of the protonated monomer species is useful to analyze the electronic structure change of porphyrin caused by quantum confinement effect or host-guest interaction. In comparison, at excitation wavelength of 457 nm, no Raman signals for both free base and aggregated forms of TSPP in homogeneous solution were detected in our experiment, indicating that the acquired Raman signals under such condition can only reflect the existence of protonated species. As we know, the strong electrostatic interaction between the end-group of TSPP (i.e., SO_3^-) and surface wall (i.e., $^+NH_3$-R) greatly changes the dipole-dipole moment of neighboring phenyl ring of TSPP molecule. It implies that for TSPP-5-M/MCM-41 sample, the greater changes in Raman signals (including Raman shift and relative intensity) pertaining to phenyl ring should be observed when compared to protonated solution TSPP, as seen from Table 2-2, 964 (0.35) vs 941(0.12) $^{-1}$cm, and 1001(0.51) vs 1011 (0.44) cm^{-1}, respectively. From the result above, the suggested band assignments based on homogeneous TSPP solution [48] are confidently confirmed and correct. The difference in spectra is also found in the low-frequency region, where the relative intensity of two bands (Part D and E) is inversed, and the shifts: 211 vs 230 cm^{-1} (core ruffling) and 309 vs 312 cm^{-1}(core doming) are illustrated in Table 2-2.

2.4 Conclusion

The experimental observation presented in this study for TSPP aggregate formed in the presence of cationic vesicle enables to conclude that the vesicle of oppositely charged head group is capable of promoting molecular aggregation by increasing local concentration of the protonated TSPP monomers on vesicle surface. The aggregation of anchored molecular units occurs via the electronic interaction between neighboring protonated TSPP monomers. The aggregated TSPP within modified MCM-41 is formed by self-alignment of protonated monomers upon acidifying the residue, similar to that in solution. Due to the difference in microenvironments, the changes in Soret band position and broadened bandwidth for aggregated TSPP formed within modified MCM-41 and in the presence of vesicle are demonstrated in characteristic absorption, and the low band shift and change in relative intensity in Raman scattering are illustrated as well.

Bibliography

[1] Chen, S. H.; Huang, J. S. In *Structure and Dynamics of Strongly Interacting Colloids and Supramolecular Aggregates in Solution*, Tartaglia, P., Eds.; Luwer: Dordrecht, **1992**.

[2] Mallamace, F. In *Scaling Concepts and Complex Fluids*, Ed.; Compositori: Bologna, **1995**.

[3] Lehn, J. M. In *Supramolecular Chemistry*, VCH: Weinheim, **1995**.

[4] White, W. I. In *The Porphyrins*: Dolphin, D., Ed.; Academic: New York, **1978**; Vol. 5, Chapter 7.

[5] Kasha, M. *Radiation Res.* **1963**, *20*, 55.

[6] Sturmer, D. M.; Heseltine, D. W. In *The Theory of the Photographic Process*, (4th. ed.); James, T. H., Ed.; MacMillian Publishing Company: New York, 1977, Chap. 8.

[7] Herz, A. H.; *Adv. Colloid. Interface Sci.* **1977**, *8*, 237.

[8] Mobius, D.; Kuhn, H. *Israel. J. Chem.* **1979**, *18*, 375.

[9] Mobius, D. *Acc. Chem. Res.* **1981**, *14*, 63.

[10] Akins, D. L. *J. Phys. Chem.* **1986**, *90*, 1530.

[11] Akins, D. L.; Lombardi, J. R. *Chem. Phys. Lett.* **1987**, *136*, 495.

[12] Akins, D. L.; Akpabli, C. K.; Li, X. *J. Phys. Chem.* **1989**, *93*, 1977.

[13] Akins, D. L.; Macklin, J. W. *J. Phys. Chem.* **1989**, *93*, 5999.

[14] Akins, D. L.; Macklin, J. W.; Parker, L. A.; Zhu, H. -R. *Chem. Phys. Lett.* **1990**, *169*, 564.

[15] Akins, D. L.; Macklin, J. W.; Zhu, H. -R. *J. Phys. Chem.* **1991**, *95*, 793.

[16] Akins, D. L.; Zhu, H. -R. *Langmuir* **1992**, *8*, 546.

[17] Akins, D. L.; Zhuang, Y. H.; Zhu, H. -R.; Liu, J. Q. *J. Phys. Chem.* **1994**, *98*, 1068.

[18] Selwyn, J. E.; Steinfeld, J. I. *J. Phys. Chem.* **1972**, *76*, 762.

[19] Ojeda, P. R.; Amashta, I. A. K.; Ochoa, J. R.; Arbeloa, I. L. *J. Chem. Soc., Faraday Trans. II* **1988**, *84*, 1.

[20] Valdes-Aguilera, O.; Neckers, D. C. *Acc. Chem. Res.* **1989**, *22*, 171.

[21] Kasha, M.; Rawls, H. R.; El-Bayoumi, M. A. *Pure. Appl. Chem.* **1965,** *11*, 37.

[22] Hessemann, J. *J. Am. Chem. Soc.* **1980**, *102*, 2167; 2176.

[23] Vincent, P. S.; Barlow, W. A. *Thin Solid Films* **1980**, *71*, 305.

[24] Fukuda, K.; Nakahara, H. *J. Colloid Interface Sci.* **1984**, *98*, 555.

[25] Mooney, W. F.; Brown, P. E.; Russel, J. C.; Costa, S. B.; Pederson, L. G.; Whitten, D. G. *J. Am. Chem. Soc.* **1984**, *106*, 5659.

[26] Mooney, W. F.; Whitten, D. G. *J. Am. Chem. Soc.* **1986**, *108*, 5712.

[27] Pasternack, R. F.; Huber, P. R.; Boyd, P.; Engasser, G.; Francesconi, L.; Gibbs, E.; Fasella, P.; Venturo, G. C.; Hinds, L. deC. *J. Am. Chem. Soc.* **1972**, *94*, 4511.

[28] Pasternack, R. F.; Francesconi, L.; Raff, D.; Spiro, E. *Inorg. Chem.* **1973**, *12*, 2606.

[29] Shelnutt, J. A.; Dobry, M. M.; Satterlee, J. D. *J. Phys. Chem.* **1984**, *88*, 4980.

[30] Schick, G. A.; Schreiman, I. C.; Wagner, R. W.; Lindsey, J. S.; Bocian, D. F. *J. Am. Chem. Soc.* **1989**, *146*, 165.

[31] Barber, D. C.; Freitag-Beeston, R. A.; Whitten, D. G. *J. Phys. Chem.* **1991**, *95*, 4074.

[32] Ohno, O.; Kaizu, Y.; Kobayashi, H. *J. Chem. Phys.* **1993**, *99*, 4128.

[33] Schick, G. A.; O'Grady, M. R.; Tawari, R. K. *J. Phys. Chem.* **1993**, *97*, 1339.

[34] van Esch, J. H.; Feiters, M. C.; Peters, A. M.; Nolte, R. J. M. *J. Phys. Chem.* **1994**, *98*, 5541.

[35] Gilman, P. B. *Photo. Sci. Eng.* **1974**, *18*, 418.

[36] Borsenberger, P. M.; Chowdry, A.; Hoesterey, D. C.; W. Mey *J. Appl. Phys.* **1978**, *44*, 5555.

[37] Waggoner, A. *J. Membrane Biol.* **1976**, *27*, 317.

[38] Chatterjee, S.; Davis, P. D.; Gottschalk, P.; Kurz, M. E.; Sauerwein, B.; Yang, X.; Schuster, G. B. *J. Am. Chem. Soc.* **1990**, *112*, 6329.

[39] Hanamura, E. *Phys. Rev. B* **1988**, *37*, 1273.

[40] Sasaki, F.; Kobayashi, S. *Appl. Phys. Lett.* **1993**, *63*, 2887.

[41] Wang, Y. *Chem. Phys. Lett.* **1986**, *126*, 209.

[42] Wang, Y. *J. Opt. Soc. Am. B* **1991**, *8*, 981.

[43] Kobayashi, S. *Mol. Crys. Liq. Crys.* **1992**, 217, 77.

[44] Okamura, M. Y.; Feher, G.; Nelson, N. In *Photosynthesis*, Govindjee, Ed.; Academic Press: New York, 1982, pp. 195-272.

[45] O'Neil, M. P.; Niemcyzk, M. P.; Svec, W. A.; Gosztola, D.; Gaines III, G. L.; Wasielewski, M. R. *Science* **1992**, *257*, 63.

[46] Wagner, R. W.; Lindsey, J. S.; Seth, J.; Palaniappan, V.; Bocian, D. F. *J. Am. Chem. Soc.* **1996**, *118*, 3996.

[47] Lawandy, N.; Firehammer, J.; Vartak, S. *Laser Focus* **1997**, *33(5)*, 137.

[48] Akins, D. L, Zhu, H. -R.; Guo, C. *J. Phys. Chem.*, **1996**, *100*, 5420.

[49] Guo, C.; Ren, B.; Akins, D. L. *J. Phys. Chem.*, **1998**.

[50] Kano, H.; Saito, T.; and Kobayashi, T. J Phys. Chem. B 2001 105(2), 413-419.

[51] Akins, D. L, Zhu, H. -R.; Guo, C. *J. Phys. Chem.*, **1994**, *98*, 3612;

Samples	Monomeric Soret band λ(nm)	Aggregated Soret band λ(nm)	Q band λ (nm)
Aggregated TSPP solution	423	490	706
TSPP-5-A/MCM-41	424	487	704
TSSP-A/3DMA	433	495	710
TSPP-5-M/MCM-41	393	--	--
Protonated HTSPP	434	--	--
Free base NaTSPP	413	--	--

Table 2-i

HTSPP λ (I/Io)	TSPP-5-M/MCM-41 λ (I/Io)	Aggregated TSPP λ (I/Io)	TSPP-5-A/MCM-41 λ (I/Io)	TSPP-A/3DMA λ (I/Io)	Assignments
195 (0.17)		208 (0.26)	202 (0.19)	211(0.35)	
230 (0.60)	211 (0.15)	240 (6.28)	241(5.92)	246 (7.80)	γ_s(por) " Core ruffling?
312 (0.41)	309(0.35)	317 (6.31)	315(4.54)	319 (6.80)	γ_s(por) " Core doming?
		365 (0.41)	363 (0.30)	366 (0.75)	ν(N---N)
408 (0.12)	408 (0.13)				?
		494 (0.15)			?
		551 (0.10)	552 (0.18)	552 (0.40)	?
573 (0.07)		581 (0.20)	579 (0.26)	584 (0.67)	?
623 (0.08)	620 (0.11)	622 (0.11)	620 (0.15)	622 (0.50)	?
700 (0.27)	703 (0.11)	700 (0.69)	700 (0.66)	703 (1.00)	?
805 (0.11)	803 (0.15)	809(0.06)	802(0.09)		?
		822 (0.08)			Phenyl
		846(0.04)			?
		856 (0.04)			?
		882 (0.10)	877(0.08)		B_{1g}, δ(pyr)
928 (0.10)		922(0.19)	914 (0.13)		?
941 (0.12)	964 (0.35)				A_{1g}, δ(pyr)? Phenyl?
989 (0.20)		986 (1.00)	986 (0.99)	990 (1.18)	-
1011 (0.44)	1001 (0.51)	1018 (0.41)	1015 (0.60)	1019 (0.72)	A_{1g}, $\nu_s(C_a\text{-}C_m)$? Phenyl?
1087 (0.17)	1082 (0.14)	1083 (0.24)	1082 (0.28)	1085 (0.50)	B2g, $\delta_{ip}(C_b\text{-}H)$
1126 (0.08)	1123 (0.16)	1125 (0.11)	1121 (0.19)	1130 (0.31)	A_{1g}, δ(C$_b$-H)
					A_{1g}, ν(C$_a$-N)
1199 (0.09)					B_{1g}, $\nu_s(C_a\text{-}C_b)$
1237 (1)	1234 (1)	1234 (1)	1232 (1)	1234 (1)	ν(C$_m$-ϕ)
1282 (0.03)	1296 (0.13)	1286 (0.08)	1282 (0.17)		B_{1g}, $\nu_s(C_a\text{-}N)$, [ν(Ca-N){NH}]*
1326 (0.24)	1325 (0.16)	1323 (0.34)	1321 (0.38)	1322 (0.38)	B_{1g}, $\nu_{as}(C_a\text{-}N)$
		1360 (0.08)			A_{2g}, $\nu_s(C_a\text{-}C_b)$
1372 (0.45)	1374(0.21)	1387 (0.11)	1387 (0.13)		A_{1g}, $\nu_s(C_a\text{-}N)$
	1437(0.13)	1430 (0.23)	1432 (0.20)	1432 (0.34)	A_{1g}, $\nu_s(C_a\text{-}C_b)$
1476 (0.42)	1475 (0.11)	1478 (0.47)	1478 (0.53)	1481 (0.50)	B_{1g}, $\nu(C_b\text{-}C_b)$, [A_{1g}, ν(Ca-N){NH}]*
1544 (1.33)	1546 (1.07)	1538 (1.56)	1537 (1.53)	1541 (1.12)	A1g, $\nu(C_b\text{-}C_b)$, [A_{1g}, $\nu(C_b\text{-}C_b)${N}]*
		1565 (0.29)	1565 (0.46)	1566 (0.45)	B_{1g}, $\nu_{as}(C_a\text{-}C_m)$
1598 (0.29)	1595(0.36)	1598 (0.23)	1595 (0.28)	1598 (0.41)	Phenyl

Table 2-2

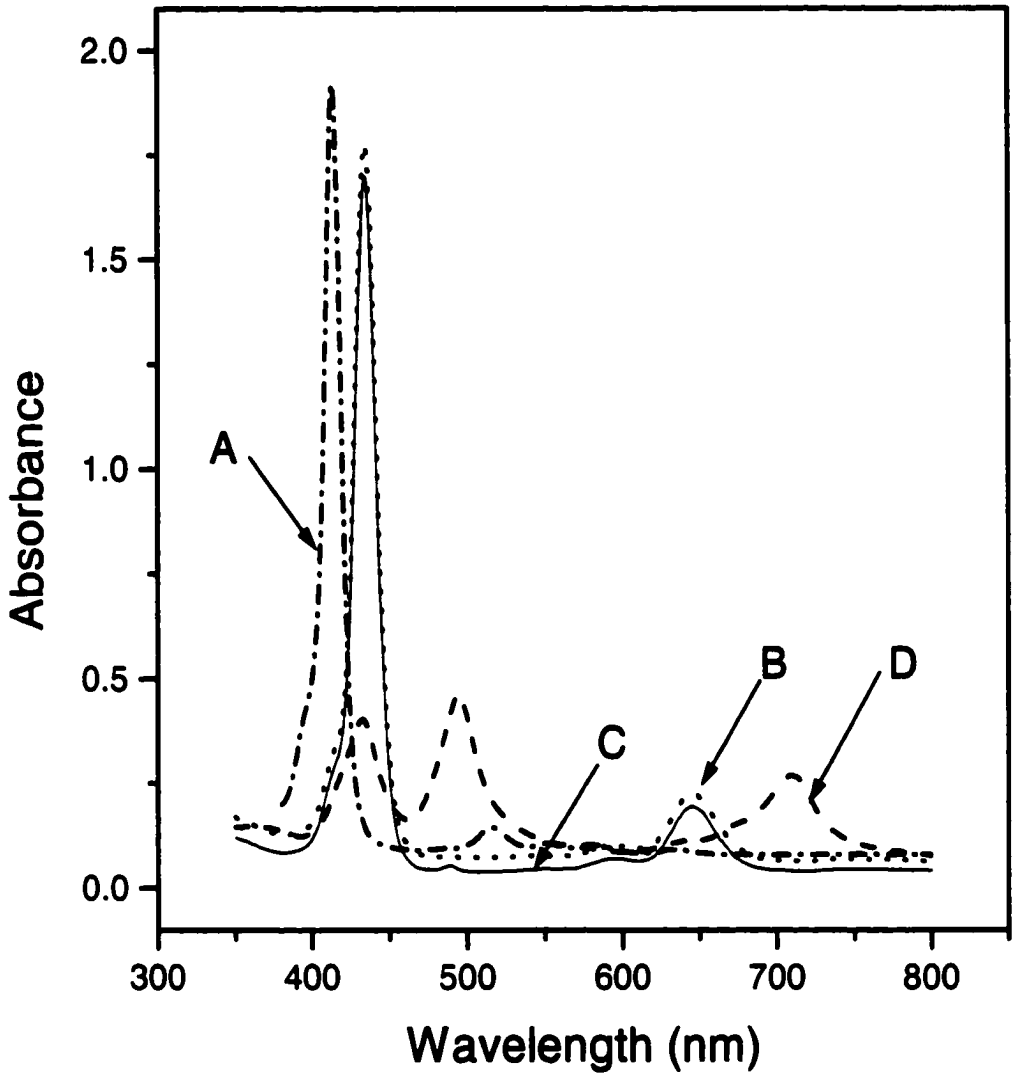

Fig. 2-1

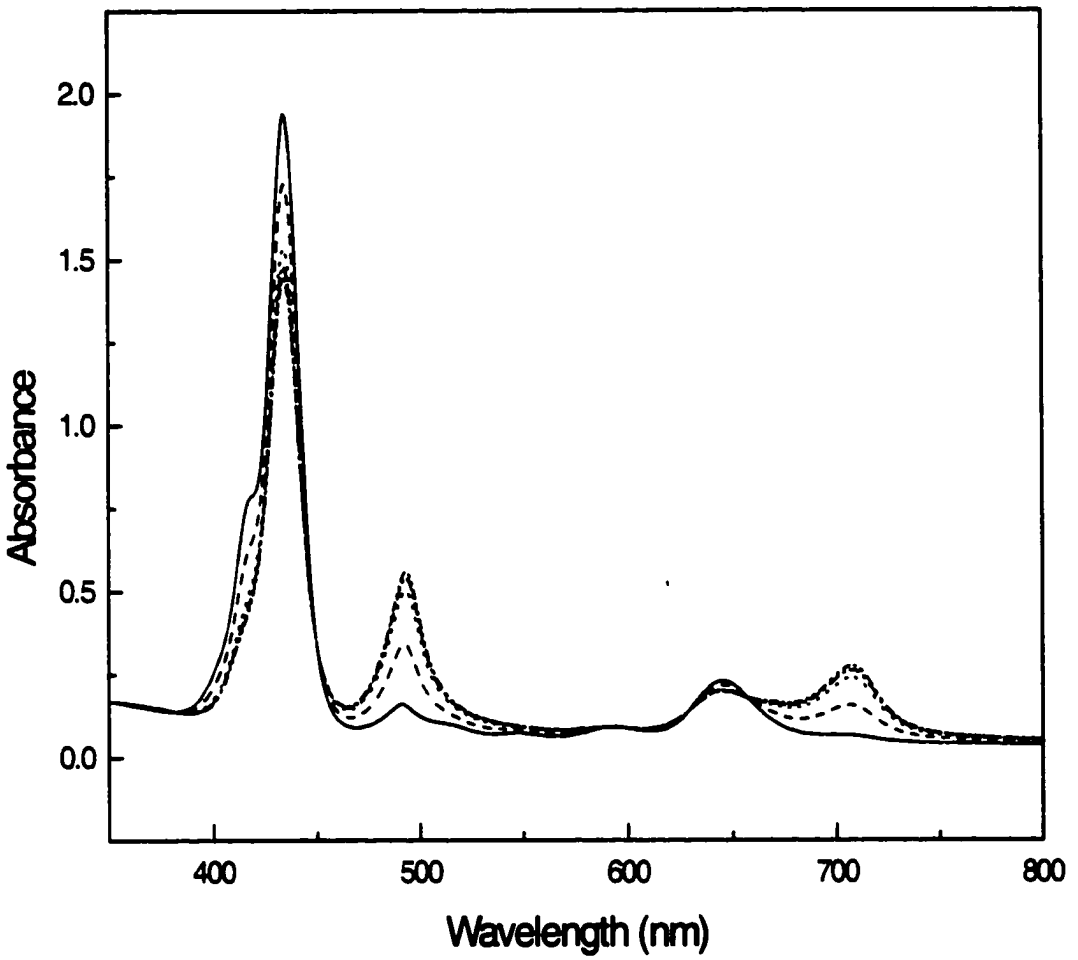

Fig. 2-2

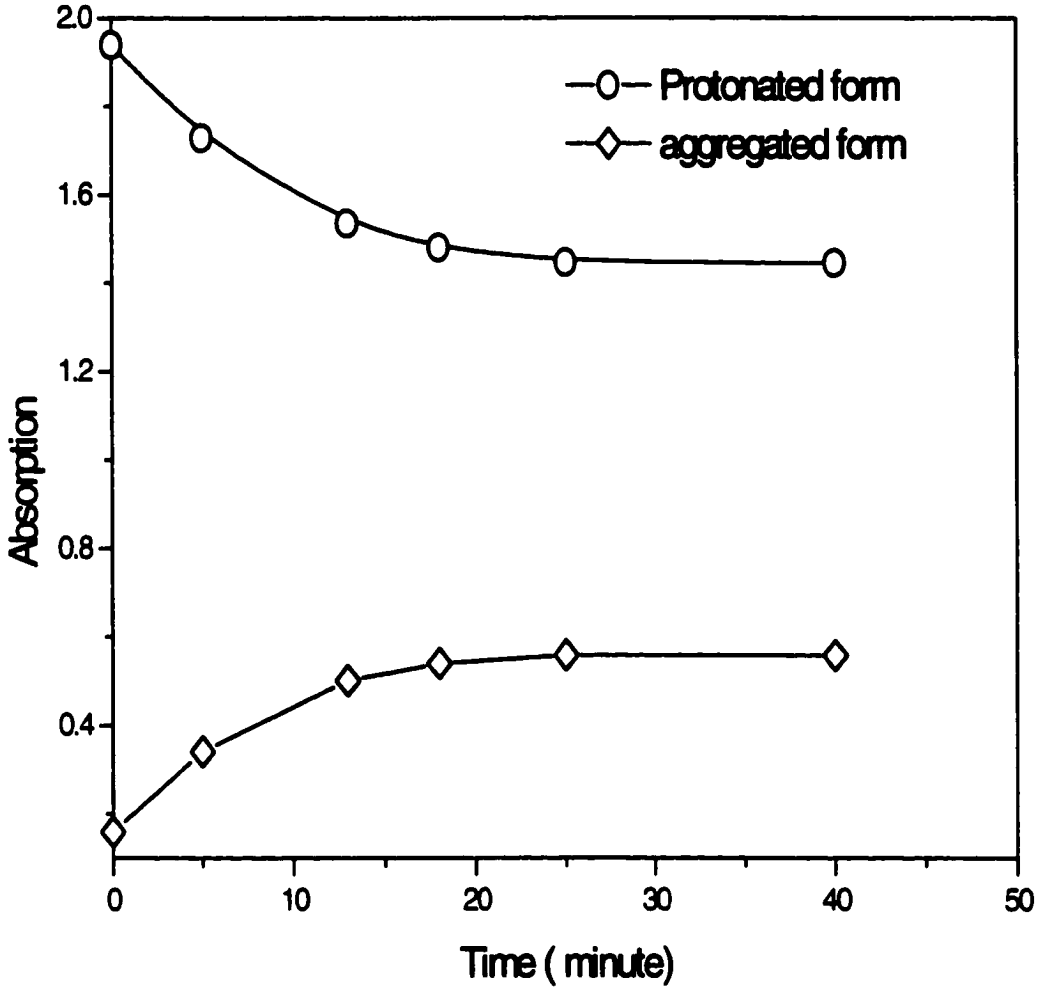

Fig. 2-3

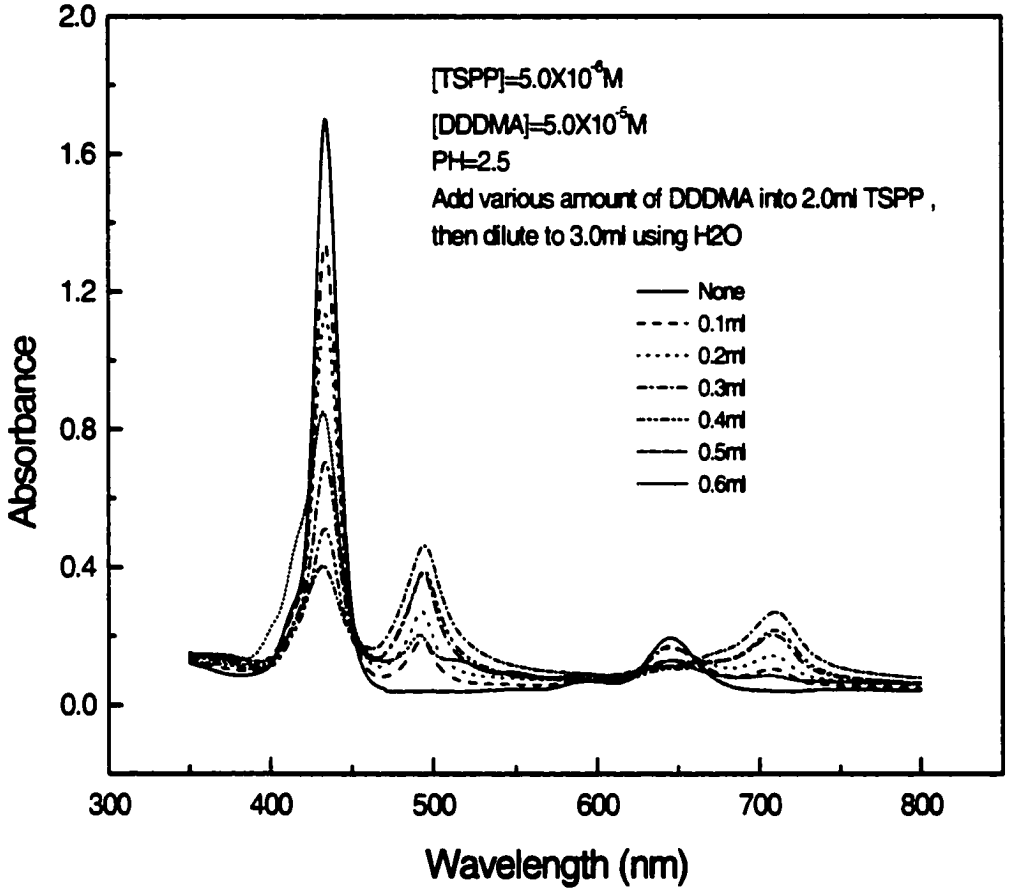

Fig. 2-4

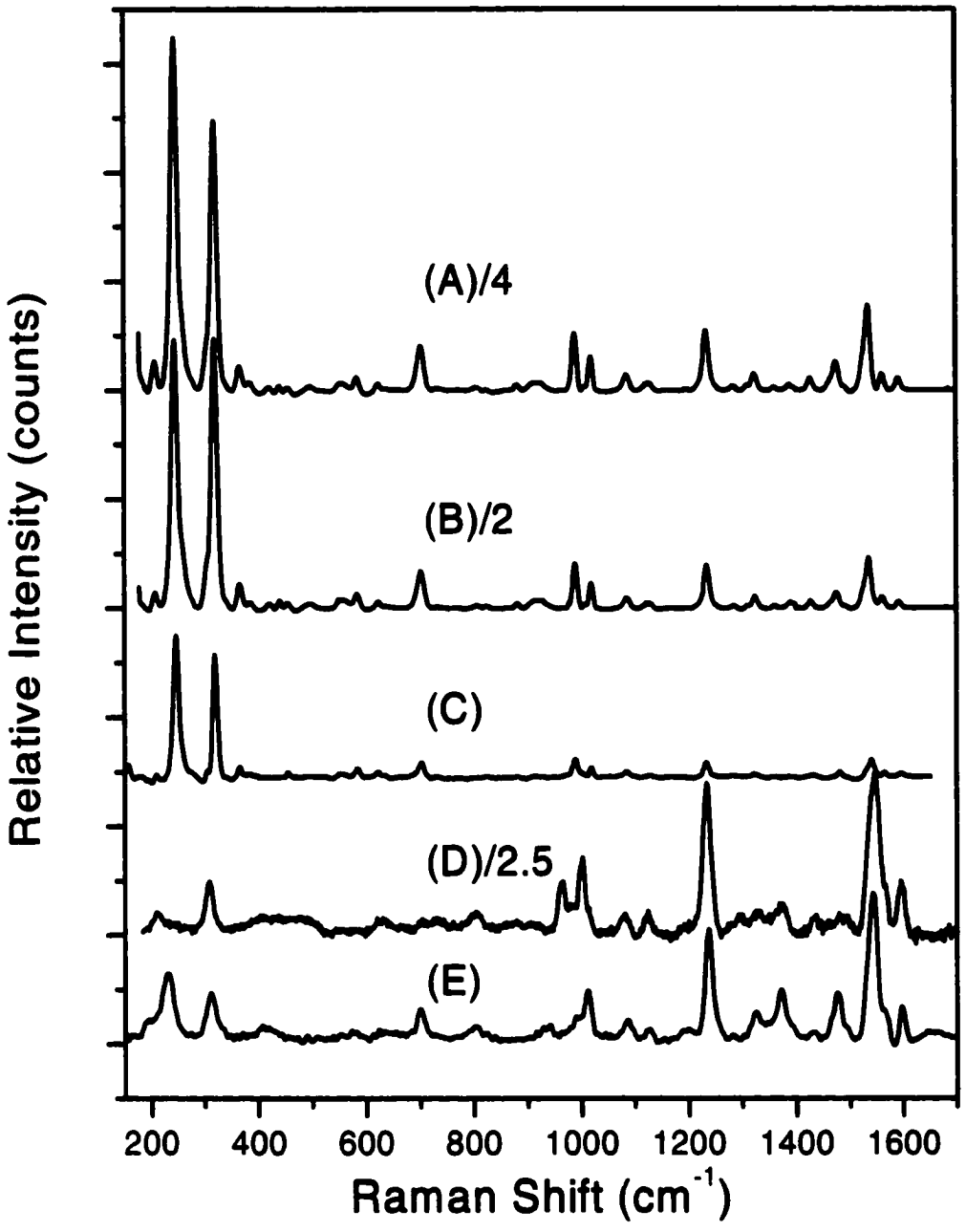

Fig. 2-5

CHAPTER 3

AGGREGATION AND EXCITON EMISSION OF A CYANINE DYE ENCAPSULATED WITHIN MESOPOROUS MCM-41

3.1 Introduction

Spectroscopic and optical dynamics properties of aggregated cyanine dyes in homogeneous systems [1,2] and as adsorbates in heterogeneous systems [3-14] have been widely investigated in Akins' s laboratory. Our interest is to examine the formation of cyanine aggregates within a mesoporous cage compound. The aim in this case would be to create an encapsulated species where constraints in aggregate length and orientation, associated with the spatially constricted and directional character of the cavity, as well as controls available in the synthesis process, result in a nanocomposite that is a new material, possessing the unique spectroscopic and other optical properties generally associated with cyanine dye aggregates, while assuming a more robust and manipulable physical form. Our ultimate goal is to exploit such new materials for optical and optoelectronic applications.

In terms of research activities described in the literature involving an occluded species, most efforts exploit the one-dimensional uniform pore sizes and thermal stability of mesoporous siliceous materials as hosts to organize either guest atoms [15], polymers [16-18], or organic and inorganic compounds [19-21], with the aims of creating composite materials with catalytic [22], environmentally remunerative [23], or

optoelectronic properties [24]. Also, recently, dye-doped microstructures and mesostructures have been advanced as novel microlasers and optoelectronic devices [25].

The focus of our present study with the occluded aggregated cyanine dye is quite distinct from that of the other investigators referenced above. Much work has been done by Akins, et al dealing with several aggregated cyanine dyes in heterogeneous systems; in particular, with aggregation of cyanine dyes on electrode surfaces [3-14] as well as on the surfaces of different colloidal particles [26,27]. In the latter case, they studied 1,1'-3, 3'-tetraethyl-5,5',6,6'-tetrachlorobenzimidazolocarbocyanine (referred to as TTBC) adsorbed onto colloidal silica [26] as well as 1,1'-diethyl-3,3'-bis-(3-sulfopropyl)-5,5',6,6'-tetrachlorobenzimidazolocarbocyanine (referred to as BIC) adsorbed onto colloidal silver [27]. It was found, for both systems, that a form of lasing occurs, defined by Akins et al. as superradiant lasing, at phenomenally low optical pumping thresholds.

In Chapter 1, we reported a technique for encapsulating tetrakis(*p*-sulfonatophenyl) porphyrin, also referred to as TSPP, within an aluminosilicate, specifically, an aluminum incorporated MCM-41, and the spectroscopic evidence confirming the encapsulation; in particular, the dramatic changes in absorption and emission spectra upon formation of the occluded aggregate. This composite system has enormous value as regards proof-of-concept and possibly in regards to its unique absorption property. But because exciton emission, which is indicative of aggregate formation, is weak (due to a transition between the Q-state and ground state), there is reduced prospect of exploiting the composite for materials or device applications. Aggregated cyanine dyes, on the other hand, typically fluoresce very intensely, and when incorporated within the pores of mesoporous materials, may represent systems with wide utility.

In recognition of the aforementioned prospect, our focus in the present chapter is on optically excited luminescence of a composite system consisting of an aggregated cyanine dye—specifically, TTBC, see Fig. 3-1—occluded within mesoporous aluminosiliceous MCM-41. The luminescence results from coherent emission from the excitonic state derived from coupled, aligned monomeric species. This quantum confinement is associated with both the restricted growth region available to the spontaneously self-assembled molecular aggregate, which forms when TTBC monomers are exposed to sufficiently basic microenvironment, and the intrinsic confinement (characterized in terms of a coherence length [28-30]) of the exciton's movement among a subset of coherently responding molecules within the physical aggregate. Such a composite evinces enhanced emission with a shortened radiative lifetime, and may have specific utility in such applications as the active element in a flat-panel display device, as the secondary emitter at a near-field optical microscope (NSOM) fiber tip, and as a monochromatic emitting component in coatings for identification of objects in robotic vision and search-and-rescue endeavors.

3.2 Experimental

3.2.1 Synthesis of Modified Al Containing MCM-41

Polycrystalline powders of the mesostructural aluminosilicate MCM-41 were prepared by using cetyltrimethylammonium bromide (CTAB) as the template [31,32]. Briefly, Na_2SiO_3 (Aldrich, ~27% SiO_2) solution and a calculated amount of $NaAlO_2$ (Alfa) solution (Si/Al = 20) were added to CTAB (Aldrich) solution according to the

molar composition ratio $5SiO_2$:$0.4Al_2O_3$:CTAB:$610H_2O$. The pH was lowered to 11 with 2 M H_2SO_4 and the mixture was stirred for more than 3 hrs at about 318 K. Then the temperature was raised to 373 K, and the reaction allowed for 72 hrs in a teflon-lined autoclave. The resulting precipitate was filtered, washed thoroughly with distilled water, and calcined in air at 773 K to obtain the final product, MCM-41 (see discussions below of XRD patterns).

To stabilize the synthesized MCM-41 and allow monomeric TTBC incorporation as well as formation of aggregated TTBC from the occluded monomers, we found it necessary to modify its interior structure through use of a silylation reagent, aminopropyltriethoxysilane (APTES; NH_2-$(CH_2)_3$-Si-$(C_2H_5O)_3$), thus linking oxygen atoms on the aluminosilicate surface and rigidifying the mesoporous framework, and satisfying guest-host intermolecular and/or electrostatic interactions as well. For our studies, the modified MCM-41 was prepared according to Ref. 33. Briefly, about 1.5 g of the calcined MCM-41 was mixed with a chloroform solution of APTES (100 ml, 0.2 M) and stirred overnight at room temperature. The precipitate was filtered and washed with chloroform and dichloromethane.

Various MCM-41/TTBC assemblies were obtained through mixing of the modified MCM-41 with TTBC monomer in different ratios. Upon basifying filtered residues containing various assemblies in a programmed way, thereby changing the pH of the microenvironment within the cavity of the aluminosilicate, conditions were attained where the J-aggregated TTBC were formed from occluded monomers. Specifics of the chemical and spectroscopic techniques are provided below.

3.2.1 Formation of TTBC/MCM-41 Composites

A typical preparation of a TTBC/MCM-41 composite involved stirring a mixture of 300 mg of modified MCM-41, 4.5 mg TTBC, and 15ml of distilled water for over 24 hrs at room temperature with the pH held at ca. 7.0 using 2 M NaOH. The solution was then centrifuged, and the transparent aqueous solution decanted. The residue was washed ca. 3 times with distilled water to remove TTBC monomers from the external surface, and then dried in air. The product is here designated TTBC-M/MCM-41, where TTBC-M indicates that monomeric TTBC is encapsulated within the modified MCM-41: absorption and emission studies (see below, section III) have confirmed the presence of monomer under the above conditions.

The formation of occluded, aggregated TTBC involves adding 2 M NaOH to the solid residue above. An immediate color change of the residue occurred from light red to dark pink. Absorption spectra of the powdered residue (see below, section III) indicated the presence of occluded J-aggregated TTBC, here designated TTBC-A/MCM-41.

3.2.3 Instrumentation

Absorption spectra were recorded using a Perkin-Elmer, Lambda 18, UV-vis-NIR spectrometer. Steady-state fluorescence spectra were acquired using a SPEX, Fluorolog-τ2 spectrofluorometer. The x-ray diffraction (XRD) instrument used was a Rigaku diffractometer using Cu $K_{\alpha 1}$ (0.154 nm) x-rays: typically run at a voltage of 40 kV and current of 30 mA. SEM was taken using an Amray 1910 FE-SEM (KLA-Tencor) which was made available to us by Dr. James Batteas of the Chemistry Department at the College of Staten Island.

Time-dependent emission measurements utilized a Hamamatsu streak camera, Model C4334, optically coupled to a charge-coupled-device (CCD) array detector. This system allowed the measurements of both the emission decay rate and the time-resolved emission spectrum. The light source is Spectra-Physics all solid state laser system and described in detail in the experimental section of Chapter 1.

3.3 Results and Discussion

Fig. 3-2 shows the SEM micrograph of a typical sample, aggregated TTBC-A/MCM-41 sample. XRD patterns of pristine calcined MCM-41, modified MCM-41, the monomer-incorporated composite (TTBC-M/MCM-41), and the aggregate-incorporated composite (TTBC-A/MCM-41) are shown in Fig. 3-3. Using Bragg's equation and comparison with reference studies [34-36], the pore size of calcined MCM-41 is estimated to be ca. 30 Å in line with result of N_2 adsorption-desorption isotherm (chapter 1). Additionally, we find, upon attachment of the (putative) monolayer of silylation product to the internal channels of the calcined MCM-41, that the pore size is narrowed to ca. 21 Å which is sufficiently large to allow TTBC, of approximate dimensions ca. (8 $\times$ 17) $Å^2$, to be incorporated into the modified MCM-41.

The XRD patterns of TTBC-M/MCM-41 and TTBC-A/MCM-41 show strong (100) peaks, suggesting that framework stability is still maintained for the modified MCM-41 when either monomeric or aggregated TTBC is incorporated. What difference in relative intensities that occur likely is attributable to electrostatic interaction between positive-

charged TTBC and the interior walls of the cage as well as with the aggregate's transverse dimension as it grows along the channel length of the aluminosilicate.

We found that monomeric TTBC could be occluded into either calcined or modified MCM-41. However, upon formation of aggregated TTBC from monomers, the (100) peak intensity for the calcined MCM-41 loses significant intensity (not shown), indicating that the framework was not sufficiently strong to allow aggregation, thus resulting in disintegration of the structure. Rigidification of the calcined MCM-41 was a prerequisite to allowing occluded aggregate formation. It is also to be noted that direct encapsulation of aggregated TTBC into the MCM-41 channels was not possible, and the "ship-in-bottle" approach, as used in our study dealing with encapsulation of TSPP into MCM-41 (Chapter 1), was used here also.

Diffuse reflectance (DR) UV-vis spectra of the samples designated TTBC-M/MCM-41 and TTBC-A/MCM-41 are shown in Fig. 3-4. Also included in this figure, for comparison purposes, are transmission UV-vis spectra of TTBC in methanol solution (where monomer exists) and in aqueous solution (at a pH concentration where aggregated TTBC forms). The prominent absorption band at 590 nm in this figure is termed the J-band and is indicative of aggregate formation. It is to be noted that we have also found, as will be detailed in a subsequent report by Akins et al, that resonance excitation of Raman scattering at 590 nm results in resonantly enhanced low frequency band (below ca. 300 cm^{-1}) that has been shown to also be diagnostic for aggregate formation [3,37].

Continuing with Figure 3-4, it is observed that the occluded monomer exhibits a blue shift for its absorption band (514 nm) when compared to the band of the solution

monomeric species (520 nm). A blue shift is also found for the encapsulated J-aggregate when compared to the solution aggregate, 580 nm and 592 nm, respectively. Such shifts can be rationalized in terms of intramolecular charge-transfer caused by host-guest interaction, which is connected to steric effects associated with the pore structure within modified MCM-41. The formation of the occluded monomer is rationalized by the fact that at pH = 7 the surface amino groups are not protonated, which makes it possible for positively charge TTBC to experience a favorable interaction with the lone pair electrons, thus facilitating monomer incorporation. The broaden structure for the monomeric band (part D) relative to that for the solution monomer (part C) can be attributed to site specific adsorption of encapsulated TTBC; suggesting that the monomer is distributed at various positions within the cage and experience, as a result, a range of perturbations.

Fluorescence spectra for solution phase and composite systems were also acquired (see Figure 4). As shown in parts A and B of Fig. 3-5, which were acquired with excitation at 490 nm, the emissions from monomeric TTBC in solution and the composite TTBC-M/MCM-41 reflect a Stokes shift relationships of their respective absorption bands shown in Fig. 3-4, but additionally the relatively greater Stokes shift (530 vs 537nm, respectively) and width of the composite suggests a larger rate for relaxation of excitonic energy. By the same argument, the similarity between the spectra of the aggregate in solution and in the composite (parts C and D, respectively; excited at 550 nm with peak positions at ca. 594 nm), both in terms of band positions and widths, can be interpreted as indicating that upon formation of the aggregate the molecules are coupled and realigned such that site specific perturbations to the exciton absorption energy, line width, and possibly other properties are diminished. In addition, when excited at 490 nm

(Part E of Fig. 3-5), strong emission at 590 nm is also observed for aggregated TTBC-A/MCM-41.

The decay curves and time-resolved fluorescence spectra foraggregated TSPP within both modified MCM-41 and in solution have been measured. Fig. 3-6, Fig. 3-6 and Fig. 3-8 show, respectively, decay curves for aggregated TTBC in MCM-41 and solution; time-resolved fluorescence of TTBC in solution and time-resolved fluorescence of TTBC in MCM-41.

For excitation at 550 nm, the emission decay kinetics for the aggregated TTBC-A/MCM-41 composite shows shortened lifetime, compared with the lifetime of solution aggregate TTBC (see Fig. 3-6). The lifetimes for aggregated TTBC-A/MCM-41 composite and solution aggregate are approximately 42 ps and 130 ps, respectively, by using single exponential fitting. From the time-resolved emission spectra (Fig. 3-7 and Fig. 3-8), the broader emission bands for TTBC-A/MCM-41, compared with those of aggregated solution. It demonstrates that there exists more microenvironment perturbation to the formed aggregate within solid sample because of heterogeneous effect, than that to the aggregate in homogeneous solution, in line with the steady state emission result above.

It is also to be noted that for TTBC-A/MCM-41, the much stronger temporal emission intensities at the initial emission stage are illustrated (see Fig. 3-7 and Fig. 3-8), thus the exciton emission for TTBC-A/MCM-41 is observed, which is anticipated in the present study.

3.4 Conclusion

The combination of XRD, UV-vis absorption and fluorescence measurements of TTBC in solution and post-formation addition to an MCM-41 aluminosilicate indicates that we are able to form monomeric and aggregated TTBC occluded in the core. Upon basifying the monomeric TTBC/MCM-41 composite, aggregated TTBC were formed from some occluded monomers. In order to facility formation of incorporated J-aggregated TTBC, surface silylation, using an alkoxysilane reagent, was performed to thicken and functionalize the walls of the aluminosilicate. The composite consisting of J-aggregated TTBC and the modified MCM-41 represents a new nanomaterial whose properties derive from exciton energies and dynamics that result from quantum confinement.

Bibliography

[1] Akins, D. L.; Özçelik, S.; Zhu, H. -R.; Guo, C. *J. Phys. Chem A.* **1997**, *101*, 3251.

[2] Özçelik, S.; Akins, D. L. *J. Phys. Chem. B* **1999**, *103*, 8926.

[3] Akins, D. L. *J. Phys. Chem.* **1986**, *90*,1530.

[4] Akins, D. L. *J. of Colloid and Interface Sci.* **1982**, *90*, 373.

[5] Li, X.; Gu, B.; Akins, D. L. *Chem. Phys. Lett.* **1984**, *105*, 263.

[6] Gu, B.; Akins, D. L. *Chem. Phys. Lett.* **1985**, *113*, 558.

[7] Akins, D. L.; Akpabli, C.; Li, X. *J. Phys. Chem.* **1989**, *93*, 1977.

[8] Akins, D. L.; Macklin, J. W. *J. Phys. Chem.* **1989**, *93*, 5999.

[9] Akins, D. L.; Macklin, J. W.; Parker, L.; Zhu, H. -R. **1990**, *169*, 564.

[10] Akins, D. L.; Macklin, J. W.; Zhu, H. ¨ R. *J. Phys. Chem.* **1990**, *95*, 793.

[11] Akins, D. L.; Zhu, H. -R. *Langmuir* **1992**, *8*, 546.

[12] Akins, D. L.; Macklin, J. W.; Zhu, H. -R. *J. Phys. Chem.* **1992**, *96*, 4515.

[13] Akins, D. L.; Zhuang, Y. H.; Zhu, H. ¨ R.; Li, J. Q. *J. Phys. Chem.* **1993**, *98*, 1068.

[14] Akins, D. L. In *J-Aggregate*; Kobayashi, T., Ed.; World Scientific: Singapore, 1996, pp 67¨ 84.

[15] Plyuto, Y.; Berquier, J.; Jacquiod, C.; Ricolleau, C.; *Chem. Commun.* **1999**, 1653.

[16] Wu, C.; Bein, T.; *Science* **1994**, *264*, 1757.

[17] Kageyama, K.; J. Tamazawa, J.; Aida, T. *Science* **1999**, *285*, 2113.

[18] Moller, K.; Bein, T.; *Chem. Mater.* **1998**, *10*, 2950.

[19] Holland, B. T.; C. Walkup, C.; Stein, A.; *J. Phys. Chem. B* **1998**, *102*, 4301.

[20] Hyung Mi, Sung-Suh, Luan, Z.; Kevan, L.; *J. Phys. Chem. B* **1997**,*49*, 10455.

[21] Stucky, G. D.; MacDougall, J. E.; *Science* **1990**, *247*, 669.

[22] Moller, K.; Bein, T. *Chem. Mater.* **1998**, *10*, 2950. (Review article, see references therein.)

[23] X. Feng, X. G. E. Fryxell, G. E.; Wang, L. Q.; Kim, A.Y.; Liu, J.; Kemner, K. M.; *Science* **1997**, *276*, 923.

[24] Chakraborty, P.; *J. Mater. Sci.* **1998**, *33*, 2235.

[25] Yang, P.; Wirnsberger, G.; Huang, H. C.; Cordero, S. R.; McGehee, M. D.; Scott, B.; Deng, T.; Whitesides, G. M.; Chmelka, B. F.; Buratto, S. K.; Stucky, G. D. *Science* **2000**, *287*, 465.

[26] Özçelik, S.; Akins, D. L. *Appl. Phys. Lett.* **1997**, *71*, 1.

[27] Özçelik, S.; Akins, D. L. *Appl. Phys. Lett.* **1998**, *73*, 1949.

[28] Grad, J.; Hernandez, G.; Mukamel, S. *Phys. Rev. A.* **1988**, *37*, 3835.

[29] Spano, F. C.; Mukamel, S. *J. Chem. Phys.* **1989**, *91*, 683.

[30] Spano, F. C.; Kuklinski, J. R.; Mukamel, S. *J. Chem. Phys.* **1991**, *94*, 7534.

[31] Kresge, C. T.; Leonowicz, M. E.; Roth, W. J.; Vartuli, J. C.; Beck, J. S.; *Nature* **1992**, *359*, 710.

[32] Beck, J. S.; Vartuli, J. C.; Roth, W. J.; Leonowicz, M. E.; Kresge, C. T.; Schmitt, K. D.; Chu, C. T.-W.; Olson, D. H.; Sheppard, E. W.; McCullen, B.; Higgins, J. B.; Schlenker, J. L. *J. Am. Chem. Soc.* **1992**, *114*, 10834.

[33] Liu, C. -J.; Li, S. -G.; Pang, W. -Q.; Che, C. -M. *Chem. Commun.*, **1997**, *65*, 78.

[34] Mercier, L.; Pinnavaia, T. J. *Adv. Mater.* **1997**, *9*, 500.

[35] Sung-Suh, Hyung Mi; Luan, Z.; Kevan, L. *J. Phys. Chem. B.*, **1997**, *101*, 10455.

[36] Stucky, G. D.; Monnier, A.; Schuth, F.; Huo, Q.; Margolese, D.; Kumar, D.; Kridhnamurty, M.; Petroff, P.; Firouzi, A.; Janicke, M.; Chmelka, B. F. *Mol. Cryst. Liq. Cryst.*, **1994**, *240*, 187.

[37] Akins, D. L.; Zhu, H. -R.; Guo, C. *J. Phys. Chem.* **1996**, *100*, 5420.

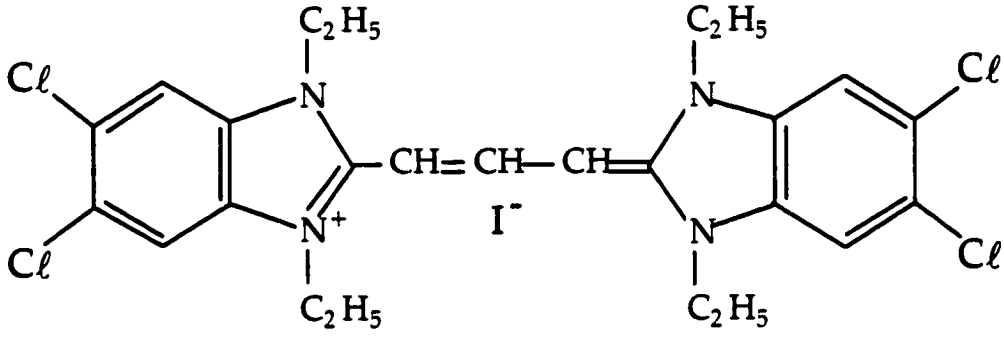

Fig. 3-1

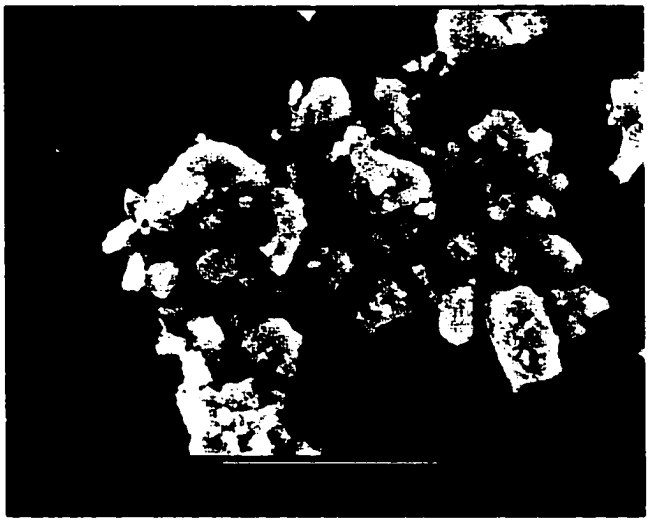

Fig. 3-2

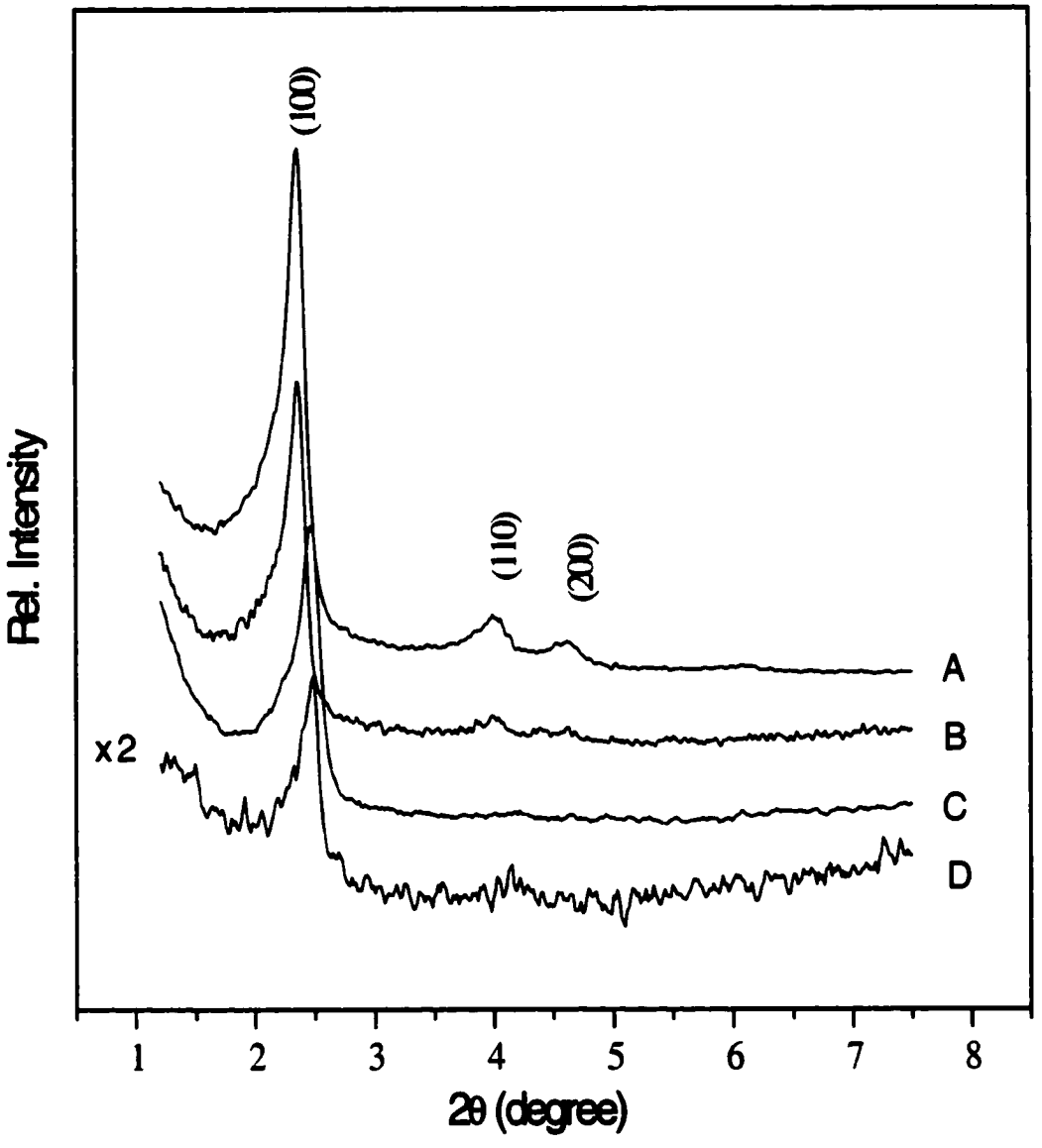

Fig 3-3

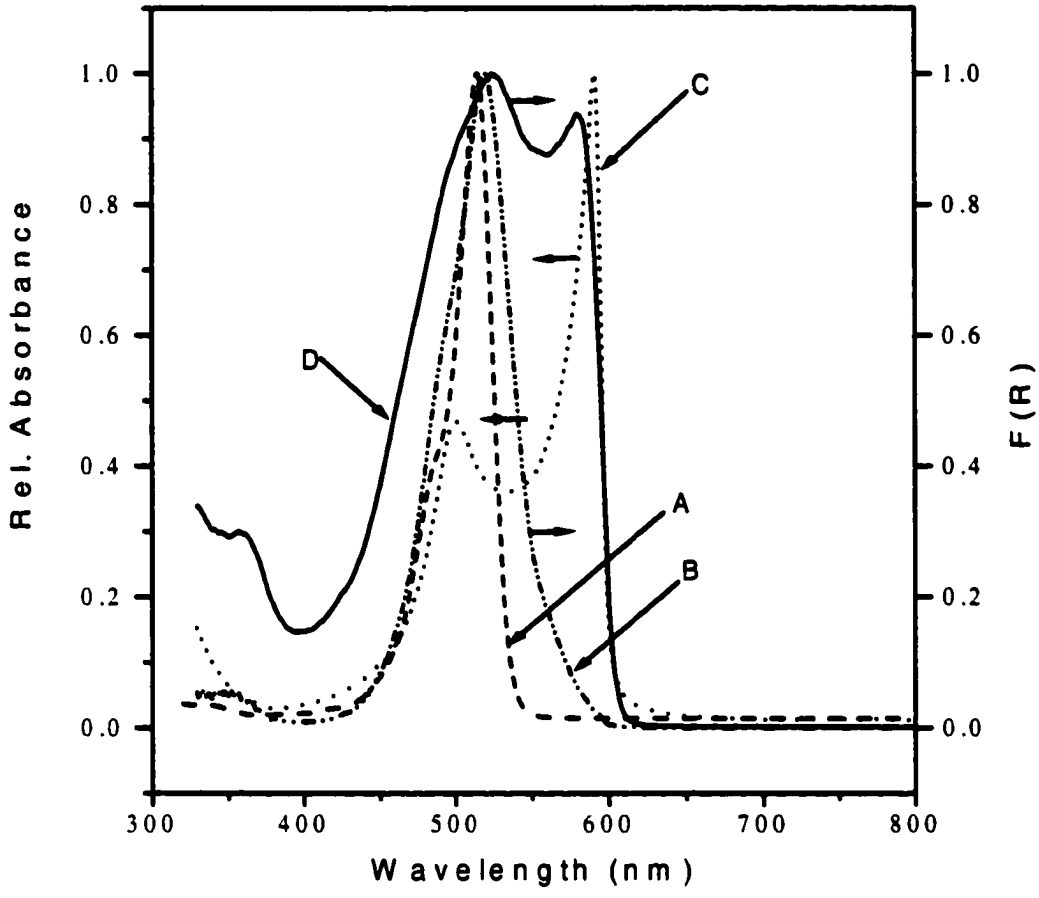

Fig. 3-4

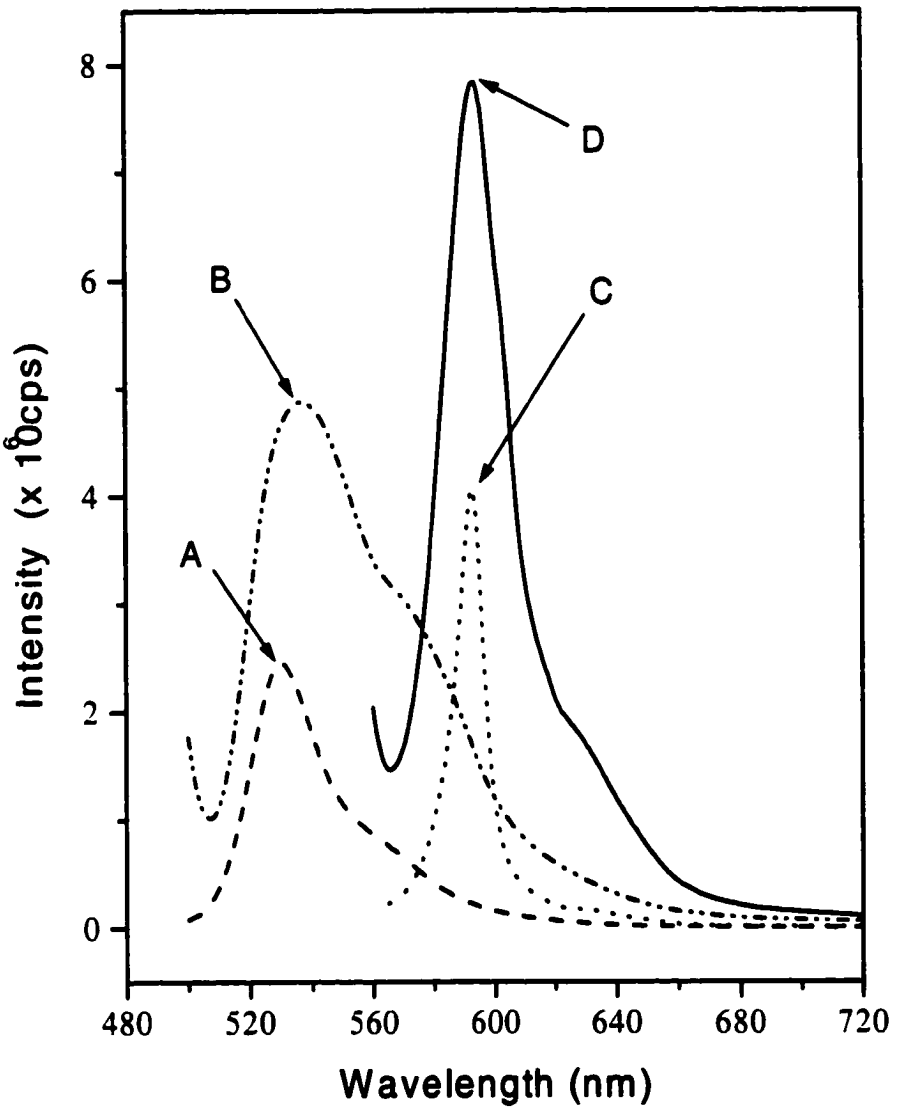

Fig. 3-5

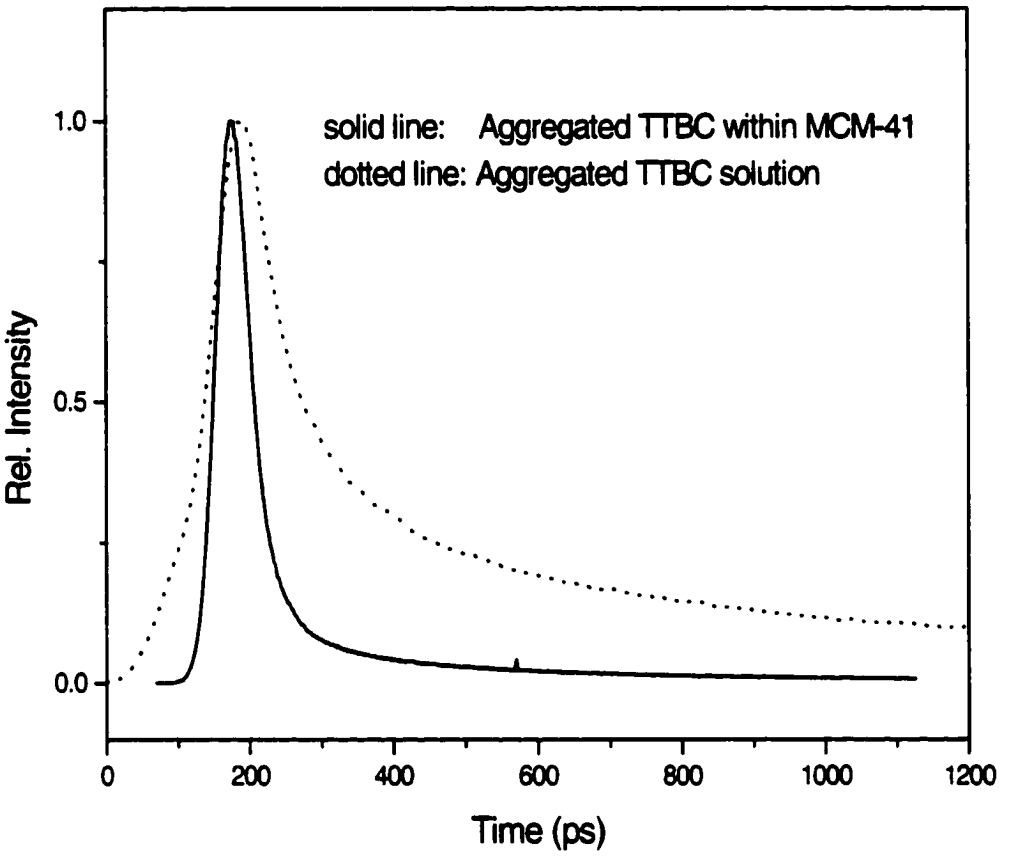

Fig. 3-6

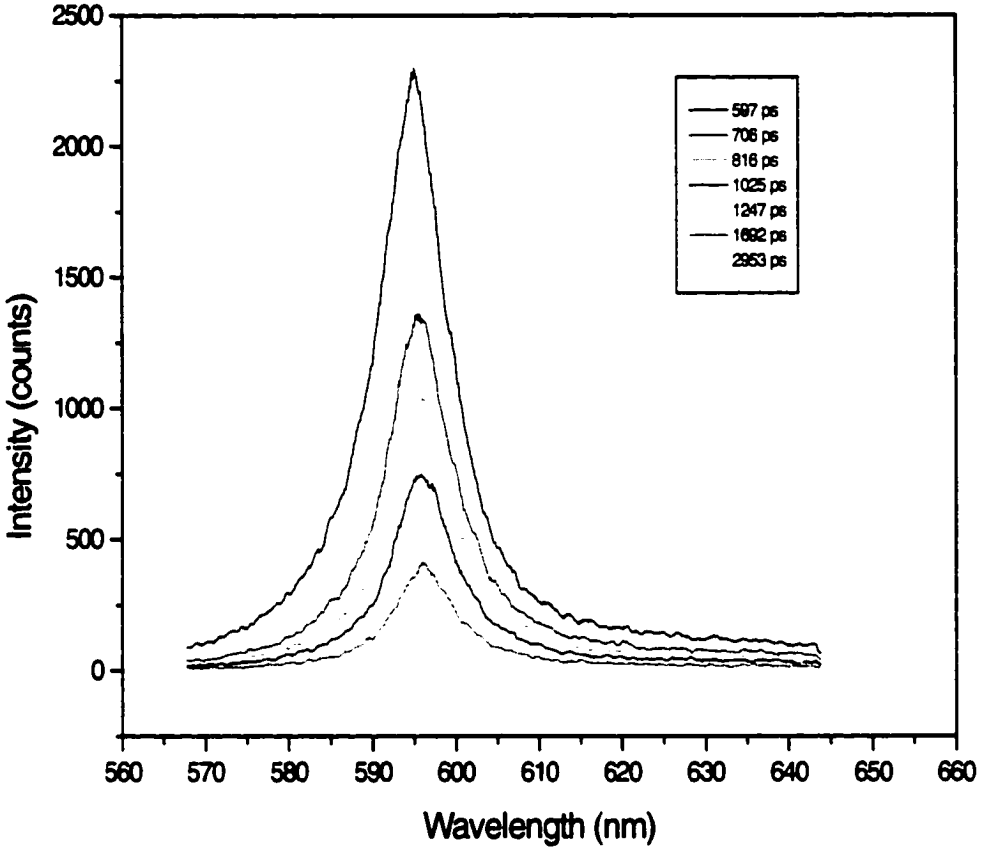

Fig. 3-7

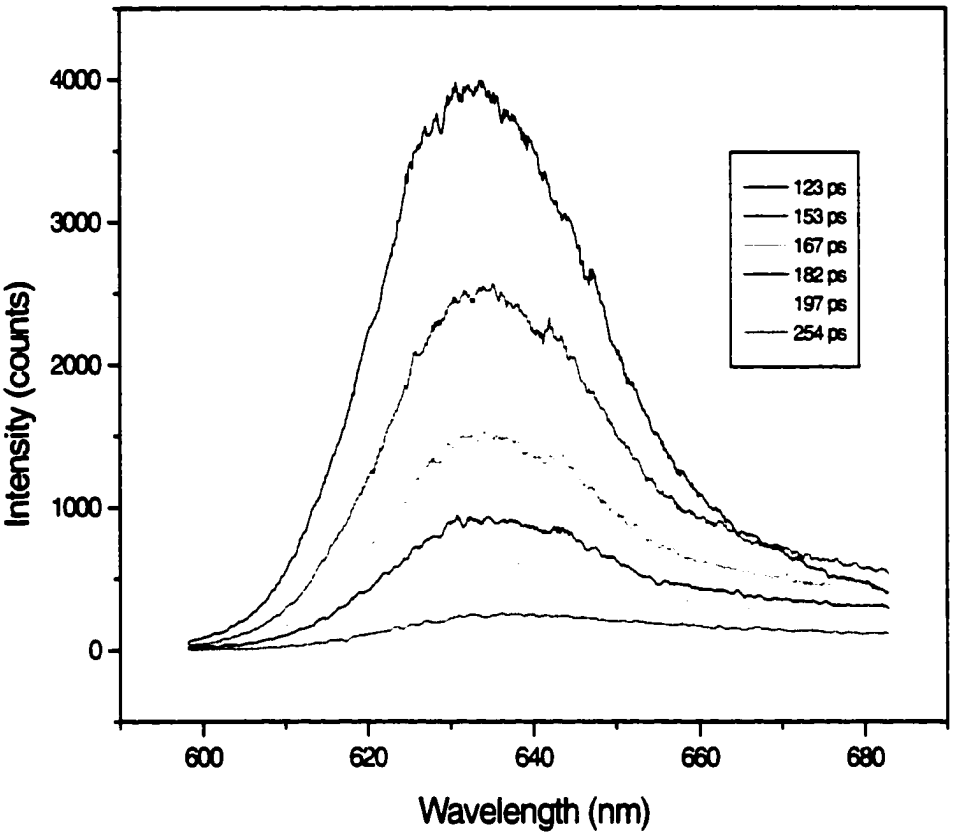

Fig. 3-8

CHAPTER 4

ABSORPTION AND EXCITON EMISSION BY AN AGGREGATED CYANINE DYE OCCLUDED WITHIN ESOPOROUS SBA-15

4.1 Introduction

Research dealing with spectral and optical dynamics properties of molecular aggregated structures is of continuing interest for a large number of scientists and engineers. Interest in molecular aggregates, at the most fundamental level, derives from the opportunity such structures present to study intermolecular interactions that have a decidedly directional character and a resulting reduced degree of freedom for both electronic and nuclear motions. At its most sophisticated level, interest in aggregates derives from the realization that aggregated molecules play crucial roles in nature; indeed, processes upon which life itself depends, such as light harvesting and the primary charge-separation steps in photosynthesis, are facilitated by aggregated species [1-4].

The primary mechanism through which molecular aggregate structures are formed in both artificial and natural systems is self-assembly through intrinsic intermolecular interactions. Often, such aggregates can be classified, based on their spectral properties, as being of J- or H-type, defined by the relative orientations of induced transition dipoles of the constituent molecules, either "head-to-tail" or "head-to-head," respectively [5]; J-aggregate structures have been the most studied. A potentially useful phenomenon associated with the alignment of the transition dipole moments in aggregates is the

coherent participation of molecules in absorption, emission and scattering, which can amplify each of these phenomena and dramatically change spectral and temporal properties. In general, any such changes result from creation of new energy states for the aggregate, due to the implicit coupling of quantum states of the constituent monomers. As a result, spectra and optical dynamics of molecular aggregates are subjects of intense interest for device applications.

We report in this chapter, further efforts to form cyanine aggregates as much as possible within one-dimensional mesoporous silicates by trying different cyanine dye from Chapter 3. These composites are being examined as potential new nanostructural material with useful optical properties, including, in some cases, high luminescence cross-section (resulting from superradiance), controllable strong attenuation of incident radiation, and for their chemical sensors prospects. As we mentioned in previous chapters, in our present study, these composites consisting of one-dimensional channel structure material and cyanine dye are quite distinct from those investigated by other investigators, whose efforts have focused on occluded molecules or atoms, with the aim to exploit their evinced catalytic, environmentally remunerative or optoelectronic properties [6-15].

Recently, studies from this laboratory have been reported on techniques for forming aggregated molecules within MCM-14 siliceous structures and some of the results are also included in previous chapters [16,17]. In one study (Chapter 1) we encapsulated tetrakis(*p*-sulfonatophenyl)porphyrin, also referred to as TSPP, within aluminum incorporated MCM-41, and provided spectroscopic evidence that confirmed the encapsulation—in particular, the dramatic changes in absorption and emission spectra

that occur upon formation of the occluded aggregate [16]. However, this system has reduced prospect for exploitation of the composite material for device or new materials applications, because exciton emission, which is indicative of aggregate formation, is weak. The weakness of the emission is due to the resultant emission from the Q-state, following internal conversion from the initially excited B-state of the porphyrin and the low emission cross section between the Q-state and the ground state. In a second study (Chapter 3), we have encapsulated monomeric and aggregated 1,1',3,3'-tetraethyl-5,5',6,6'-tetrachlorobenzimidazolocarbocyanine (referred to as TTBC) within MCM-41 and found strong excitonic emission from the aggregated composite [17]. But, for this latter case, the amount of aggregated TTBC formed within the channels of MCM-41, as a result of the synthetic approach used, did not dominate the emission from the sample, since a substantial amount of monomer remained within the mesoporous channels. Moreover, from XRD studies we ascertained that the structural integrity of the aluminosilicate was somewhat compromised upon forming the occluded aggregate. Consequently, this sample also had diminished promise as regards applications.

In the present study, we have replaced MCM-41 with SBA-15, which has a thicker wall structure, which can be varied in the range 31 to 64 Å, than the 10 to 15 Årange commonly found for MCM-41. We have additionally developed an encapsulation strategy and used a cyanine dye that leads, mainly, to the formation of the aggregated species within the mesoporous core of the silicate.

SBA-15 was first synthesized in 1998 [18], and is similar to MCM-41 in structure, composition and pore size. And the latter can be varied in the range from 46 to 300 Åby choice of template (*vide infra*) and hydrothermal treatment.

In the present chapter, we report the preparation and optically excited luminescence of a nanocomposite consisting of a cyanine dye (specifically, TDBC, see Diagram 1) occluded within modified mesoporous SBA-15 (*vide infra*). Both monomeric and J-aggregated TDBC was encapsulated within modified SBA-15 by host-guest interaction. J-aggregated TDBC was formed from TDBC monomers within the channels by changing the pH of the microenvironment within the cavity. As detailed in our recent publications regarding composites derived from aluminosilicates and aggregated molecules [16,17], luminescence results from coherent emission from the excitonic state derived from coupled, aligned monomeric species within such quantum confinement systems.

4.2 Experimental

4.2.1 Synthesis of Modified SBA-15

Polycrystalline powders of the mesostructural siliceous SBA-15 were prepared by using triblock copolymer as the template [18,19]. Briefly, 6.0 g of triblock poly(ethylene oxide)-poly(propylene oxide)-poly(ethylene oxide) ($EO_{20}PO_{70}EO_{20}$, Pluronic 123, Aldrich) was dissolved in 170 ml of 2 M aqueous HCl with stirring. Then 13.5 ml of tetraethyl orthosilicate (TEOS, Aldrich) was added drop wise to the resultant solution at room temperature. The mixture was stirred for 24 hrs at 313 K. Then the temperature was raised to 373 K, and the reaction allowed for 48 hrs in a Teflon-lined autoclave. The resulting precipitate was filtered, dried, and calcined in air at 773 K to obtain the final product, SBA-15 (see discussion below of XRD patterns).

To functionalize the synthesized SBA-15, in order to promote monomeric TDBC incorporation as well as formation of aggregated TDBC from the occluded monomers—by satisfying guest-host intermolecular and/or electrostatic interactions, we modified the surface of the SBA-15 through use of a silylation reagent, aminopropyltriethoxysilane (APTES; NH_2-$(CH_2)_3$-Si-$(C_2H_5O)_3$), which links oxygen atoms on the silicate surface.

For our studies, the modified SBA-15 was prepared by using a similar approach as we used in the modification of MCM-41 [16]. Briefly, about 0.5 g of the calcined SBA-15 was mixed with a chloroform solution of APTES (25 ml, 0.2 M) and stirred overnight at room temperature. The precipitate was filtered and washed with chloroform and dichloromethane.

Various TDBC/SBA-15 assemblies were obtained through mixing of the modified SBA-15 with TDBC monomer in different ratios. Upon basifying filtered residues containing various assemblies in a programmed way, thereby changing the pH of the microenvironment within the cavity of the silicate, conditions were attained where the J-aggregated TDBC were formed from occluded monomers. Specifics of the chemical and spectroscopic techniques are provided below.

4.2.2 Formation of TDBC/SBA-15 Composites

A typical preparation of a TDBC/SBA-15 composite involved stirring a mixture of 300 mg of modified SBA-15, 15 ml of TDBC solution (derived from 3.0 mg TDBC dissolved in 15 ml of water:methanol mixed solvent of volume ratio (H_2O:CH_3OH) of 9:1 for at least 24 hrs at room temperature, with the pH held at ca. 4.5 (using 2 M H_2SO_4). The solution was then centrifuged, and the transparent aqueous solution decanted. The

residue was washed at least 3 times with distilled water to remove TDBC monomers from the external surface and then dried in air. The product is here designated TDBC-M/SBA-15, where TDBC-M indicates that monomeric TDBC is encapsulated within the modified SBA-15.

The formation of occluded, aggregated TDBC involved adding 2 M NaOH to the solid occluded monomer residue described above. An immediate color change of the residue occurred from white to dark pink. Absorption spectra of the powdered residue (see below, section III) indicated the presence of occluded J-aggregated TDBC, here designated TDBC-A/SBA-15.

4.2.3 Instrumentation

Absorption spectra were recorded using a Perkin-Elmer, Lambda 18, UV-vis-NIR spectrometer. Steady-state fluorescence spectra were acquired using a SPEX, Fluorolog-τ2 spectrofluorometer. The x-ray diffraction (XRD) instrument used was a Rigaku diffractometer using Cu $K_{\alpha 1}$ (0.154 nm) x-rays: typically run at a voltage of 40 kV and current of 30 mA. SEM was taken using an Amray 1910 FE-SEM (KLA-Tencor), which was made available to us by Dr. James Batteas of the Chemistry Department at the College of Staten Island.

Time-dependent emission measurements utilized a Hamamatsu streak camera, Model C4334, optically coupled to a charge-coupled-device (CCD) array detector. This system allowed the measurements of both the emission decay rate and the time-resolved emission spectrum. The light source is Spectra-Physics all solid state laser system and described in detail in experimental section of Chapter 1.

4.3 Results and Discussion

XRD patterns of pristine calcined SBA-15, modified SBA-15, and the aggregate-incorporated composite (TDBC-A/SBA-15) are shown in Figure 4-1. Using Bragg's equation and comparison with reference studies [18], an interplanar spacing $d_{100} \approx 77$ Å for calcined SBA-15 was observed, and the pore size and wall thickness of calcined SBA-15 are estimated to be ca. 50 and 40 Å respectively. Additionally, we found, upon attachment of the (putative) monolayer of silylation product, that the pore size was narrowed to ca. 42 Å which is sufficiently large to allow TDBC to be incorporated into the modified SBA-15.

The XRD patterns of modified SBA-15 and TDBC-A/SBA-15 show strong (100) peaks, suggesting that framework stability of the mesoporous material is well maintained for modified SBA-15 when aggregated TDBC is formed in its interior. It is to be noted that there is almost no change in relative intensities of (110) and (200) scattering reflections for aggregated TDBC-A/SBA-15 composite in comparison to calcined SBA-15 and modified SBA-15. In our prior work [16,17], when an aggregated cyanine dye (TTBC) or an aggregated porphyrin (TSPP) was formed within modified MCM-41, although the MCM-41 ordered structure was maintained, the relative intensities of (110) and (200) reflections were dramatically decreased. Our observation for SBA-15 is interpreted as indicating that the thicker wall aids in maintaining structural integrity when occluded, aggregated TDBC is formed. Moreover, a greater stability of SBA-15 compared to MCM-41 has been demonstrated through its stability in boiling water [18], which MCM-41 does not survive. For the present study, silylation is mainly used to functionalize SBA-15 so as to satisfy the requirement for host-guest interaction, while, in

our earlier studies, silylation of MCM-41 was used both to rigidify the framework upon incorporation of the aggregated species and to functionalize the interface for appropriate guest-host interaction [16,17].

Fig. 4-2 shows the SEM micrograph of synthesized SBA-15. The rod shown in Fig. 4-2 is about 2.5 μm in length and 0.2 μm in diameter. For practical application, the rod-shaped SBA-15 with uniform pore size is desirable to encapsulate aggregated cyanine dye molecules within the channels.

It is also to be noted that direct encapsulation of aggregated TDBC into the MCM-41 channels was not possible, and the "ship-in-bottle" approach, as used in our earlier studies [16,17], was used here also. Thus, to meet host-guest requirement, it is necessary to first encapsulate the monomers in the modified SBA-15 and then to form aggregated TDBC within the pores of SBA-15.

The diffuse reflectance (DR), UV-vis spectrum of the sample designated TDBC-A/SBA-15 is shown in Fig. 4-3. Also included in this figure, for comparison purposes, are transmission UV-vis spectra of TDBC in methanol solution (where monomer exists) and in aqueous solution (at a pH where aggregated TDBC forms). The prominent absorption bands near 590 nm in the figure are attributable to the J-band and are diagnostic for presence of aggregated molecules. The band at ca. 518 nm is attributed to the solution monomeric species. The lack of a spectrum for the TDBC-M/SBA-15 composite in Fig. 4-3 is due to the colorless nature of the sample for the pH (i.e., 4.5) at which individual molecules become occluded within the aluminosilicate, ostensibly due to a change of the chemical form of monomer to, possibly, a protonated form of the dye,

which characteristically does not absorb light in the visible region [20,21]. In this latter case, the protonation would be expected to involve the proton associated with the surface NH_3^+ groups on the surface.

We further note that in Fig. 4-3 a blue shift is found for the occluded J-aggregate when compared to the solution aggregate, 583 nm versus 587 nm, respectively. Such a shift can be rationalized in terms of charge-transfer caused by host-guest interaction, which is connected to steric effects associated with the pore structure within modified SBA-15. The presence of sites with different interaction strengths with the occluded species is expected to lead to broadening of the absorption spectrum relative to that of the solution aggregates, as is shown for TDBC-A/SBA-15 in Fig. 4-3 upon comparing parts C and B, respectively.

We also note that the intensity of the shoulder of the aggregate absorption in Fig. 4-3 (Part C), with wavelength near that of the solution monomer absorption peak, might at first thought be attributed to the monomer's absorption, however, as revealed in Figure 3, which pertains to the fluorescence of the same sample, the emission also contains the mirror image of this apparent feature. We thus attribute this feature to a vibronic band of the aggregate. We additionally conclude, based on this assignment of the shoulder in the absorption spectrum, that the majority of TDBC in TDBC-A/SBA-15 composite exists in aggregated form. It might be noted that our prior work with occluded TTBC suggested that only about half of the occluded TTBC molecules existed in the aggregated state in the channels of MCM-41 [17], thus the present system represents a better fit to our initial goal of constructing a system in which the aggregated form of the cyanine dye is the majority species present in the core of the aluminosilicate.

Fluorescence spectra for solution phase and composite system are contained in Figure 4-4. As shown in parts B and C of Fig. 4-4, which were acquired with excitation at 550 nm, the emissions from aggregated TDBC in solution and the composite TDBC-A/MCM-41 reflect a Stokes shift relationships of their respective absorption bands shown in Fig. 4-3. The exciton band at ca. 590 nm for each sample is observed, which is exactly what to be expected for mirror emission associated with corresponding absorption shown in Fig. 4-3. A similar result is also illustrated for the emission of monomeric TDBC in methanol (part A). The similarity between the spectra of the aggregate in solution and in the composite, both in terms of band positions and widths, can be interpreted as indicating that upon formation of the aggregate the molecules are coupled and realigned such that site specific perturbations to the exciton absorption energy, line width, and possibly other properties are diminished.

The decay curves and time-resolved fluorescence spectra for aggregated TDBC within both modified SBA-15 and in solution have been measured. Fig.4-5, Fig. 4-6 and Fig. 4-7 show, respectively, decay curves for aggregated TDBC in SBA-15 and solution; time-resolved fluorescence of TDBC in solution and time-resolved fluorescence of TDBC in SBA-15.

For excitation at 550 nm, the emission decay kinetics for the aggregated TDBC-A/SBA-15 composite shows shortened lifetime, compared with the lifetime of solution aggregate sample (see Fig. 4-5). The lifetimes for aggregated TDBC-A/SBA-15 composite and solution aggregate are approximately 77 ps and 205 ps, respectively, by using single exponential fitting. From the time-resolved emission spectra (Fig. 4-6 and Fig. 4-7), the broader emission bands for TDBC-A/SBA-15, compared with those of

aggregated solution. It demonstrates that there exists more microenvironment perturbation to the formed aggregate within solid sample because of heterogeneous effect, than that to the aggregate in homogeneous solution, in line with the steady state emission result above. It is also to be noted that for TDBC-A/SBA-15, the much stronger temporal emission intensities at the initial emission stage are illustrated (see Fig. 4-6 and Fig. 4-7), thus the exciton emission for TDBC-A/MCM-41 is observed, which is anticipated in the present study. In addition, the red-shift of emission peaks for TDBC-A/MCM-41 is also demonstrated, in line with the steady state fluorescence result.

4.4 Conclusion

The combination of XRD, UV-vis absorption and fluorescence measurements of TDBC in solution and post-formation addition to SBA-15 silicate indicates that we are able to form aggregated TDBC occluded in the core. Upon basifying the monomeric TDBC/SBA-15 composite, aggregated TDBC is formed from occluded monomers. In order to facilitate formation of incorporated J-aggregated TDBC, surface silylation, using an alkoxysilane reagent, was performed to functionalize the walls of the silicate. The composite consisting of J-aggregated TDBC and the modified SBA-15 represents a new nanomaterial whose spectroscopic properties emanate from quantum confinement associated with coherently responding molecules, associated with the coherence length, and whose structural form is further dictated by the restricted growth region defined by the one-dimensional nanoporous structure of the silicate.

Bibliography

[1] Pearlstein, R. M. In *Photosynthesis*, Amesz, J., Ed.; Elsevier: Amsterdam **1987**, pp. 299-317.

[2] Warshel, A.; Parson, W. W. *J. Am. Chem. Soc.* **1987**, *109*, 6152.

[3] Creighton, S.; Hwang, J. -K.; Warshel, A.; Parson, W. W.; Norris, J. *Biochemistry* **1988**, *27*, 774.

[4] Michel-Beyerle, M. E.; Plato, M.; Deisenhofer, J.; Michel, H.; Bixon, M.; Jorter, L. *Biochem. Biophys. Acta* **1988**, *932*, 52.

[5] Kasha, M. *Radiation Res.* **1963**, *20*, 55.

[6] Plyuto, Y.; Berquier, J.; Jacquiod, C.; Ricolleau, C. *Chem. Commun.* **1999**, 1653.

[7] Wu, C.; Bein, T. *Science* **1994**, *264*, 1757.

[8] Kageyama, K.; Tamazawa, J.; Aida, T. *Science* **1999**, *285*, 2113.

[9] Moller, K.; Bein, T. *Chem. Mater.* **1998**, *10*, 2950.

[10] Holland, B. T.; C. Walkup, C.; Stein, A. *J. Phys. Chem. B* **1998**, *102*, 4301.

[11] Sung-Suh, H.; Luan, Z.; Kevan, L. *J. Phys. Chem. B* **1997**, *49*, 10455.

[12] Stucky, G. D.; MacDougall, J. E. *Science* **1990**, *247*, 669.

[13] Moller, K.; Bein, T. *Chem. Mater.* **1998**, *10*, 2950. (Review article, see references therein.)

[14] Feng, X.; Fryxell, G. E.; Wang, L. Q.; Kim, A.Y.; Liu, J.; Kemner, K. M. *Science* **1997**, *276*, 923.

[15] Chakraborty, P. *J. Mater. Sci.* **1998**, *33*, 2235.

[16] Xu, W.; Guo, H.; Akins, D. L. *J. Phys. Chem. B.*, **2001**, *105*, 1543.

[17] Xu, W.; Guo, H.; Akins, D. L. *J. Phys. Chem. B.*, **2001**, *105*, 7687.

[18] Zhao, D.; Feng, J.; Huo, Q.; Melosh, N.; Fredrickson, G. H.; Chmelka B. F.; Stucky G. D. *Science* **1998**, *297*, 548.

[19] Zhao, D.; Huo, Q.; Feng, J.; Chmelka, B. F.; Stucky, G. D. J. Am. Chem. Soc. 1998, 120, 6024.

[20] Akins, D. L.; Macklin, J. W. *J. Phys. Chem.* **1989**, *93*, 5999.

[21] Herz, A. H. *Adv. Colloid. Interfacial Sci.* **1977**, *8*, 237.

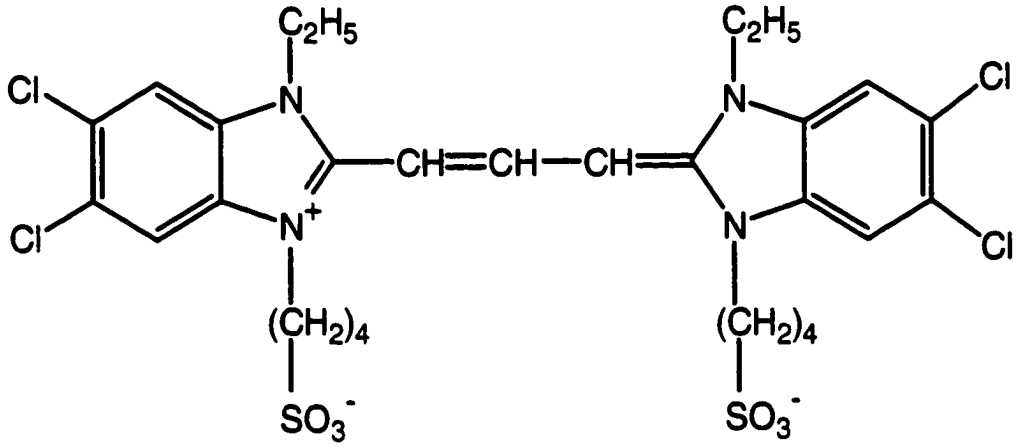

Diagram 4-1

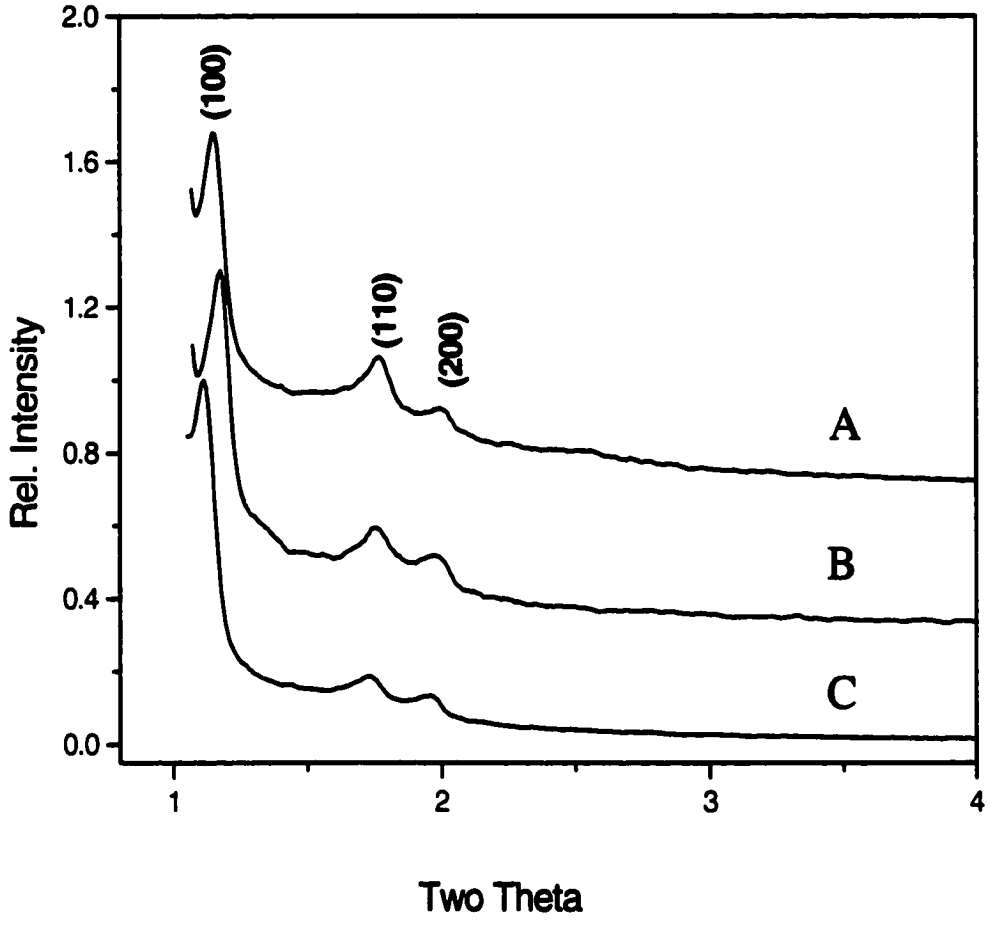

Fig. 4-1

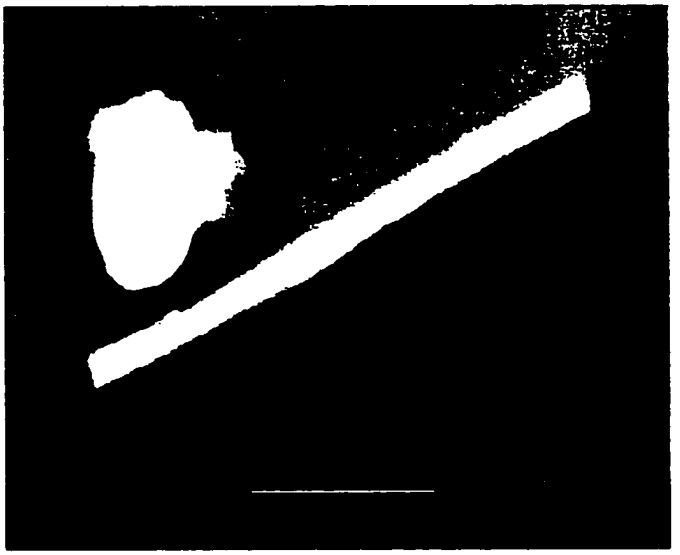

Fig. 4-2

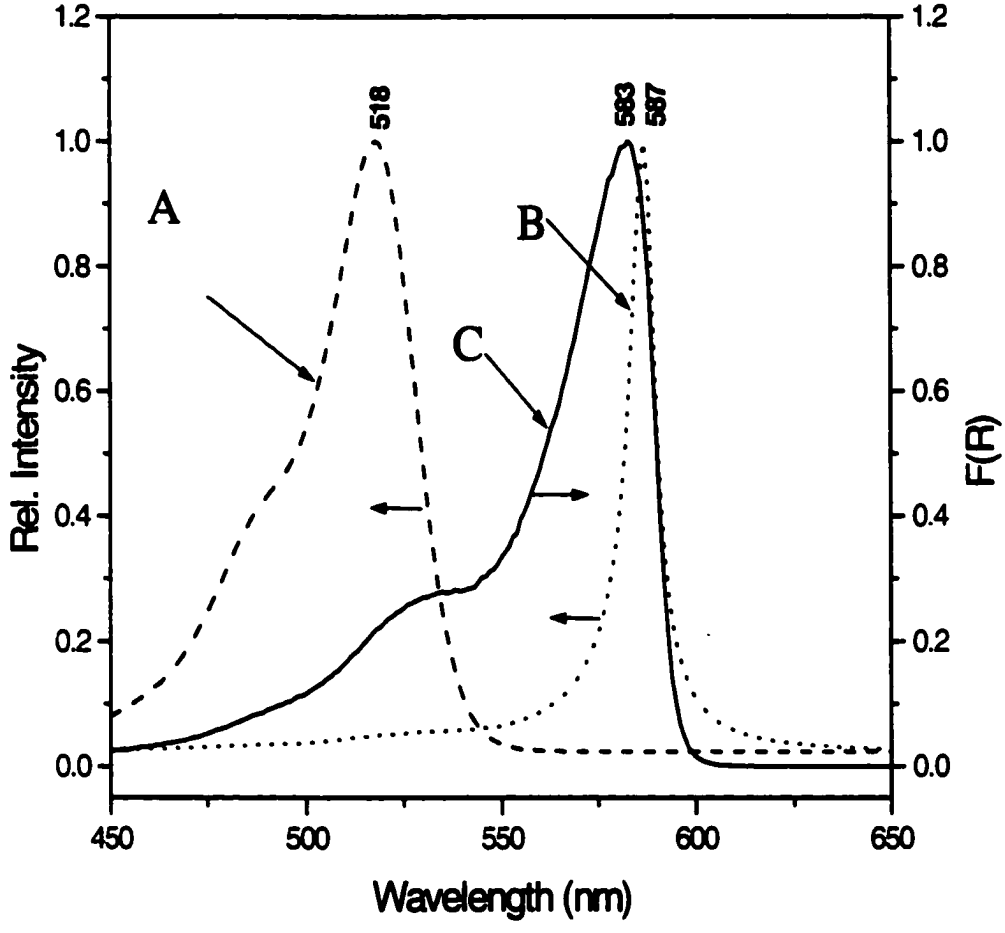

Fig. 4-3

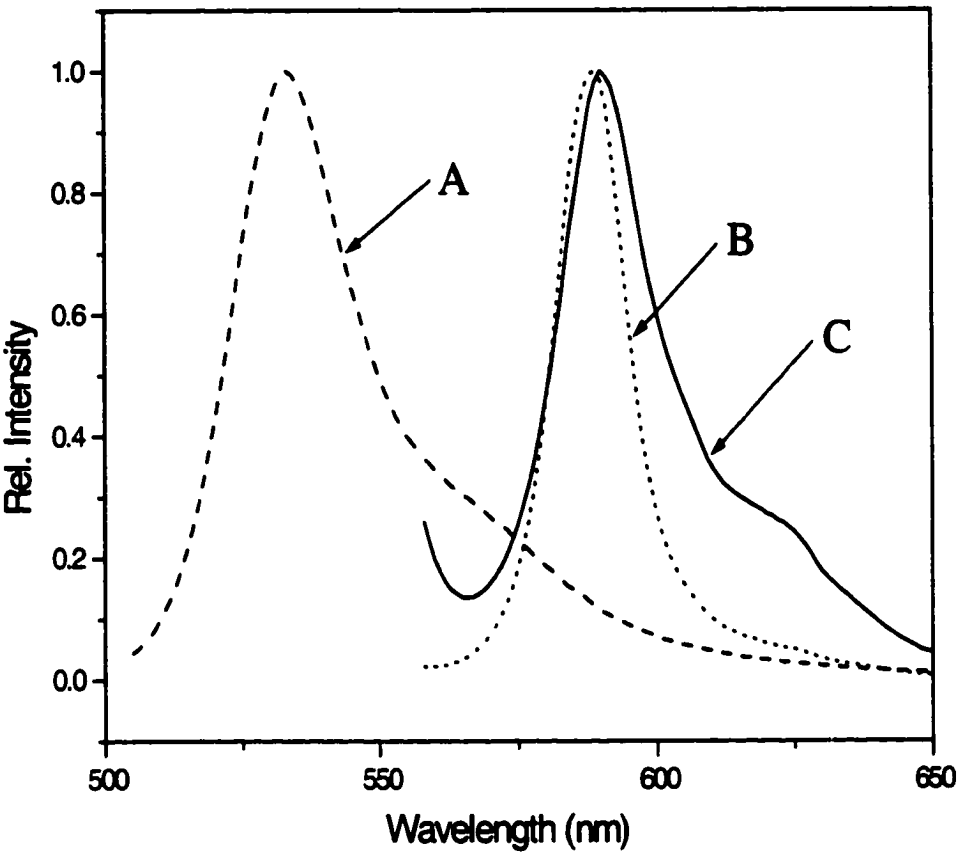

Fig. 4-4

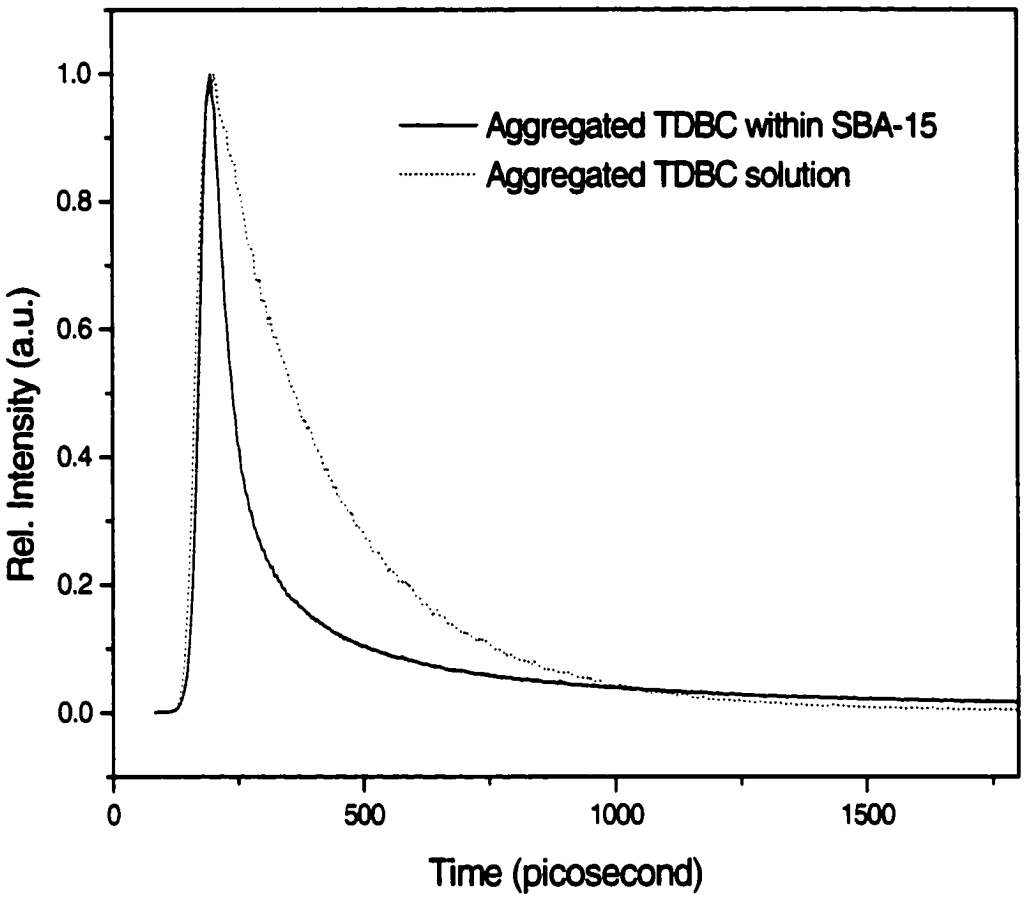

Fig. 4-5

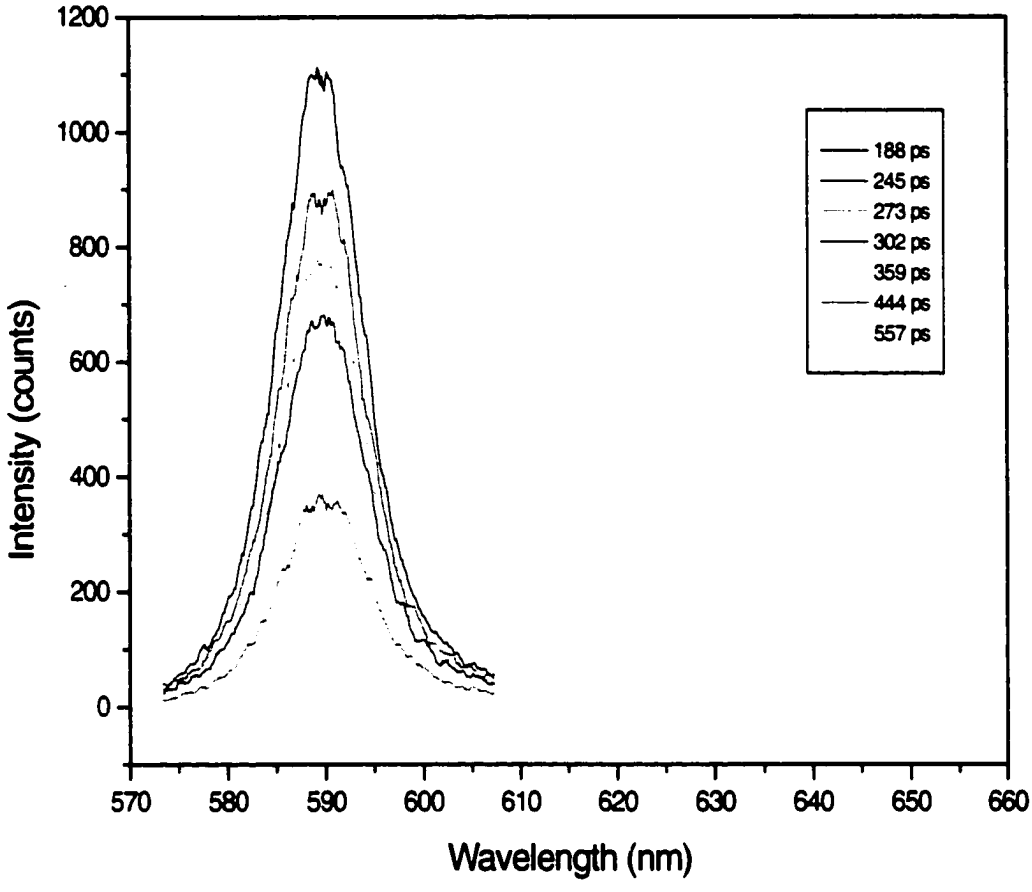

Fig. 4-6

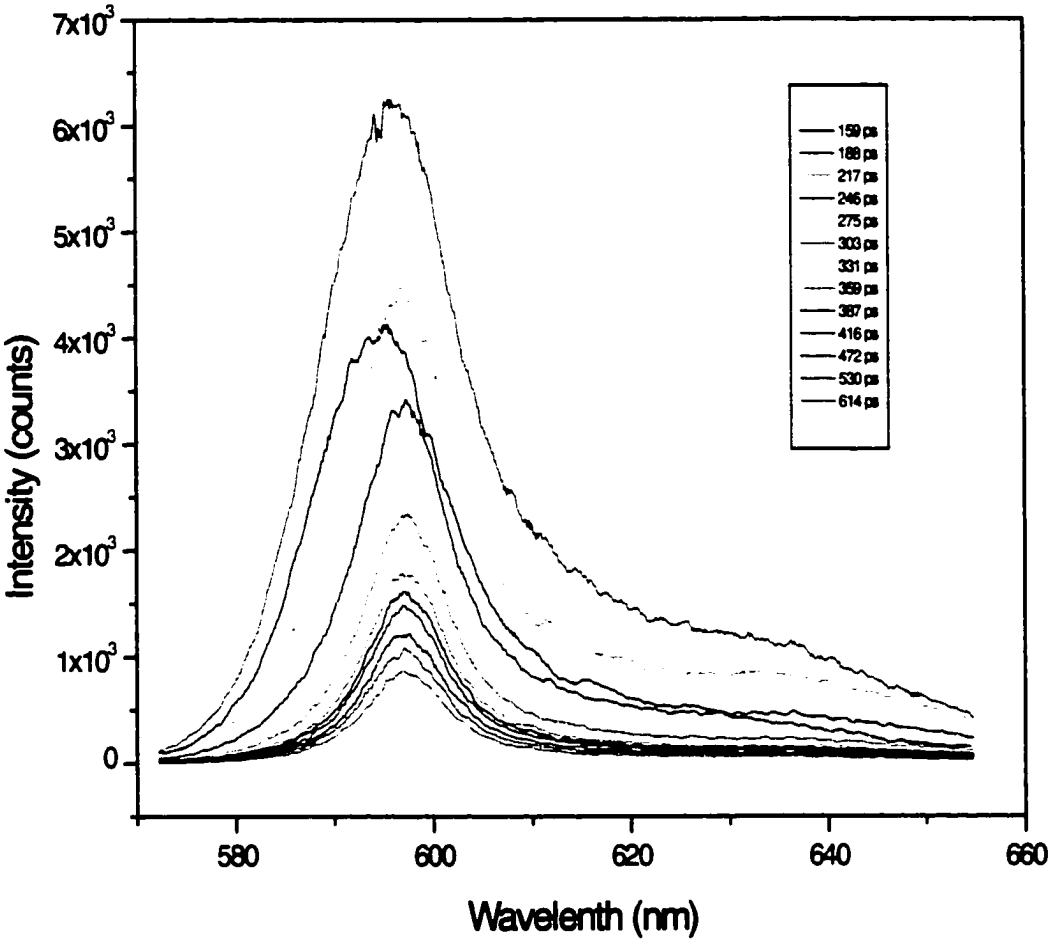

Fig. 4-7

Bibliography

References of Chapter 1

[1] Okamura, M. Y.; Feher, G.; Nelson, N. In *Photosynthesis*, Govindjee, Ed.; Academic Press: New York, **1982**, pp. 195-272.

[2] Pearlstein, R. M. In *Photosynthesis*, Amesz, J., Ed.; Elsevier: Amsterdam, **1987**, pp 299-317.

[3] O'Neil, M. P.; Niemcyzk, M. P.; Svec, W. A.; Gosztola, D.; Gaines III, G. L.; Wasielewski, M. R. *Science* **1992**, *257*, 63.

[4] Wagner, R. W.; Lindsey, J. S.; Seth, J.; Palaniappan, V.; Bocian, D. F. *J. Am. Chem. Soc.* **1996**, *118*, 3996.

[5] Akins, D. L.; Zhu, H.-R.; Guo, C. *J. Phys. Chem.* **1994**, *98*, 3612.

[6] Akins, D. L.; Zhu, H.-R.; Guo, C. *J. Phys. Chem.* **1996**, *100*, 5420.

[7] Akins. D. L. In *J-Aggregate*; Kobayashi, T., Ed.; World Scientific: Singapore, 1996, pp 67- 94.

[8] Guo, C.; Ren, B.; Akins, D. L. *J. Phys. Chem. B.* **1998**, *102*, 8751.

[9] Guo, C.; Ren, B.; Akins, D. L. *J. Phys. Chem.* In revision, **2000**.

[10] Beck, J. S.; Vartuli, J. C.; Roth, W. J.; Leonowicz, M. E.; Kresge, C. T.; Schmitt, K. D.; Chu, C. T.-W.; Olsen, D. H.; Sheppard, E. W.; McCullen, B.; Higgins, J. B.; Schlenker, J. L. *J. Am. Chem. Soc.* **1992**, *114*, 10834.

[11] Grad, J.; Hernandez, G.; Mukamel, S. *Phys. Rev. A.* **1988**, *37*, 3835.

[12] Spano, F. C.; Mukamel, S. *J. Chem. Phys.* **1989**, *91*, 683.

[13] Spano, F. C.; Kuklinski, J. R.; Mukamel, S. *J. Chem. Phys.* **1991**, *94*, 7534.

[14] Kresge, C. T.; Leonowicz, M. E.; Roth, W. J.; Vartuli, J. C.; Beck, J. S. *Nature* **1992**, *359*, 710.[15] Liu, C. -J.; Li, S. -G.; Pang, W. -Q.; Che, C. -M. *Chem. Commun.*, **1997**, *65*, 78.

[16] Mercier, L.; Pinnavaia, T. J. *Adv. Mater.* **1997**, *9*, 500.

[17] (a) Feng, X.; Fryxell, G. E.; Wang, L. Q.; Kim, A. Y.; Liu, J.; Kemner, K. M. *Science* **1997**, *276*, 923. (b) Liu, J.; Feng, X.; Fryxell, G. E.; Wang, L. Q.; Kim, A. Y.; Gong, M. *Adv. Mater.* **1998**, *10*, 161.

[18] (a) Cauvel, A.; Renard, G.; Brunel, D. *J. Org. Chem.* **1997**, *62*, 749. (b) Brunel, D.; Cauvel, A.; Fajula, F.; DiRenzo, F. *Stud. Surf. Sci. Catal.* **1995**, *97*, 173.

[19] Sutra, P.; Brunel, D. *Chem. Commun.* **1996**, 2485.

[20] Bellocq, N.; Brunel, D.; Lasperas, M.; Moreau, P. *Stud. Surf. Sci. Catal.* **1997**, *108*, 485.

[21] (a) Subba Rao, Y. V.; De Vos, D. E.; Bein, T.; Jacobs, P. A. *Chem. Commun.* **1997**, 355. (b) Subba Rao, Y. V.; De Vos, D. E.; Jacobs, P. A. *Angew. Chem., Int. Ed. Engl.* **1997**, *36*, 2661.

[22] Diaz, J. F.; Balkus, K. J., Jr.; Bedioui, F.; Kurshev, V.; Kevan, L. *Chem. Mater.* **1997**, *9*, 61.

[23] Barrett, E. P.;Joyner, L. G.; Halenda, P. P. *J. Am. Chem. Soc.* **1951**, *73*, 373.

[24] (a) Sung-Suh, Hyung Mi; Luan, Z.; Kevan, L. *J. Phys. Chem. B.*, **1997**, *101*, 10455. (b) Stucky, G. D.; Monnier, A.; Schuth, F.; Huo, Q.; Margolese, D.; Kumar, D.; Kridhnamurty, M.; Petroff, P.; Firouzi, A.; Janicke, M.; Chmelka, B. F. *Mol. Cryst. Liq. Cryst.*, **1994**, *240*, 187.

[25] (a) Sindorf, D.W.; Macier, G.E. *J Am. Chem. Soc.* **1983**, *105*, 3769. (b) Sindorf, D. W.; Maciel, G. E. *J. Am. Chem. Soc.* **1981**, *103*, 4263.

[26] (a) Akins, D. L.; Özçelik, S.; Zhu, H. -R.; Guo, C. *J. Phys. Chem.* **1996**, *100*, 14396. (b) Ohno, O.; Kaizu, Y.; Kobayashi, H. *J. Chem. Phys.*, **1993**, *99*, 4128.

[27] Akins, D. L. *J. Phys. Chem.* **1986**, *90*,1530.

[28] Akins, D. L.; Akpabli, C. K.; Li, X. *J. Phys. Chem.* **1989**, *93*, 1977.

[29] Kasha, M. *Radiat. Res.* **1963**, *20*, 55.

[30] Khairutdinov, R. F.; Serpone, N. *J. Phys. Chem. B* **1999**, *103*, 761.

References of Chapter 2

[1] Chen, S. H.; Huang, J. S. In *Structure and Dynamics of Strongly Interacting Colloids and Supramolecular Aggregates in Solution*, Tartaglia, P., Eds.; Luwer: Dordrecht, **1992**.

[2] Mallamace, F. In *Scaling Concepts and Complex Fluids*, Ed.; Compositori: Bologna, **1995**.

[3] Lehn, J. M. In *Supramolecular Chemistry*, VCH: Weinheim, **1995**.

[4] White, W. I. In *The Porphyrins*: Dolphin, D., Ed.; Academic: New York, **1978**; Vol. 5, Chapter 7.

[5] Kasha, M. *Radiation Res.* **1963**, *20*, 55.

[6] Sturmer, D. M.; Heseltine, D. W. In *The Theory of the Photographic Process*, (4th. ed.); James, T. H., Ed.; MacMillian Publishing Company: New York, 1977, Chap. 8.

[7] Herz, A. H.; *Adv. Colloid. Interface Sci.* **1977**, *8*, 237.

[8] Mobius, D.; Kuhn, H. *Israel. J. Chem.* **1979**, *18*, 375.

[9] Mobius, D. *Acc. Chem. Res.* **1981**, *14*, 63.

[10] Akins, D. L. *J. Phys. Chem.* **1986**, *90*, 1530.

[11] Akins, D. L.; Lombardi, J. R. *Chem. Phys. Lett.* **1987**, *136*, 495.

[12] Akins, D. L.; Akpabli, C. K.; Li, X. *J. Phys. Chem.* **1989**, *93*, 1977.

[13] Akins, D. L.; Macklin, J. W. *J. Phys. Chem.* **1989**, *93*, 5999.

[14] Akins, D. L.; Macklin, J. W.; Parker, L. A.; Zhu, H. -R. *Chem. Phys. Lett.* **1990**, *169*, 564.

[15] Akins, D. L.; Macklin, J. W.; Zhu, H. -R. *J. Phys. Chem.* **1991**, *95*, 793.

[16] Akins, D. L.; Zhu, H. -R. *Langmuir* **1992**, *8*, 546.

[17] Akins, D. L.; Zhuang, Y. H.; Zhu, H. -R.; Liu, J. Q. *J. Phys. Chem.* **1994**, *98*, 1068.

[18] Selwyn, J. E.; Steinfeld, J. I. *J. Phys. Chem.* **1972**, *76*, 762.

[19] Ojeda, P. R.; Amashta, I. A. K.; Ochoa, J. R.; Arbeloa, I. L. *J. Chem. Soc., Faraday Trans. II* **1988**, *84*, 1.

[20] Valdes-Aguilera, O.; Neckers, D. C. *Acc. Chem. Res.* **1989**, *22*, 171.

[21] Kasha, M.; Rawls, H. R.; El-Bayoumi, M. A. *Pure. Appl. Chem.* **1965**, *11*, 37.

[22] Hessemann, J. *J. Am. Chem. Soc.* **1980**, *102*, 2167; 2176.

[23] Vincent, P. S.; Barlow, W. A. *Thin Solid Films* **1980**, *71*, 305.

[24] Fukuda, K.; Nakahara, H. *J. Colloid Interface Sci.* **1984**, *98*, 555.

[25] Mooney, W. F.; Brown, P. E.; Russel, J. C.; Costa, S. B.; Pederson, L. G.; Whitten, D. G. *J. Am. Chem. Soc.* **1984**, *106*, 5659.

[26] Mooney, W. F.; Whitten, D. G. *J. Am. Chem. Soc.* **1986**, *108*, 5712.

[27] Pasternack, R. F.; Huber, P. R.; Boyd, P.; Engasser, G.; Francesconi, L.; Gibbs, E.; Fasella, P.; Venturo, G. C.; Hinds, L. deC. *J. Am. Chem. Soc.* **1972**, *94*, 4511.

[28] Pasternack, R. F.; Francesconi, L.; Raff, D.; Spiro, E. *Inorg. Chem.* **1973**, *12*, 2606.

[29] Shelnutt, J. A.; Dobry, M. M.; Satterlee, J. D. *J. Phys. Chem.* **1984**, *88*, 4980.

[30] Schick, G. A.; Schreiman, I. C.; Wagner, R. W.; Lindsey, J. S.; Bocian, D, F. *J. Am. Chem. Soc.* **1989**, *146*, 165.

[31] Barber, D. C.; Freitag-Beeston, R. A.; Whitten, D. G. *J. Phys. Chem.* **1991**, *95*, 4074.

[32] Ohno, O.; Kaizu, Y.; Kobayashi, H. *J. Chem. Phys.* **1993**, *99*, 4128.

[33] Schick, G. A.; O'Grady, M. R.; Tawari, R. K. *J. Phys. Chem.* **1993**, *97*, 1339.

[34] van Esch, J. H.; Feiters, M. C.; Peters, A. M.; Nolte, R. J. M. *J. Phys. Chem.* **1994**, *98*, 5541.

[35] Gilman, P. B. *Photo. Sci. Eng.* **1974**, *18*, 418.

[36] Borsenberger, P. M.; Chowdry, A.; Hoesterey, D. C.; W. Mey *J. Appl. Phys.* **1978**, *44*, 5555.

[37] Waggoner, A. *J. Membrane Biol.* **1976**, *27*, 317.

[38] Chatterjee, S.; Davis, P. D.; Gottschalk, P.; Kurz, M. E.; Sauerwein, B.; Yang, X.; Schuster, G. B. *J. Am. Chem. Soc.* **1990**, *112*, 6329.

[39] Hanamura, E. *Phys. Rev. B* **1988**, *37*, 1273.

[40] Sasaki, F.; Kobayashi, S. *Appl. Phys. Lett.* **1993**, *63*, 2887.

[41] Wang, Y. *Chem. Phys. Lett.* **1986**, *126*, 209.

[42] Wang, Y. *J. Opt. Soc. Am. B* **1991**, *8*, 981.

[43] Kobayashi, S. *Mol. Crys. Liq. Crys.* **1992**, 217, 77.

[44] Okamura, M. Y.; Feher, G.; Nelson, N. In *Photosynthesis*, Govindjee, Ed.; Academic Press: New York, 1982, pp. 195-272.

[45] O'Neil, M. P.; Niemcyzk, M. P.; Svec, W. A.; Gosztola, D.; Gaines III, G. L.; Wasielewski, M. R. *Science* **1992**, *257*, 63.

[46] Wagner, R. W.; Lindsey, J. S.; Seth, J.; Palaniappan, V.; Bocian, D. F. *J. Am. Chem. Soc.* **1996**, *118*, 3996.

[47] Lawandy, N.; Firehammer, J.; Vartak, S. *Laser Focus* **1997**, *33(5)*, 137.

[48] Akins, D. L, Zhu, H. -R.; Guo, C. *J. Phys. Chem.*, **1996**, *100*, 5420.

[49] Guo, C.; Ren, B.; Akins, D. L. *J. Phys. Chem.*, **1998**.

[50] Kano, H.; Saito, T.; and Kobayashi, T. J Phys. Chem. B 2001 105(2), 413-419.

[51] Akins, D. L, Zhu, H. -R.; Guo, C. *J. Phys. Chem.*, **1994**, *98*, 3612;

References of Chapter 3

[1] Akins, D. L.; Özçelik, S.; Zhu, H. -R.; Guo, C. *J. Phys. Chem A.* **1997**, *101*, 3251.

[2] Özçelik, S.; Akins, D. L. *J. Phys. Chem. B* **1999**, *103*, 8926.

[3] Akins, D. L. *J. Phys. Chem.* **1986**, *90*,1530.

[4] Akins, D. L. *J. of Colloid and Interface Sci.* **1982**, *90*, 373.

[5] Li, X.; Gu, B.; Akins, D. L. *Chem. Phys. Lett.* **1984**, *105*, 263.

[6] Gu, B.; Akins, D. L. *Chem. Phys. Lett.* **1985**, *113*, 558.

[7] Akins, D. L.; Akpabli, C.; Li, X. *J. Phys. Chem.* **1989**, *93*, 1977.

[8] Akins, D. L.; Macklin, J. W. *J. Phys. Chem.* **1989**, *93*, 5999.

[9] Akins, D. L.; Macklin, J. W.; Parker, L.; Zhu, H. -R. **1990**, *169*, 564.

[10] Akins, D. L.; Macklin, J. W.; Zhu, H. ¨ R. *J. Phys. Chem.* **1990**, *95*, 793.

[11] Akins, D. L.; Zhu, H. -R. *Langmuir* **1992**, *8*, 546.

[12] Akins, D. L.; Macklin, J. W.; Zhu, H. -R. *J. Phys. Chem.* **1992**, *96*, 4515.

[13] Akins, D. L.; Zhuang, Y. H.; Zhu, H. ¨ R.; Li, J. Q. *J. Phys. Chem.* **1993**, *98*, 1068.

[14] Akins, D. L. In *J-Aggregate*; Kobayashi, T., Ed.; World Scientific: Singapore, 1996, pp 67¨ 94.

[15] Plyuto, Y.; Berquier, J.; Jacquiod, C.; Ricolleau, C.; *Chem. Commun.* **1999**, 1653.

[16] Wu, C.; Bein, T.; *Science* **1994**, *264*, 1757.

[17] Kageyama, K.; J. Tamazawa, J.; Aida, T. *Science* **1999**, *285*, 2113.

[18] Moller, K.; Bein, T.; *Chem. Mater.* **1998**, *10*, 2950.

[19] Holland, B. T.; C. Walkup, C.; Stein, A.; *J. Phys. Chem. B* **1998**, *102*, 4301.

[20] Hyung Mi, Sung-Suh, Luan, Z.; Kevan, L.; *J. Phys. Chem. B* **1997**,*49*, 10455.

[21] Stucky, G. D.; MacDougall, J. E.; *Science* **1990**, *247*, 669.

[22] Moller, K.; Bein, T. *Chem. Mater.* **1998**, *10*, 2950. (Review article, see references therein.)

[23] X. Feng, X. G. E. Fryxell, G. E.; Wang, L. Q.; Kim, A.Y.; Liu, J.; Kemner, K. M.; *Science* **1997**, *276*, 923.

[24] Chakraborty, P.; *J. Mater. Sci.* **1998**, *33*, 2235.

[25] Yang, P.; Wirnsberger, G.; Huang, H. C.; Cordero, S. R.; McGehee, M. D.; Scott, B.; Deng, T.; Whitesides, G. M.; Chmelka, B. F.; Buratto, S. K.; Stucky, G. D. *Science* **2000**, *287*, 465.

[26] Özçelik, S.; Akins, D. L. *Appl. Phys. Lett.* **1997**, *71*, 1.

[27] Özçelik, S.; Akins, D. L. *Appl. Phys. Lett.* **1998**, *73*, 1949.

[28] Grad, J.; Hernandez, G.; Mukamel, S. *Phys. Rev. A.* **1988**, *37*, 3835.

[29] Spano, F. C.; Mukamel, S. *J. Chem. Phys.* **1989**, *91*, 683.

[30] Spano, F. C.; Kuklinski, J. R.; Mukamel, S. *J. Chem. Phys.* **1991**, *94*, 7534.

[31] Kresge, C. T.; Leonowicz, M. E.; Roth, W. J.; Vartuli, J. C.; Beck, J. S.: *Nature* **1992**, *359*, 710.

[32] Beck, J. S.; Vartuli, J. C.; Roth, W. J.; Leonowicz, M. E.; Kresge, C. T.; Schmitt, K. D.; Chu, C. T.-W.; Olson, D. H.; Sheppard, E. W.; McCullen, B.; Higgins, J. B.; Schlenker, J. L. *J. Am. Chem. Soc.* **1992**, *114*, 10834.

[33] Liu, C. -J.; Li, S. -G.; Pang, W. -Q.; Che, C. -M. *Chem. Commun.*, **1997**, *65*, 78.

[34] Mercier, L.; Pinnavaia, T. J. *Adv. Mater.* **1997**, *9*, 500.

[35] Sung-Suh, Hyung Mi; Luan, Z.; Kevan, L. *J. Phys. Chem. B.*, **1997**, *101*, 10455.

[36] Stucky, G. D.; Monnier, A.; Schuth, F.; Huo, Q.; Margolese, D.; Kumar, D.; Kridhnamurty, M.; Petroff, P.; Firouzi, A.; Janicke, M.; Chmelka, B. F. *Mol. Cryst. Liq. Cryst.*, **1994**, *240*, 187.

[37] Akins, D. L.; Zhu, H. -R.; Guo, C. *J. Phys. Chem.* **1996**, *100*, 5420.

References of Chapter 4

[1] Pearlstein, R. M. In *Photosynthesis*, Amesz, J., Ed.; Elsevier: Amsterdam **1987**, pp. 299-317.

[2] Warshel, A.; Parson, W. W. *J. Am. Chem. Soc.* **1987**, *109*, 6152.

[3] Creighton, S.; Hwang, J. -K.; Warshel, A.; Parson, W. W.; Norris, J. *Biochemistry* **1988**, *27*, 774.

[4] Michel-Beyerle, M. E.; Plato, M.; Deisenhofer, J.; Michel, H.; Bixon, M.; Jorter, L. *Biochem. Biophys. Acta* **1988**, *932*, 52.

[5] Kasha, M. *Radiation Res.* **1963**, *20*, 55.

[6] Plyuto, Y.; Berquier, J.; Jacquiod, C.; Ricolleau, C. *Chem. Commun.* **1999**, 1653.

[7] Wu, C.; Bein, T. *Science* **1994**, *264*, 1757.

[8] Kageyama, K.; Tamazawa, J.; Aida, T. *Science* **1999**, *285*, 2113.

[9] Moller, K.; Bein, T. *Chem. Mater.* **1998**, *10*, 2950.

[10] Holland, B. T.; C. Walkup, C.; Stein, A. *J. Phys. Chem. B* **1998**, *102*, 4301.

[11] Sung-Suh, H.; Luan, Z.; Kevan, L. *J. Phys. Chem. B* **1997**, *49*, 10455.

[12] Stucky, G. D.; MacDougall, J. E. *Science* **1990**, *247*, 669.

[13] Moller, K.; Bein, T. *Chem. Mater.* **1998**, *10*, 2950. (Review article, see references therein.)

[14] Feng, X.; Fryxell, G. E.; Wang, L. Q.; Kim, A.Y.; Liu, J.; Kemner, K. M. *Science* **1997**, *276*, 923.

[15] Chakraborty, P. *J. Mater. Sci.* **1998**, *33*, 2235.

[16] Xu, W.; Guo, H.; Akins, D. L. *J. Phys. Chem. B.*, **2001**, *105*, 1543.

[17] Xu, W.; Guo, H.; Akins, D. L. *J. Phys. Chem. B.*, **2001**, *105*, 7687.

[18] Zhao, D.; Feng, J.; Huo, Q.; Melosh, N.; Fredrickson, G. H.; Chmelka B. F.; Stucky G. D. *Science* **1998**, *297*, 548.

[19] Zhao, D.; Huo, Q.; Feng, J.; Chmelka, B. F.; Stucky, G. D. J. Am. Chem. Soc. 1998, 120, 6024.

[20] Akins, D. L.; Macklin, J. W. *J. Phys. Chem.* **1989**, *93*, 5999.

[21] Herz, A. H. *Adv. Colloid. Interfacial Sci.* **1977**, *8*, 237.